AD_____

Award Number: DAMD17-98-1-8482

TITLE: Gene Discovery in Prostate Cancer: Functional Identification and Isolation of PAC-1, a Novel Tumor Suppressor Gene Within Chromosome 10p

PRINCIPAL INVESTIGATOR: Ann M. Killary, Ph.D.

CONTRACTING ORGANIZATION: University of Texas
MD Anderson Cancer Center
Houston, Texas 77030-4095

REPORT DATE: September 1999

TYPE OF REPORT: Annual

PREPARED FOR: U.S. Army Medical Research and Materiel Command
Fort Detrick, Maryland 21702-5012

NOTICE

LIMITED RIGHTS LEGEND

Award Number: DAMD17-98-1-8482
Organization: University of Texas
M.D. Anderson Cancer Center
Location of Limited Rights Data (Pages):

THIS TECHNICAL REPORT HAS BEEN REVIEWED AND IS APPROVED FOR PUBLICATION.

[illegible]
10/30/00

REPORT DOCUMENTATION PAGE

Form Approved
OMB No. 074-0188

1. AGENCY USE ONLY (Leave blank)	2. REPORT DATE	3. REPORT TYPE AND DATES COVERED
	September 1999	Annual (1 Sep 98 - 31 Aug 99)

4. TITLE AND SUBTITLE
Gene Discovery in Prostate Cancer: Functional Identification and Isolation of PAC-1, a Novel Tumor Suppressor Gene Within Chromosome 10p

5. FUNDING NUMBERS
DAMD17-98-1-8482

6. AUTHOR(S)
Ann M. Killary, Ph.D.

7. PERFORMING ORGANIZATION NAME(S) AND ADDRESS(ES)
University of Texas
MD Anderson Cancer Center

Houston, Texas 77030-4095

E-MAIL:
akillary@mdanderson.org

8. PERFORMING ORGANIZATION REPORT NUMBER

9. SPONSORING / MONITORING AGENCY NAME(S) AND ADDRESS(ES)
U.S. Army Medical Research and Materiel Command
Fort Detrick, Maryland 21702-5012

10. SPONSORING / MONITORING AGENCY REPORT NUMBER

11. SUPPLEMENTARY NOTES

12a. DISTRIBUTION / AVAILABILITY STATEMENT
Distribution authorized to U.S. Government agencies only (proprietary information, Sep 99). Other requests for this document shall be referred to U.S. Army Medical Research and Materiel Command, 504 Scott Street, Fort Detrick, Maryland 21702-5012.

12b. DISTRIBUTION CODE

13. ABSTRACT ***(Maximum 200 Words)***
We have previously identified a novel genetic locus *PAC-1* (*Prostatic Adenocarcinoma-1*) involved in tumor suppression of human prostate carcinoma. Introduction of human chromosome 10p into prostate adenocarcinoma cells resulted in tumor suppression and a restoration of the cell death pathway in vivo. The specific aims of this award involve both an expression based and positional cloning based strategy to identify PAC-1. As a first step in this strategy, we identified a region of homozygous deletion within a prostate cell line that falls within a region we identified as having tumor suppressor functional activity in vivo. Thus, we report the narrowing of the region containing *PAC-1* to a homozygous deletion region. The next step in the strategy will be to clone the homozygous deletion region and identify this important tumor suppressor gene for prostate cancer.

14. SUBJECT TERMS
Prostate Cancer, tumor suppressor genes, functional identification

15. NUMBER OF PAGES
54

16. PRICE CODE

17. SECURITY CLASSIFICATION OF REPORT	18. SECURITY CLASSIFICATION OF THIS PAGE	19. SECURITY CLASSIFICATION OF ABSTRACT	20. LIMITATION OF ABSTRACT
Unclassified	Unclassified	Unclassified	Unlimited

NSN 7540-01-280-5500

Standard Form 298 (Rev. 2-89)
Prescribed by ANSI Std. Z39-18
298-102

FOREWORD

Opinions, interpretations, conclusions and recommendations are those of the author and are not necessarily endorsed by the U.S. Army.

_N/A__ Where copyrighted material is quoted, permission has been obtained to use such material.

_N/A__ Where material from documents designated for limited distribution is quoted, permission has been obtained to use the material.

_X__ Citations of commercial organizations and trade names in this report do not constitute an official Department of Army endorsement or approval of the products or services of these organizations.

X In conducting research using animals, the investigator(s) adhered to the "Guide for the Care and Use of Laboratory Animals," prepared by the Committee on Care and use of Laboratory Animals of the Institute of Laboratory Resources, national Research Council (NIH Publication No. 86-23, Revised 1985).

X For the protection of human subjects, the investigator(s) adhered to policies of applicable Federal Law 45 CFR 46.

In conducting research utilizing recombinant DNA technology, the investigator(s) adhered to current guidelines promulgated by the National Institutes of Health.

In the conduct of research utilizing recombinant DNA, the investigator(s) adhered to the NIH Guidelines for Research Involving Recombinant DNA Molecules.

N/A In the conduct of research involving hazardous organisms, the investigator(s) adhered to the CDC-NIH Guide for Biosafety in Microbiological and Biomedical Laboratories.

Ann Killary 1/07/90

PI - Signature Date

Table of Contents

1.0 INTRODUCTION

The search for tumor suppressor genes involved in prostate cancer has been primarily based on the compilation of many years of research in the cytogenetics of prostate cancer as well more recent molecular genetic investigation.

2.0 *BODY

2.1 Cytogenetic Evaluation Of Human Prostate Cancer. Recent advances in the cytogenetic analysis of short term cultures of primary prostatic adenocarcinoma have allowed a more thorough investigation of nonrandom chromosomal aberrations associated with prostate cancer. The most consistent cytogenetic finding in primary prostate cancer is a normal diploid karyotype. Brothman and coworkers reported clonal aberrations in 9/30 primary prostate cancer cultures (1). These included loss of the Y chromosome, a partial trisomy for chromosome 4, and translocations involving the long arms of chromosomes 5 and 7. Other nonrandom changes reported by Micale and coworkers included gain of 7 and loss of the Y chromosome (2). Also clonal gains of chromosomes 8, 12 and 18 and losses of chromosome 14 and 19 were observed. Recently, Lundgren et al. reported that 24/57 primary prostatic adenocarcinomas had a normal diploid karyotype (3). Eighteen of 57 contained structural rearrangements involving 18 of 22 autosomes and the X chromosome. The most common loss was of human chromosome Y. In addition to this loss, the most common aberrations were seen on chromosomes 1, 7 and 10 in which deletions, inversions, insertions, duplications and translocations were reported. The breakpoints on human chromosome 7 were in band 7q22 and on human chromosome 10 in 10q24. Monosomy of 8 and rearrangements of the short arm of chromosome 8 leading to loss of 8p21-pter was seen in four tumors.

Thus, there is no single, high frequency cytogenetic aberration observed in prostate cancer. However, a consistent loss of the Y chromosome was observed in all studies. In addition, loss or rearrangements of chromosomes 1, 7, 8 and 10 were also reported. These types of studies are valuable to pinpoint regions within the human genome that could contain genes involved in the initiation or progression of the disease that could be further characterized by molecular genetic approaches.

2.2 Genetic Alterations in Human Prostate Cancer. While cytogenetic analysis can be used to narrow the search for genes involved in prostate cancer, much of the analysis of these tumors is complicated by the heterogeneity of the tumor cell population. Morphologically distinct, genotypically distinct foci within the tumor are characteristic of prostate cancer. In addition, normal epithelium and stroma are found within the tumor mass that complicate cytogenetic analysis of tumors. Detailed loss of heterozygosity (LOH) studies in combination with cytogenetic analysis are extremely valuable to identify key regions of the genome that contain putative tumor suppressor genes. Carter and coworkers studied 28 prostate tumor samples for loss of heterozygosity of DNA markers corresponding to 11 different

* *Unpublished data to be protected*

chromosome arms (4). LOH was observed on 10q and 16q in 30% of informative tumors samples. Allelotyping studies by Kunimi et al. reported LOH on 8p (50%), 10p (55%), 10q (30%), 16q (60%), and 18q (43%) (5). A common region of LOH has recently been identified by Bova et al. who demonstrated high frequency loss of alleles at 8p21.2-8p22 in prostate tumors (6). Homozygous deletion of the MSR locus was detected in one prostate sample. These data together indicate that the most common regions of LOH include chromosomes 8p, 10p, 10q, 16q, and 18q. These regions potentially contain tumor suppressor genes involved in either the initiation and/or progression of this devastating disease.

2.3 **Functional Studies to Identify Tumor Suppressor Genes**. Cytogenetic aberrations and loss of heterozygosity studies have pointed to at least five different chromosomes or chromosomal regions that may contain tumor suppressor loci involved in prostate cancer. Functional studies are further required to prove that a particular chromosome or chromosomal region encodes a tumor suppressor locus. Previous studies have shown that it is possible to complement the genetic defect in particular human cancers (which show high frequency allele loss on a defined chromosome) by the introduction of normal copy of that chromosome containing a putative tumor suppressor gene. Studies have demonstrated the functional involvement of genetic loci on human chromosome 11 in cervical carcinoma (7) and Wilms Tumor (8), human chromosome 6 in melanoma (9), human chromosomes 5 and 18 in colon carcinoma (10) and the identification of the pten tumor suppressor gene within chromosome 10q. Functional studies such as these have not been reported for prostate cancer. Metastasis suppressor genes have been identified, however, on the short arm of human chromosome 11 and the long arm of chromosome 10 which suppressed the metastasis of a highly metastatic rat prostate carcinoma line (23, 24).

We have previously functionally defined a novel genetic locus within human chromosome 10pter-q1 that mediates both the in vivo tumor suppresison and the in vitro apoptosis of prostatic adenocarcinoma cells. A defined fragment of human chromosome 10 was transferred into a prostatic carcinoma cell line PC-3H via microcell fusion. Microcell hybrids containing only the region 10pter-q11 were suppressed for tumorigenicity following injection of hybrids into nude mice. Furthermore, complemented hybrids underwent programmed cell death in vitro via a mechanism of apoptosis that does not involve nuclear localizatio of p53. These data functionally define a novel genetic locus PAC-1 (Prosatic Adenocarcinoma-1) involved in tumor suppression of human prostatic adenocarcinoma and furthermore strongly suggest that the cell death pathway can be functionally restored in prostatic adenocarcinoma cells in vivo. The major goals of this funded award are to utilize an expression based and positional cloning based strategy to identify PAC-1 within chromosome 10p.

2.4 **Hypothesis:** Our hypothesis is that an important tumor suppressor gene for prostate cancer resides within chromosome 10p and that it can be isolated by a novel concerted functional genetic, physical mapping and molecular biologic approach.

* *Unpublished data to be protected*

2.5 Technical Objectives

In this proposal, a novel experimental system is described that should result in the isolation of caddidate cDNAs encoding the tumor suppressor gene PAC-1.

2.6 Isolation of Candidate cDNAs for PAC-1 from the Region of Nonoverlap in Defined Deletion Hybrids.

1) PCR-select cDNA subtraction has identified candidate cDNAs for a novel gene for kidney cancer in our laboratory. PCR-select subtraction will be used to identify partial cDNAs that are expressed in suppressed hybrid deletion clones and not expressed in unsuppressed clones.

2) Positional cloning efforts will involve identification of all known STSs (including microsatellite markers and ESTs) mapping to homozygous deletion region to screen PAC and BAC libraries. Fingerprinting of clones will facilitate construction of a contig across the nonoverlap region between suppressed and unsuppressed hybrid clones.

3) cDNAs defined by the above approaches in combination with cDNAs defined by complementary approaches of cDNA enrichment and exon trapping (described in the ACS objectives) will be mapped into the region of nonoverlap on chromosome 10p. Mapping will be accomplished by screening suppressed and unsuppressed hybrids (ACS grant) as well as by mapping to slot blots of P1/PAC/BAC clones used to construct contigs across the region of nonoverlap (Army objectives). cDNAs that map into the region will be sequenced and used to screen for differential expression in prostate cell lines and prostate tumors (Army grant).

4) cDNAs that map into the nonoverlap region and which are differentially expressed in prostate tumor/normal samples as well as hybrid lines and prostate cell lines will be used to screen cDNA libraries to isolate full length cDNAs for the candidate PAC-1 tumor suppressor gene. Candidate cDNAs will be cloned into expression vectors for future functional studies.

5). Tissue distribution of candidate PAC-1 tumor suppressor gene will be determined.

2.7 Methods

2.8 Microsatellite Analyses

Polymorphic microsatellite markers generated by Genethon, but also polymorphic tetranucleotide repeats from the Cooperative Human Linkage Center (CHLC), random genome-wide sequence-tagged sites (STSs) generated from sheared whole human DNA, and STSs generated from sequences in the database of expressed sequence tags (dbEST)were used to screen PC-3H and prostate tumors for loss of heterozygosity and homozygous deletion. For the microsatellite analyses the forward primer for each locus will be labeled with 32P using T4 polynucleotide

* *Unpublished data to be protected*

kinase. The forward primer (10 pmoles) will be incubated with 0.5-2.5 (Ci of [gamma-32P]ATP at 37∞C for 45 min in a thermal cycler followed by an incubation at 65∞C for 10 min. The labeled primer will be used in the following PCR reaction: The labeled primer is combined with 10 pmoles of unlabeled reverse primer, and 50-100 ng of template DNA and water. A drop of oil is added to prevent evaporation and the DNA is denatured at 96∞C for 5 min, and soaked at 80∞C. While the reaction soaks at 80∞C a MAP master mix is added to each tube (Research Genetics) containing Hepes PCR buffer, dNTP's, 1.5 mM MgCl, 0.5 u amplitaq. The samples are then subjected to 25 cycles of PCR consisting of a denaturation step at 94∞C for 40 seconds followed an annealing step at 45∞C for 30 sec with an elongation step at 72∞C for 30 sec with a final elongation at 72∞C for 2 min. The reaction is stopped and the samples heated to 90∞C for 5 min. The samples are separated on a 6% sequencing gel containing 30% formamide at 60 watts and visualized by autoradiography.

2.9 Molecular Cytogenetic Analysis

For these experiments, human DNA will be amplified using PCR from monochromosomal hybrids containing either human chromosomes 10 or 10p. Amplified DNA will be used as probe for in situ hybridization onto metaphase spreads from PC-3H and other prostate cell lines and tumors. Chromosome-specific probes are prepared by PCR amplification of human-specific DNA from each monochromosomal hybrid using inter-Alu primers. For the reaction, 100 ng of hybrid DNA is incubated with 50 pmoles of each of the alu primers in buffer containing 15 mM Magnesium and 1.25 units of Taq polymerase (Perkin-Elmer Cetus). The DNA is denatured at 94∞C for five minutes followed by five cycles of 1 min at 94∞C, 1 min at 65∞C, and 3 min at 72∞C. An elongation step of 10 min at 72∞C is then performed: samples are cooled and products run on a 2% agarose gel. The primers are then removed from the PCR product using Centricon-100 columns. Chromosome-specific DNA is then labeled with biotin-14 dATP using nick translation. For hybridization, the biotinylated probe and 50X COT 1 (Gibco) unlabeled DNA and 10% Dextran sulfate, 2X SSC, and 50% formamide are denatured at 75∞C for 10 min. The DNA is allowed to reanneal at 37∞C for 20 min and hybridized to processed metaphases from tumor cell lines. Hybridization is detected using fluorescein-avidin conjugate and amplified using biotinylated anti-avidin antibody.

Cytogenetic preparations will be processed for G banding and photographed. G banded slides will then be destained by incubation 10 min at 95% methanol. Destained slides will then be utilized for fluorescence in situ hybridization using pSV2neo or locus-specific probes for each chromosome. For in situ hybridization, chromosome preparations will be treated with RNaseA and denatured with 70% formamide/2X SSC at 71∞C. The slides will then be hybridized with biotinylated probe in 2X SSC, 50% formamide and sonicated salmon sperm DNA. Hybridization will be carried out for 16 hr at 37∞C. The slides then will be washed in 50% formamide/2X SSC at 37∞C and hybridization detected by incubating the slides in a fluorescein-avidin conjugate and amplified using biotinylated anti-avidin antibody. The preparations will be mounted in antifade containing propidum iodide as a counterstain.

**Unpublished data to be protected*

3.0 KEY RESEARCH ACCOMPLISHMENTS

3.1 Physical and Functional Mapping of a Novel Tumor Suppressor Gene within Chromosome 10p

3.2 Discovery of Homozgyous Deletion in Prostate Carcinoma Cell Line that potentially signals location of tumor suppressor gene

3.3 Identification of BAC clones containing homozygous deletion region for sequencing

4.0 REPORTABLE OUTCOMES

Wong, P.E., Lovell, M.M., Goodacre, A., and Killary, A.M. A functional genomic approach for the identification of *PAC-1*, a novel chromosome 10 tumor suppressor gene. American Journal Human Genetics 65(4):A330 (1999).

5.0 RESULTS

5.1 The Model System

Human prostatic adenocarcinoma cell line PC-3H was used as a recipient cell line for the transfer of defined regions of human chromosome 10 dominantly tagged with neo. PC-3 was established from the poorly differentiated adenocarcinoma from a vertebral body metastasis in a patient with hormone-insensitive prostate cancer. PC-3 has been well characterized for in vitro growth as well as for growth in nude mice. Cytogenetics performed in our laboratory on PC-3 obtained from the American Type Culture Collection (ATCC) indicated that the cell line was near triploid with a modal chromosome number of 62.

5.2 Positional Cloning of PAC-1 within Chromosome 10p

Cytogenetic analysis, fluorescence in situ hybridization and comparative genomic hybridization were used to characterize PC-3H in an attempt to identify specific regions of copy number losses, rearrangements or homozygous deletion that might narrow the search for PAC-1 within chromosome 10p. A subcloned line PC-3H was developed for these studies. PC-3H contained no recognizable chromosome 10 by high resolution cytogenetics. However, chromosome painting analysis using chromosome 10-specific DNA as a probe indicated that fragments of chromosome 10 were scattered through the genome. Further FISH studies indicated the presence of 10p material scattered throughout PC-3H. Comparative genomic hybridization studies were performed in an attempt to identify copy number changes that result in loss of a particular region of 10p. Results indicated that PC-3H is homozygous for all microsatellite markers screened within chromosome 10p (>20 markers). Given the high degreee of heterozgosity of the markers studies (>75%), it is likely that PC-3H is hemizygous for the short arm of chromosome 10.

Since PC-3H appeared to be hemizygous for the short arm of chromosome 10, we performed a high density screen of PC-3H using 41 microsatellite markers within 10p. Results indicated homozygosity for 40 markers (Fig. 1). A single microsatellite marker was homozygously deleted in PC-3H. To confirm the homozygous deletion, multiplex PCR was used to screen PC-3H using the microsatellite marker that had been found by multiple PCR reactions to be homozygously deleted. In addition a second 10p marker proximal to the marker tested which generated a PCR product 100 bp smaller that the marker under examination was also amplified in the same PCR reaction. Again results confirmed the homozgyous deletion of a single marker within chromosome 10p (Fig. 2). Current efforts are underway to further confirm the homzygous deletion using Southern analysis. The microsatellite marker is too small to use a probe for Southern analysis, so we are in the process of utilizing a commercial product from Genosphere which utilizes dendrimer technology to amplify small oligonucleotides by bining of dendrimers to oligonucleotides specific for the sequence.

We were also able to confirm that the microsatellite marker was correctly mapped to within chromosome 10p by identifying BAC clones containing the marker and which map to chromosome 10p. We are currently attempting to sequence the BAC clone from the microsatellite marker not only as a means of generating a good probe for Southern analysis, but also as a means to identify exons that flank the homozygous deletion region. BAC clones can then be used to design terminal specific primers for a further round of screening if necessary to isolate overlapping clones To complete the contig spanning the minimal region flanking the homozygous deletion, two approaches will be taken. First, additional entry clones will be obtained using all the STSs mapping to the region to screen a P1 library. We have obtained a P1 library developed by Sternberg and coworkers, consisting of 130,000-140,000 clones with an average insert size of 70-95 kb providing 3-4 fold coverage of the human genome. Cosmid and P1 clones will be fingerprinted to initiate construction of a contig. The second method will be to fill in the gaps by synthesizing end sequences to screen gridded libraries. Fingerprinting of these clones should complete the contig.

We have also identified ESTs (expressed sequence tags) that flank the microsatellite marker that is homozgyously deleted and are screening them for differential expression in microcell hybrid clones containing 10p and suppressed for tumors in vivo versus the PC-3H parental cell line. ESTs mapped into chromosome 10p have been obtained from the European Informatics Institute, the Stanford RH database, the Whitehead Institute, dbEST, the Washington University -Merck EST Project and the I.M.A.G.E. consortium. ESTs that map into the nonoverlap region will be obtained. The corresponding clones are available from Research Genetics and can be used in Southern and Northern analysis.

Finally, in collaboration with Dr. Jacob Kagan, we are screening prostate tumor samples for loss of heterozygosity and homozygous deletion using microsatellite markers that include and flank the homozgyous deletion marker.

6.0 CONCLUSIONS

In summary, positional cloning of PAC-1 from chromosome 10p has been tremendously aided by the discovery of a homozygous deletion of a single microsatellite marker within the chromosome10 region. Other studies (funded by the American Cancer Society) have utilized defined microcell hybrid clones carrying deletions of 10p to further narrow the region of functional tumor suppressor activity. Very interesting, the results obtained from the ACS study directly complement the funded studies from the DOD in that a region of functional tumor suppressor activity was limited to approximately 2 Mb within chromosome 10p. The homozygous deletion region falls within this region defined using functional genetic approaches. We therefore conclude that we have narrowed the search for PAC-1 within chromosome 10p and have identified a novel and exciting homozygous deletion that should led to the identification of a new tumor suppressor gene in prostate cancer.

REFERENCES

1. Carter, B.S., Ewing, C.M., Ward,W.S., Treiger, R.F., Aalders, T.W., Schalken, J.A., Epstein, J.I. and Isaacs, W.B. Allelic loss of chromosome 16q and 10q in human prostate cancer. Proc. Natl. Acad. Sci. USA, 87: 8751-8755, 1990.

2. Kunimi, K., Bergerheim, U.S.R. , Larsson, L.-L., Ekman, P., and Collins, V.P. Allelotyping of human prostatic adenocarcinoma. Genomics, 11:530-536, 1991.

3. Bova, G.S., Carter, B.S., Bussemakers, M.J.G., Emi, M., Fujiwara, Y., Kyprianou, N., Jacobs, S.C., Robinson, J.C., Epstein,J.I., Walsh, P.C., and Isaacs, W.B. Homozygous deletion and frequent allelic loss of chromosome 8p22 in human prostate cancer. Cancer Res., 53: 3869-3873, 1993.

4. Saxon, P.J., Srivatsan, E.S. and Stanbridge, E.J. Introduction of human chromosome 11 via microcell transfer controls tumorigenic expression of HeLa cells. EMBO, 5(13): 3461-3466, 1986.

5. Weissman, B.E., Saxon, P.J., Pasquale,S.R., Jones, G.R., Geiser, A.G. and Stanbridge, E.J. Introduction of a normal human chromosome 11 into a Wilms' tumor cell line controls its tumorigenic expression. Science, 236: 175-180, 1987.

6. Trent, J.M., Stanbridge, E.J., McBride, H.L., Meese, E.U., Casey, G., Araujo, D.E., Witkowski, C.M. and Nagle, R.B. Tumorigenicity in human melanoma cell lines controlled by introduction of human chromosome 6. Science, 247: 568-571, 1990.

7. Dowdy, S.F., Fasching, C.L, Araujo, D., Lai, K.-M., Livanos, E., Weissman, B.E. and Stanbridge, E.J. Suppression of tumorigenicity in Wilms tumor by the p15.5-p14 region of chromosome 11. Science, 254: 293-295, 1991.

8. Sanchez, Y., Lovell, M., Marin, M.C., Wong, P., Wolf, E., McDonnell, T.J. and Killary, A.M. Tumor suppression and apoptosis of human prostate carcinoma mediated by a genetic locus within human chromosome 10pter-q11. Proc. Natl. Acad. Sci., USA, 93: 2331-2556, 1996.

Table I. Markers Screened for Homozygous Deletion in PC-3H

D10S515 (pter)	D10S526	D10S1477	D10S582
D10S558	D10S1154	D10S1661	D10S1673
D10S594	D10S591	D10S504	D10S89
D10S1145	D10S1153	D10S1125	D10S111
D10S559	D10S179	D10S1714	D10S593
D10S1716	D10S1152	D10S518	D10S600
D10S602	D10S189	D10S1423	D10S204
D10S1161	D10S1779	D10S595	D10S601
D10S1142	D10S585	D10S211	
D10S514	D10S1705	D10S1734	
D10S1706	D10S191	D10S1789	

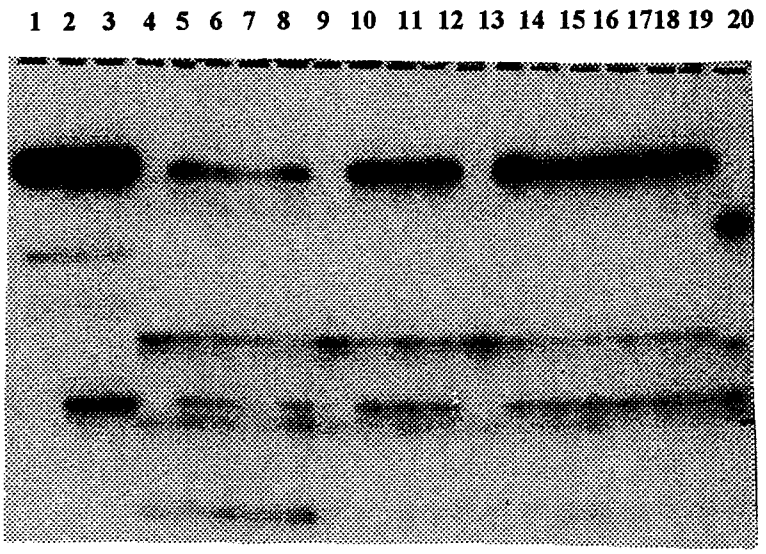

Fig. 1. Multiplex PCR to confirm homozygous deletion. 1) A9; 2) hybrid with introduced chromosome 10; 3) hybrid in A9 with introduced human chromosome 10p; 4) PC-3H (note homozygous deletion in marker homozygous in PC-3H and heterozygosity for proximal 10p marker 3 cM centromeric to marker; 5-20) various deletion hybrids containing portions of chromosome 10p.

APPENDICES I

Gene Discovery in Prostate Cancer: Functional Identification and Isolation of PAC-1, A Novel Tumor Suppressor Gene within Chromosome 10p

Proc. Natl. Acad. Sci. USA
Vol. 91, pp. 3383–3387, April 1994
Genetics

A tumor suppressor locus within 3p14-p12 mediates rapid cell death of renal cell carcinoma *in vivo*

YOLANDA SANCHEZ*, ADEL EL-NAGGAR†, SEN PATHAK‡, AND ANN MCNEILL KILLARY*§

*Hematopathology Program, Division of Laboratory Medicine, †Division of Pathology, and ‡Department of Cell Biology, The University of Texas M. D. Anderson Cancer Center, Houston, TX 77030

Communicated by Raymond L. White, December 20, 1993 (received for review July 30, 1993)

ABSTRACT **High frequency loss of alleles and cytogenetic aberrations on the short arm of chromosome 3 have been documented in renal cell carcinoma (RCC). Potentially, three distinct regions on 3p could encode tumor suppressor genes involved in the genesis of this cancer. We report that the introduction of a centric fragment of 3p, encompassing 3p14-q11, into a highly malignant RCC cell line resulted in a dramatic suppression of tumor growth in athymic nude mice. Another defined deletion hybrid contained the region 3p12-q24 of the introduced human chromosome and failed to suppress tumorigenicity. These data functionally define a tumor suppressor locus, nonpapillary renal carcinoma-1 (*NRC-1*), within 3p14-p12, the most proximal region of high frequency allele loss in sporadic RCC as well as the region containing the translocation breakpoint in familial RCC. Furthermore, we provide functional evidence that *NRC-1* controls the growth of RCC cells by inducing rapid cell death *in vivo*.**

Detailed cytogenetic investigation and loss of heterozygosity (LOH) studies have shown that the primary genetic aberration in human nonpapillary renal cell carcinoma (RCC) involves the short arm of human chromosome 3. In the rare familial form of the disease, defined translocations have been identified with breakpoints in the region of 3p13-p14 (1–3). High frequency LOH in sporadic RCC has been observed in two distinct regions on 3p encompassing 3p13-p14.3 and 3p21.3 (4–11). A third, more distal region mapping to 3p25 has been implicated in the etiology of Von Hippel–Lindau disease (12–14), an autosomal dominant disorder with many clinical manifestations including the development of bilateral kidney cysts. These cysts progress to RCC in some individuals (15, 16). Thus, three regions on 3p could be involved in the genesis of nonpapillary RCC.

Previous studies have shown that it is possible to complement the genetic defect in particular human cancers (that show high-frequency LOH on a specific chromosome) by the introduction of a normal copy of that chromosome containing a putative tumor suppressor gene (17–22). Using this approach, Shimizu *et al.* (21) modulated the tumorigenicity of the cell line YCR by the introduction of a human translocation chromosome containing 3p.

For our studies, we dissected 3p into defined regions using a functional assay to determine if a particular region alone could confer tumor suppression in RCC. We report the definition of a tumor suppressor locus within the most proximal region of high-frequency LOH in sporadic RCC as well as the region containing the translocation breakpoint in familial RCC.

MATERIALS AND METHODS

Cell Lines and Construction of Hybrids. The sporadic nonpapillary RCC cell line SN12C was derived from the primary kidney tumor of a 43-year-old man and carries a t(3;8) translocation with a breakpoint at 3p14 (23). A subcloned line (SN12C.19) of mixed granular/clear cell morphology was isolated and used for these studies. The microcell hybrid HA(3)BB containing human chromosomes 3 has been described (24). HA(3)IIaa contains a centric fragment of 3p (3p14-q11) in the A9 (mouse fibrosarcoma) background.

Microcell Fusion. The method of microcell fusion has been described (24, 25). Briefly, HA(3)BB cells were incubated in Colcemid at 0.06 μg/ml (48 hr) to induce micronucleation. Microcells were isolated after centrifugation of micronucleate cell populations in cytochalasin B (10 μg/ml) at 27,000 × *g* for 70 min (28–32°C). Microcells were resuspended in 4 ml of phytohemagglutinin P and added to a 70–80% confluent monolayer of RCC cells in each of two 25-cm² flasks. After a 15- to 20-min incubation (37°C) in phytohemagglutinin P, microcells were fused to RCC cells in 1 ml of 50% (wt/wt) polyethylene glycol (Koch Chemicals, England) for 1 min. Twenty-four hours postfusion, hybrid clones were selected by plating in medium containing G418 at 750 μg/ml and hypoxanthine/aminopterin/thymidine (A9 is hypoxanthine phosphoribosyltransferase negative). Each fusion produced between 87 and 134 G418-resistant clones.

Fluorescence *in Situ* Hybridization (FISH). Chromosome preparations were hybridized at 37°C with biotinylated human placental (100 ng), pSV2neo (400 ng), or D3S3 (400 ng) DNAs in 2× SSC/50% (vol/vol) formamide/10% dextran sulfate/sonicated salmon sperm DNA. After a wash in 50% formamide/2× SSC at 42°C for total human DNA and 37°C for pSV2neo and D3S3, the probe was detected with fluorescein-avidin and biotinylated anti-avidin antibody.

For chromosome painting, 400 ng of chromosome-specific DNA (26) and 50× C_0t 1 unlabeled DNA were hybridized as above to chromosome preparations. Posthybridization washing was performed at 42°C followed by 2× SSC at 37°C and detection as above.

***In Vivo* Growth Assays.** Microcell hybrid and parental RCC cells were injected subcutaneously at 5×10^6 cells into each of three 5- to 6-week-old male athymic nude mice (Harlan–Sprague–Dawley). Tumor volumes were monitored biweekly. Tumors were excised, explanted into culture, and maintained without G418 for chromosome analysis. For staging tumorigenicity assays, hybrid lines and parental controls were injected into each of six athymic nude mice.

RESULTS

Construction and Characterization of Monochromosomal Microcell Hybrid Clones. The monochromosomal hybrid HA(3)BB (24), which contains an intact, *neo*-marked human chromosome 3 in the A9 cell background, served as the donor line for microcell fusion into SN12C.19 (25, 27). Thirty of 87

The publication costs of this article were defrayed in part by page charge payment. This article must therefore be hereby marked "*advertisement*" in accordance with 18 U.S.C. §1734 solely to indicate this fact.

Abbreviations: LOH, loss of heterozygosity; RCC, renal cell carcinoma; FISH, fluorescence *in situ* hybridization.

§To whom reprint requests should be addressed.

Table 1. Characterization of microcell hybrid clones

Cell line injected into nude mice	Chromosome 3 retention in RCC background
SN12C.19	—
SN19(3)D	Intact 3
SN19(3)CCC	Intact 3
SN19(3)VV	Intact 3
SN19(3)A	Intact 3 (pericentric inversion)
SN19(3)WW	Intact 3 (2 copies)
SN19(3)N	Del(3p13) t(3;11)
SN19(3)EEE	3p12-q24
SN19(3i)YY	3p14-q11
SN19(3i)FF	3p14-q11
SN19(3i)LL	3p14-q11

microcell hybrid clones were screened by FISH using chromosome 3-specific DNA as a probe to detect the presence of the introduced human chromosome. Seven hybrids were characterized further by FISH using pSV2neo as a probe and by G-banding to determine if the introduced chromosome had suffered any rearrangements upon entry into the recipient cell background. Karyotypic examination of microcell hybrid clones revealed that 3 of 7 SN19(3) series hybrids contained an intact, unrearranged copy of the introduced chromosome 3 (Table 1). One hybrid [SN19(3)EEE] contained large terminal deletions of 3p and 3q and retained only 3p12-q24 (Table 1).

Introduction of Human Chromosome 3 Results in RCC Tumor Suppression. Five of these SN19(3) series microcell hybrids and parental RCC cells were injected (at 5×10^6 cells) subcutaneously into each of three athymic nude mice. After 8 weeks, RCC cells formed tumors of an average wet weight of 0.9–1.0 g. In three separate experiments, the introduction of chromosome 3 into SN12C.19 resulted in dramatic tumor suppression in all hybrids containing an intact chromosome 3 (Fig. 1*a*). The only SN19(3) microcell hybrid that formed large tumors was SN19(3)EEE, which contained only 3p12-q24. These data provide functional evidence for a tumor suppressor locus on human chromosome 3 that must reside either distal to 3q24 or, more probably, distal to p12 on the short arm of human chromosome 3.

Identification and Characterization of Fragment-Containing Clones. To define the exact region containing the tumor suppressor gene on 3p, we analyzed a collection of A9 microcell clones generated previously (24) that had been screened with 52 chromosome 3-specific PCR primers and shown to contain 3p fragments (A.M.K. and S. L. Naylor, unpublished results). PCR (29) and Southern analyses (7, 30) were performed on these fragment-containing hybrids using primers to β-galactosidase (*GLB1*), which maps to 3p21-p22 (29), or D3S3 as a probe for 3p12-p14 (31). Any clones that were positive for D3S3 and negative for *GLB1* were further analyzed by FISH using total human DNA as a probe. One clone [HA(3)II] was identified that contained one to five 3p fragments per metaphase and of the size range of 15–20 megabases. Subcloning HA(3)II produced the hybrid clone HA(3)IIaa (Fig. 2*a*), which contains a single, centric fragment of 3p encompassing 3p14-q11. FISH using pSV2neo (Fig. 2*b*) and D3S3 as probes (Fig. 2*c*) confirmed the origin of the fragment and the location of the integration site near the centromere on 3q. As further evidence that the 3p fragment was not a discontinuous and rearranged fragment of chromosome 3, chromosome painting of normal human metaphase spreads was performed by inter-*Alu* PCR amplification of human DNA from HA(3)IIaa. The results indicated that the 3p fragment mapped back exclusively to the region 3p14-q11 (Fig. 2*d*). HA(3)IIaa was also screened by PCR using primers within the Von Hippel–Lindau disease (*VHL*) gene, which maps to 3p25 (32). Results indicated that the fragment in HA(3)IIaa did not contain the *VHL* gene (data not shown).

The 3p fragment was transferred into SN12C.19 via microcell fusion. FISH using a chromosome 3-specific centromeric repeat probe (D3Z1) (33), pSV2neo, and D3S3 was carried out to confirm retention of the 3p fragment in the human RCC cell background (data not shown). *In vitro* growth of hybrid clones was monitored in 10% serum, and population doubling times were determined after 8–12 days of logarithmic growth. Results indicated very similar doubling times for parental RCC cells (22 hr) and 4 SN(19)3 hybrids

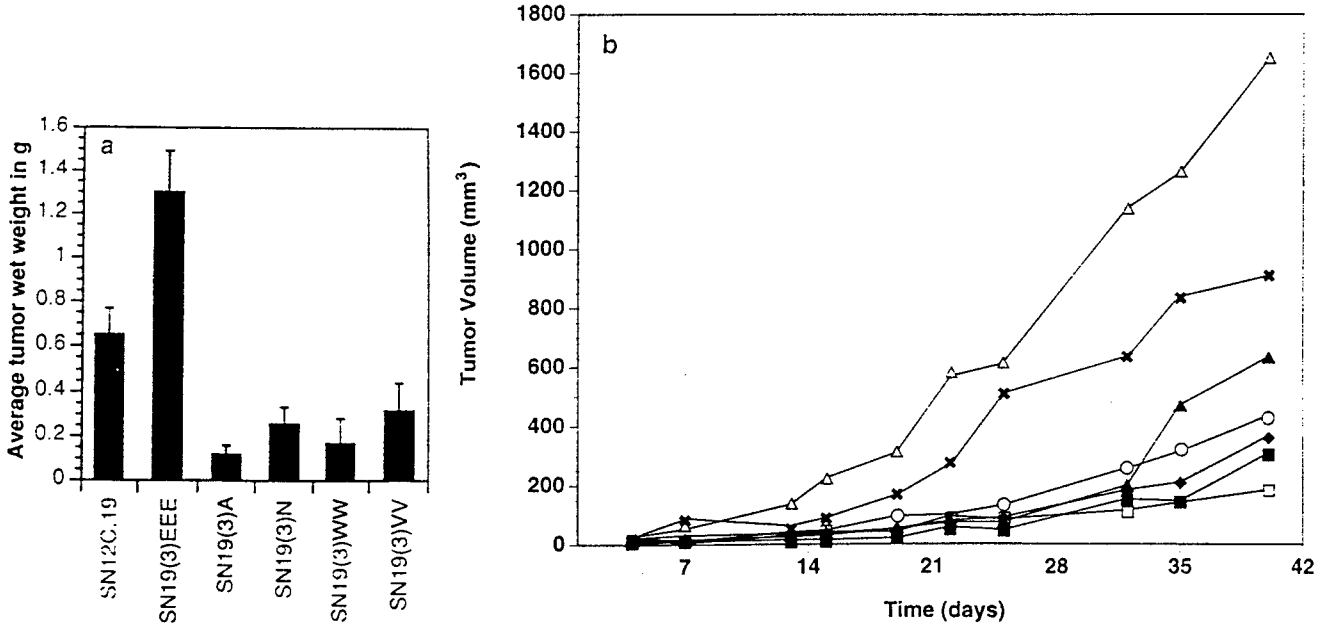

FIG. 1. Tumorigenicity assays. (*a*) Wet weights of tumors formed after injection of microcell hybrids and parental SN12C.19 cells into nude mice. (*b*) Average tumor volumes from staging tumorigenicity assay. Lines tested include SN19(3i)LL (▲), SN19(3i)FF (○), SN19(3i)YY (◆), SN19(3)WW (■), SN19(3)A (□), SN12C.19 (×), and SN19(3)EEE (△). Tumor volumes were calculated by the following formula: $[(W)^2 \times (L)]/2$ (28).

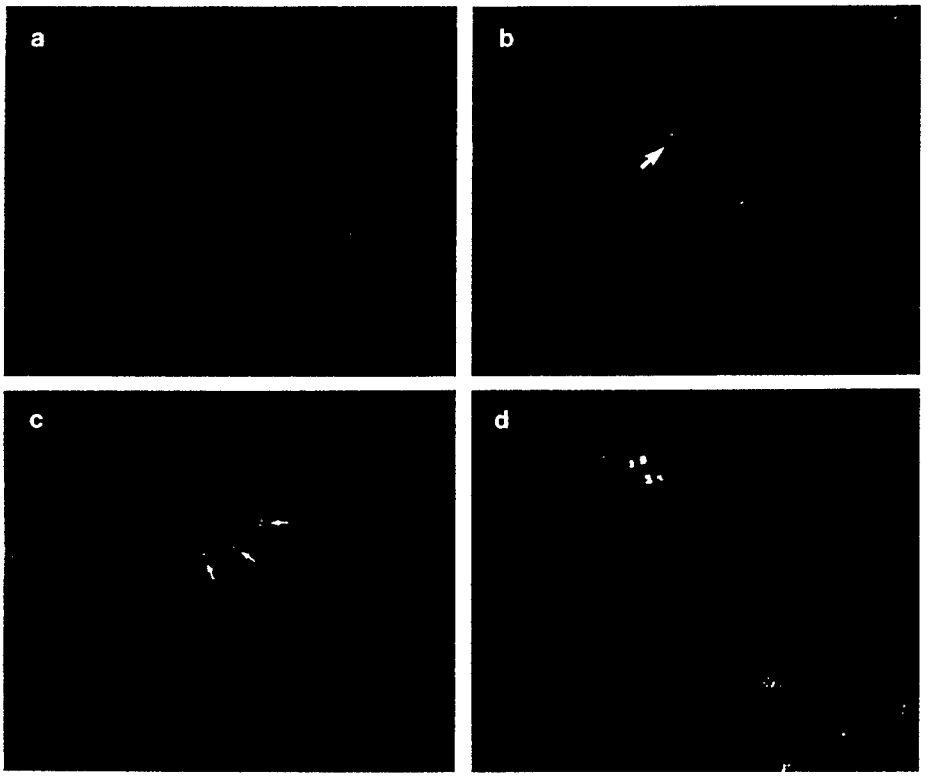

FIG. 2. FISH. (*a*) Total human DNA was used as a probe to detect the presence of the small 15- to 20-megabase fragment 3p14-q11 in HA(3)IIaa. (*b*) pSV2neo was used to detect *neo* in HA(3)IIaa. (*c*) D3S3 (3p14) was used to characterize fragments in HA(3)II prior to subcloning. Note three copies of the 3p fragment in the A9 cell. (*d*) Chromosome painting of a normal human metaphase spread using chromosome 3-specific DNA from HA(3)IIaa. The 3p fragment maps back exclusively to 3p14-q11.

containing chromosome 3 (average of 24 hr), as well as SN19(3)EEE, the control hybrid containing 3p12-q24 (26 hr), and SN19(3i)YY, the hybrid containing the introduced 3p14-q11 (27 hr).

Tumor Suppression Concomitant with Rapid Cell Death of RCC Mediated by the Introduction of Human Chromosome 3 or 3p Centric Fragment. For *in vivo* analyses, five SN19(3i) microcell hybrids were tested for tumorigenicity in athymic nude mice. In three different experiments, after 6 weeks *in vivo*, three 3p fragment-containing hybrids [SN19(3i)LL, SN19(3i)FF, and SN19(3i)YY] showed dramatic tumor suppression (Fig. 1*b*). Two of the clones failed to exhibit significant suppression (data not shown). Potentially, these clones could represent hybrids that segregated or rearranged the 3p fragment *in vivo*. To test this theory, the small tumors (formed following injection of chromosome 3 and fragment-containing clones into nude mice) were excised six weeks postinjection and histopathologically analyzed for mitotic index, necrosis, degree of invasiveness, vascularity, and cellular pleomorphism (34). In all cases, the small tumors derived from suppressed hybrid clones were found to be as highly malignant as the parental line SN12C.19 (data not shown). We reasoned that the hybrid cells must have been initially suppressed for growth *in vivo*, and at some time point, loss or inactivation of the tumor suppressor locus within this region resulted in tumor outgrowth. FISH experiments indicated that hybrid clones retained the centric fragment at high frequency (average of 93%) at the time of injection. At the end of the experiment, explants derived from small tumors in suppressed fragment-containing clones showed loss of the fragment with an average retention of 59%.

Histopathology was also performed on tumor tissue from a staging tumorigenicity assay. We wanted to determine if, at a given time point, segregation or inactivation of the suppressor locus from the injected cell population could be correlated with changes in tumor morphology and rapid expansion of the tumor cell population. Tumor volumes were determined biweekly, and tumors were excised weekly postinjection for histopathological analysis. Three fragment-containing clones and three hybrids containing an intact human chromosome 3 were injected subcutaneously (at 5×10^6 cells) into each of six athymic nude mice. SN19(3)EEE, which contains 3p12-q24, was injected along with the parental SN12C.19 cells.

At the end of the first week postinjection, the parental cell line and SN19(3)EEE displayed *in vivo* parameters of a mixed clear cell/granular cell nonpapillary carcinoma with high mitotic index, a high degree of invasiveness, and vascularization typical of RCC (Fig. 3, panel *1a*). However, the small tumors derived from the chromosome 3 and fragment-containing microcell hybrid clones contained a central core of dead or necrotic cells (Fig. 3, panels *1b* and *1c*). This high degree of necrosis is very unusual in such small tumors of 4–20 mm^3. Necrosis is usually associated with rapidly growing tumors of much larger size. Four of the six clones examined showed 60–70% necrosis. Two clones showed defined areas of necrosis but <60% cell death at the end of the first week [SN19(3)WW and SN19(3i)FF], and these were the most suppressed clones at the end of the first week *in vivo*. Slower *in vivo* growth might reflect such differences in the degree of necrosis at the end of the first week. Clearly, SN19(3i)FF was more necrotic at the end of the second week *in vivo*.

Rapid cell death *in vivo* was common to all suppressed fragment-containing clones and clones containing an intact chromosome 3. It was not apparent in parental cells or in control cells containing 3p12-q24. With time, tumors from the suppressed clones became vascularized (Fig. 3, panels *2b* and *2c*), similar to tumors from the parent and control clones (Fig.

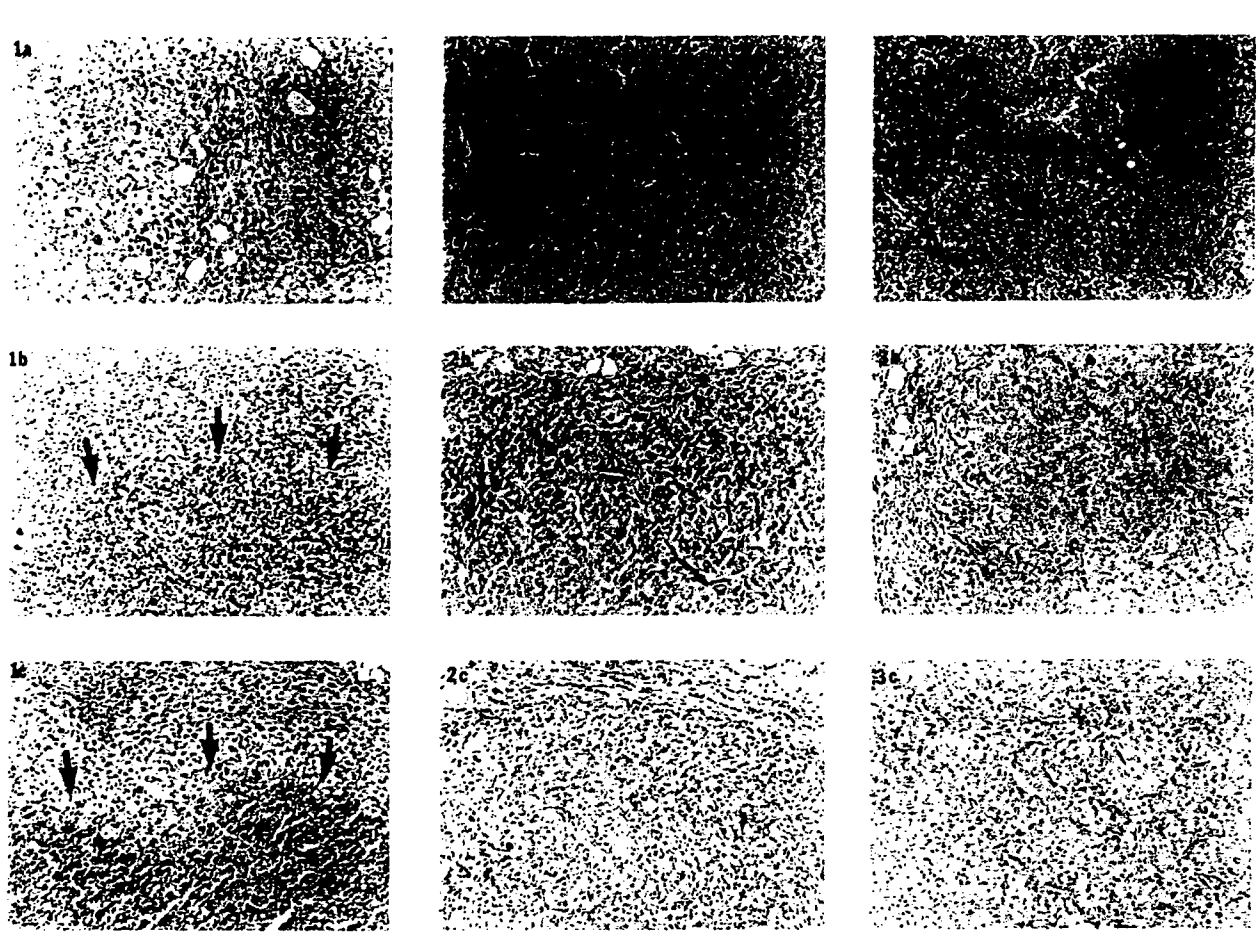

FIG. 3. Histopathology performed on tumors from the staging tumorigenicity assay. Clones tested include SN19(3)EEE, which contains 3p12-q24, at the end of week 1 (panel *1a*), week 2 (panel *2a*), and week 3 (panel *3a*) *in vivo*; SN19(3)A, the clone containing an intact chromosome 3, at the end of week 1 (panel *1b*), week 2 (panel *2b*), and week 3 (panel *3b*); SN19(3)LL, the hybrid clone containing only the region 3p14-q11, at week 1 (panel *1c*), week 2 (panel *2c*), and week 3 (panel *3c*). Note the high degree of cell death and/or necrosis evident at the end of week 1 in the SN19(3)A and SN19(3)LL (denoted by arrows). Cell death is not at all evident in the control clone containing 3p12-q24.

3, panel *2b*), with no significant necrosis. At the end of the experiment, tumor cells from the suppressed clones were highly aggressive by histopathological criteria (Fig. 3, panels *3b* and *3c*) and resembled tumors from the parent cell line and control clone (Fig. 3, panel *1a*). The parental RCC cell line and SN19(3)EEE were highly necrotic at the end of the experiment, as might be expected for large, rapidly dividing tumor cell populations.

DISCUSSION

Thus, introduction of the centric fragment encompassing 3p14-q11 into SN12C.19 resulted in dramatic tumor suppression resulting from rapid cell death following injection of cells into nude mice. Hybrids containing 3p12-q24 not only formed tumors equivalent to or larger than those formed by parental RCC cells but also morphologically resembled the parent line with no evidence of early cell death. These data define a genetic locus in the most proximal region of high frequency LOH in sporadic RCC as well as the region containing the translocation breakpoint in familial RCC (Fig. 4). We have designated the locus nonpapillary renal carcinoma 1 (*NRC-1*). Furthermore, by a concerted genetic and pathological analysis, we have shown a function for *NRC-1* prior to isolation of the gene. The function of *NRC-1* correlates directly with the induction of rapid cell death *in vivo*. The cell death observed does not seem to be a random rejection event as described by Stanbridge and Ceredig (35) on day 1 following injection of both tumorigenic and nontumorigenic HeLa × fibroblast hybrids into nude mice. Both tumorigenic and nontumorigenic hybrids exhibited cell death on day 1 followed by differentiation of the nontumorigenic cells by day 4. In sharp contrast to these results, in our studies all suppressed fragment-containing clones, chromosome 3-containing clones, the control tumorigenic hybrid SN19(3)EEE, and parental cells had very similar doubling times *in vitro*, yet *in vivo*, rapid cell death was only observed in the hybrids containing the intact chromosome 3 and the region 3p14-q11. Neither the parental RCC cells nor the control line SN19(3)EEE showed a central core of dying cells with no evidence of differentiation in any of the clones. In the suppressed clones, cells surrounding the core were viable most probably because of access to growth factors in the periphery of the tumor, which could explain how cells containing the tumor suppressor locus could escape growth control *in vivo*. Clearly, loss of the centric fragment from the tumor population at the end of the experiment was evident in some but not all of the cells in the tumor explants. Thus, *NRC-1* could function to mediate growth factor dependence in the RCC cells *in vivo*. *In vitro* experiments have confirmed a striking effect of the transferred fragment on the ability of RCC cells to proliferate in reduced serum concentrations (Y.S. and A.M.K., unpublished results).

To our knowledge, these experiments are the first report of the direct transfer of a centric fragment in a functional tumor suppression assay. Transfer of this small region of 3p was made possible by simple screening of A9 hybrid clones after microcell fusion. These results indicate the utility of this

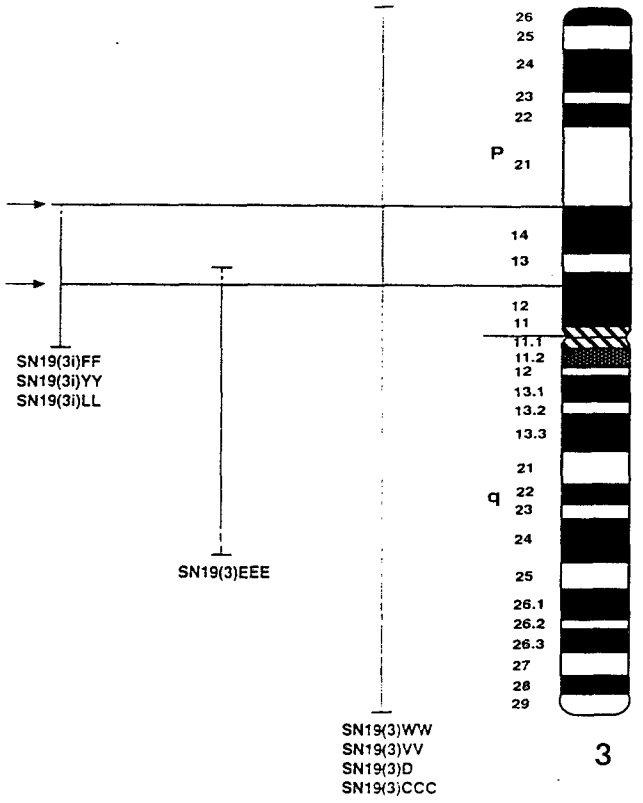

FIG. 4. Regional assignment of *NRC-1*. Depicted are suppressed hybrids containing an intact chromosome 3 as well as clones carrying 3p14-q11 in an RCC background; one hybrid is illustrated that was not suppressed *in vivo* and contained 3p12-q24. The region of nonoverlap containing *NRC-1* is denoted by arrows. Vertical dashed lines correspond to the breakpoint regions of fragment-containing clones.

system for the isolation of fragments surrounding the *neo* integration site in a tagged human chromosome. Furthermore, if the *neo* integration site is located close to the centromere, unrearranged centric fragments can be obtained. A potential caveat for these types of functional studies is the definitive proof of complementation. For our studies, the RCC recipient cell line contains a t(3;8) with a breakpoint in 3p14; however, without access to normal tissue from this patient, it is difficult to determine in this established cell line informative homozygous loss or inactivation at a particular locus. Nevertheless, this type of functional assay system in concert with molecular genetic and cytogenetic analyses of hybrid clones is a powerful approach for the definition of tumor suppressor genes.

Results from this study indicate that the proximal region of 3p is intimately involved in sporadic RCC. The interaction of this locus with more distal loci, such as the *VHL* gene, in the development of RCC remains to be determined. Recently, the *VHL* gene was isolated, and mutations were detected in VHL patients and in sporadic RCC cell lines (32). The finding that *NRC-1* functions to induce cell death *in vivo* provides strong evidence that this locus is involved in the genesis of nonpapillary RCC and potentially could play an important role in Von Hippel–Lindau disease-associated RCC as well.

We thank M. Lovell for excellent cytogenetic analyses, M. J. Siciliano and G. Lozano for critical reading of the manuscript, and G. Clinkscales for excellent assistance in the preparation of this manuscript. This work was supported by Grants GM37999, HG00042, and CA16672 from the National Institutes of Health, the Mather Charitable Foundation, and a National Institutes of Health Minority Access to Research Careers Predoctoral Fellowship to Y.S.

1. Cohen, A. J., Leu, F. P., Berg, S., Marchetto, D. J., Tsai, S. & Jacobs, S. C. (1979) *N. Engl. J. Med.* **301**, 592–595.
2. Kovacs, G., Brusa, P. & De-Riese, W. (1989) *Int. J. Cancer* **43**, 422–427.
3. Pathak, S., Strong, L. C., Ferrell, R. E. & Trindade, A. (1982) *Science* **217**, 939–941.
4. Zbar, B., Brauch, H., Talmadge, C. & Linehan, M. (1987) *Nature (London)* **327**, 721–724.
5. Kovacs, G., Erlandsson, R., Boldog, F., Ingvarsson, S., Müller-Brechlin, R., Klein, G. & Sümegi, J. (1988) *Proc. Natl. Acad. Sci. USA* **85**, 1571–1575.
6. Carroll, P. R., Murty, V. V. S., Reuter, V., Jhanwar, S., Fair, W. R., Whitmore, W. F. & Chaganti, R. S. K. (1987) *Cancer Genet. Cytogenet.* **26**, 253–259.
7. Bergerheim, U., Nordenskjold, M. & Collins, V. P. (1989) *Cancer Res.* **49**, 1390–1396.
8. Ogawa, O., Kakehi, Y., Ogawa, K., Koshiba, M., Sugiyama, T. & Yoshida, O. (1991) *Cancer Res.* **51**, 949–953.
9. Yamakawa, K., Morita, R., Takahashi, E.-I., Hori, T.-A., Ishikawa, J. & Nakamura, Y. (1991) *Cancer Res.* **51**, 4707–4711.
10. Anglard, P., Tory, K., Brauch, H., Weiss, G. H., Latif, F., Merino, M. J., Lerman, M. I., Zbar, B. & Linehan, W. M. (1991) *Cancer Res.* **51**, 1071–1077.
11. Yamakawa, K., Takahashi, E.-I., Murata, M., Okui, K., Yokoyama, S. & Nakamura, Y. (1992) *Genomics* **14**, 412–416.
12. Maher, E. R., Bentley, E., Yates, J. R. W., Latif, F., Lerman, M., Zbar, B., Affara, A. & Ferguson-Smith, M. A. (1991) *Genomics* **10**, 957–960.
13. Seizinger, B. R., Rouleau, G. A., Ozelius, L. J., Lane, A. H., Farmer, G. E., Lamiell, J. M., Haines, J., Yuen, J. W. M., Collins, D., Majoor-Krakauer, D., Bonner, T., Matthew, C., Rubenstein, A., Halperin, J., McConkie-Rosell, A., Green, J. S., Trofatter, J. A., Ponder, B. A., Eierman, L., Bowmer, M. I., Schimke, R., Oostra, B., Aronin, N., Smith, D. I., Drabkin, H., Waziri, M. H., Hobbs, W. J., Martuza, R. L., Conneally, P. M., Hsia, Y. E. & Gusella, J. F. (1988) *Nature (London)* **332**, 268–269.
14. Tory, K., Brauch, H., Linehan, M., Barba, D., Oldfield, E., Filling-Katz, M., Seizinger, B., Yakamura, Y., White, R., Marshall, F. F., Lerman, M. I. & Zbar, B. (1989) *J. Natl. Cancer Inst.* **81**, 1097–1101.
15. Goodman, M. D., Goodman, B., Lubin, M. B., Braunstein, G., Rotter, J. I. & Schreck, R. R. (1990) *Cancer* **65**, 1150–1154.
16. Kovacs, G., Emanuel, A., Neumann, H. P. H. & Kung, H. (1991) *Genes Chromosomes Cancer* **3**, 256–262.
17. Saxon, P. J., Srivatsan, E. S. & Stanbridge, E. J. (1986) *EMBO J.* **5**, 3461–3466.
18. Weissman, B. E., Saxon, P. J., Pasquale, S. R., Jones, G. R., Geiser, A. G. & Stanbridge, E. J. (1987) *Science* **236**, 175–180.
19. Trent, J. M., Stanbridge, E. J., McBride, H. L., Meese, E. U., Casey, G., Araujo, D. E., Witkowski, C. M. & Nagle, R. B. (1990) *Science* **247**, 568–571.
20. Tanaka, K., Oshimura, M., Kikuchi, R., Seki, M., Hayashi, T. & Miyaki, M. (1991) *Nature (London)* **349**, 340–342.
21. Shimizu, M., Yokota, J., Mori, N., Shuin, T., Shinoda, M., Terada, M. & Oshimura, M. (1990) *Oncogene* **5**, 185–194.
22. Dowdy, S. F., Fasching, C. L., Araujo, D., Lai, K.-M., Livanos, E., Weissman, B. E. & Stanbridge, E. J. (1991) *Science* **254**, 293–295.
23. Naito, von Eschenback, C., Giavazzi, R. & Fidler, I. J. (1986) *Cancer Res.* **46**, 4109–4115.
24. Killary, A. M., Wolf, M. E., Giambernardi, T. A. & Naylor, S. L. (1992) *Proc. Natl. Acad. Sci. USA* **89**, 10877–10881.
25. McNeill, C. A. & Brown, R. L. (1980) *Proc. Natl. Acad. Sci. USA* **77**, 5394–5398.
26. Liu, P., Siciliano, J., Seong, D., Craig, J., Zhao, U., deJong, P. J. & Siciliano, M. J. (1993) *Cancer Genet. Cytogenet.* **65**, 93–99.
27. Fournier, R. E. K. (1981) *Proc. Natl. Acad. Sci. USA* **78**, 6349–6353.
28. Osborne, C. K., Coronado, E. B. & Robinson, J. P. (1987) *Eur. J. Cancer Clin. Oncol.* **23**, 1189–1196.
29. Theune, S., Fung, J., Todd, S., Sakaguchi, A. Y. & Naylor, S. L. (1991) *Genomics* **9**, 511–516.
30. Southern, E. M. (1975) *J. Mol. Biol.* **98**, 503–517.
31. Gerber, M. J., Miller, W. E., Drabkin, H. A. & Scoggin, C. H. (1986) *Cytogenet. Cell Genet.* **42**, 72–74.
32. Latif, F., Tory, K., Gnarra, J., Yao, M., Duh, F.-M., Orcutt, M. L., Stackhouse, T., Kuzmin, I., Modi, W., Geil, L., Schmidt, L., Zhou, F., Li, H., Wei, M. H., Chen, F., Glenn, G., Choyke, P., Walther, M. M., Weng, Y., Duan, D.-S. R., Dean, M., Glavac, D., Richards, F. M., Crossey, P. A., Ferguson-Smith, M. A., LePaslier, D., Chumakov, I., Cohen, D., Chinault, A. C., Maher, E. R., Linehan, W. M., Zbar, B. & Lerman, M. I. (1993) *Science* **260**, 1317–1320.
33. Waye, J. S. & Willard, H. F. (1989) *Chromosoma* **97**, 475–480.
34. Mostofi, F. K., ed. (1981) in *International Classification of Tumours* (World Health Org., Geneva), No. 25, pp. 1–23.
35. Stanbridge, E. J. & Ceredig, R. (1981) *Cancer Res.* **41**, 573–580.

[CANCER RESEARCH 58, 3533–3537, August 15, 1998]

Physical and Functional Mapping of a Tumor Suppressor Locus for Renal Cell Carcinoma within Chromosome 3p12[1]

Steven Trent Lott,[2] Mercedes Lovell, Susan L. Naylor, and Ann McNeill Killary

Division of Laboratory Medicine, Section of Experimental Laboratory Medicine, The University of Texas M. D. Anderson Cancer Center, Houston, Texas 77030-4095 [S. T. L., M. L., A. M. K.], and Department of Cellular and Structural Biology, The University of Texas Health Science Center at San Antonio, San Antonio, Texas 78284 [S. L. N.]

Abstract

Using a functional genetic approach, we previously identified a novel genetic locus, *NRC-1* (*N*onpapillary *R*enal *C*ell *C*arcinoma *1*), that mediated tumor suppression and rapid cell death of renal cell carcinoma (RCC) cells *in vivo*. For these experiments, a defined subchromosomal fragment of human chromosome 3p was transferred into a sporadic RCC cell line via microcell fusion, and microcell hybrid clones were tested for tumorigenicity *in vivo*. The results indicated functional evidence for a novel tumor suppressor locus within the 3p14–p12 interval known to contain the most common fragile site of the human genome (*FRA3B*), the *FHIT* gene, and the breakpoint region associated with the familial form of RCC. We now report the physical mapping of the *NRC-1* critical region by detailed microsatellite analyses of novel microcell hybrid clones containing transferred fragments of chromosome 3p in the RCC cell background that were phenotypically suppressed or unsuppressed for tumorigenicity *in vivo*. The results limit the region containing the tumor suppressor locus within chromosome 3p12. The *FHIT* gene, *FRA3B*, and the familial RCC breakpoint region were excluded from the *NRC-1* critical region. Furthermore, the *NRC-1* locus falls within a well-characterized homozygous deletion region of 5–7 Mb associated with a small cell lung carcinoma cell line, U2020, suggesting that a more general tumor suppressor gene may reside in this region.

Introduction

Sporadic RCC[3] is characterized by high-frequency LOH and cytogenetic aberrations involving the short arm of human chromosome 3 (1–5). Using these strategies, as many as three to four separate regions of 3p have been identified that may contain putative tumor suppressor genes involved in the etiology of RCC. The telomeric region of 3p (3p25) contains the von Hippel Lindau (*VHL*) gene (6). Germ-line mutation of *VHL* predisposes to the development of a number of different tumor types including spinal hemangioblastomas, retinal angiomas, pheochromocytomas, and renal and pancreatic cysts (6). *VHL* is mutated in 57% of sporadic clear cell renal carcinoma, and methylation of the gene may account for the vast majority of RCC without *VHL* mutation (7, 8). Transfection of the *VHL* gene into RCC cells *in vitro* results in the suppression of tumorigenic growth after the injection of transfectants into athymic nude mice, suggesting a significant role for the *VHL* gene as a tumor suppressor gene for sporadic RCC (9). LOH studies, cytogenetic analyses of RCC tumors, and our own functional studies have implicated other regions of 3p as candidate regions to contain important tumor suppressor genes for RCC as well.

Studies focused on virtually all types of lung cancer as well as ovarian, uterine cervical, and testicular carcinoma imply that a region more centromeric than 3p25 may contain a putative tumor suppressor gene(s). High-frequency LOH has been demonstrated for SCLC (100%), RCC (95–100%), and ovarian carcinoma (57%) in the 3p21–p24 region (5, 10, 11). We have previously functionally defined a 2-Mb fragment encompassing 3p21–p22 that mediated tumor suppression in a mouse fibrosarcoma model system (12). Homozygous deletions have also been documented in SCLC lines that map into the 2-Mb region identified by functional approaches (13, 14).

We have concentrated on the most centromeric region of 3p in which high-frequency LOH has been documented in sporadic RCC (1–3). In the rare familial form of RCC, specific translocations in this region with breakpoints within 3p14 have been observed (15). The breakpoint region is near the *FRA3B* region containing the most common fragile site in the human genome (16). In addition, the *FHIT* gene has been isolated from the breakpoint region in familial RCC (17). Aberrant transcripts and homozygous deletions of *FHIT* in a number of cancers including lung, breast, and gastrointestinal tumors have indicated its possible role as a tumor suppressor gene (17). The extent of *FHIT* involvement in RCC has not been clearly determined.

Functional evidence for a tumor suppressor gene in the most centromeric region of 3p has been demonstrated by previous experiments in which an intact human chromosome 3 and subsequently a centric fragment of 3p encompassing 3p14–3q11 (by cytogenetic analysis) were transferred into a sporadic nonpapillary RCC cell line, SN12C.19 (18). All hybrids containing the introduced, intact copy of chromosome 3 (four of four) were suppressed for tumor formation after the injection of hybrids in nude mice. A fifth hybrid clone [SN19(3)EEE] contained terminal deletions of both the short and long arms of the introduced chromosome 3 and retained only the region 3p12–q24 in the RCC background. This hybrid formed larger tumors than did the parental control, SN12C.19, which suggested that the 3p tumor suppressor locus potentially mapped telomeric to 3p12. In addition, microcell hybrid clones were generated by the transfer of a centric 3p fragment in the SN12C.19 background. In all experiments, the 3p fragment mediated a dramatic tumor suppression and the induction of rapid cell death after the s.c. injection of hybrid cells into nude mice (18). These data functionally defined tumor suppressor locus *NRC-1* within 3p12-p14 and distinct from the *VHL* gene at 3p25. We now report the microsatellite polymorphism analysis of microcell hybrid clones that were phenotypically suppressed or unsuppressed for tumorigenicity *in vivo*. Results narrow the region on chromosome 3p containing *NRC-1* to a 5–7-Mb region within 3p12 that has also been shown to be homozygously deleted in the SCLC

Received 2/4/98; accepted 6/24/98.

The costs of publication of this article were defrayed in part by the payment of page charges. This article must therefore be hereby marked *advertisement* in accordance with 18 U.S.C. Section 1734 solely to indicate this fact.

[1] Supported by National Cancer Institute Grant R01 CA-62027 and the Marie I. Morgan Fund for Kidney Cancer Research (to A. M. K.). S. T. L. was supported by National Cancer Institute Training Grant 5 T32 CA-09299-18.

[2] To whom requests for reprints should be addressed, at Division of Laboratory Medicine, Box 54, The University of Texas M. D. Anderson Cancer Center, 1515 Holcombe Boulevard, Houston, TX 77030-4095. Phone: (713) 792-7835; Fax: (713) 745-0251; E-mail: sa95047@odin.mdacc.tmc.edu.

[3] The abbreviations used are: RCC, renal cell carcinoma; LOH, loss of heterozygosity; SCLC, small cell lung carcinoma; RT, reverse transcription; FISH, fluorescence *in situ* hybridization.

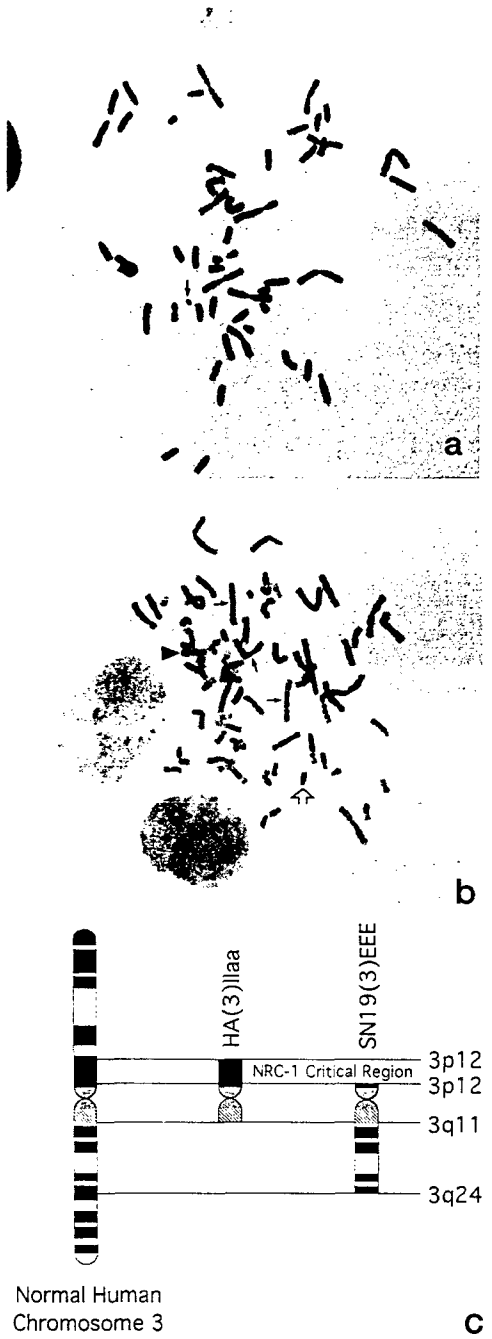

Fig. 1. *a*. G banded metaphase spread of the mouse/human-interspecific hybrid HA(3)IIaa. This hybrid contains a single centric fragment of human chromosome 3 (indicated by the *arrow*) in a mouse A9 fibrosarcoma background. Transfer of this fragment by microcell-mediated chromosome transfer into the sporadic RCC cell line SN12C.19 resulted in tumor suppression of the resulting hybrids *in vivo*. *b*. G banded metaphase spread of the hybrid SN19(3)EEE. This hybrid was constructed via microcell-mediated chromosome transfer of a normal chromosome 3 into SN12C.19. During this process, a terminal deletion fragment of the transferred normal human chromosome 3 (indicated by the *open arrow*) was generated. The three copies of chromosome 3 already present in the SN12C.19 cell line are indicated by *solid arrows*. The derivative chromosome 8 resulting from an unbalanced t(3;8) is indicated by a *solid arrowhead*. This hybrid was not suppressed for tumor formation *in vivo*. *c*. ideogram illustrating the *NRC-1* region as defined by the centric fragment of chromosome 3 in hybrid HA(3)IIaa, which was suppressed for tumorigenicity *in vivo*, and the terminal deletion of the introduced chromosome 3 present in the hybrid SN19(3)EEE, which was not suppressed for tumorigenicity *in vivo*.

cell line U2020. This region does not include the *FRA3B* fragile site, the *FHIT* gene, or the breakpoint region associated with familial RCC. These data provide the first functional evidence for a tumor suppressor locus within 3p12.

Materials and Methods

DNA and RNA Isolation from Cell Lines and Hybrids. DNA from cultured cells was isolated using a high salt technique. Briefly, cells were lysed in lysis buffer I [40 mM Tris-HCl (pH 7.5), 1.3 M sucrose, 20 mM $MgCl_2$, and 1% Triton X-100]. After centrifugation, the pelleted nuclei were resuspended in 4.5 ml of lysis buffer II (75 mM NaCl and 24 mM EDTA) and 0.5 ml of sarkosyl-proteinase K solution (2 mg of proteinase K and 1 ml of 10% sarkosyl). Samples were incubated overnight at 37°C with constant rocking. DNA was precipitated by the addition of 1.5 ml of NaCl-saturated H_2O and 6.5 ml of isopropanol. DNA was resuspended in TE [10 mM Tris (pH 8) and 1 mM EDTA] and assessed by spectrophotometry for concentration and purity. RNA was isolated using Trizol (Life Technologies, Inc., Grand Island, NY) according to the manufacturer's suggested protocol.

Cytogenetic Analysis. High-resolution G banding of metaphase spreads was performed as described previously (19).

Microsatellite PCR. Microsatellite PCR was performed using primers synthesized by Research Genetics (Huntsville, AL). Before amplification, the forward primer was end-labeled with ^{32}P by T4 polynucleotide kinase (Promega, Madison, WI). PCR amplification was performed in a 25-μl reaction volume containing 0.63 μM of forward and reverse primers, 100 ng of template DNA, 0.2 mM deoxynucleotide triphosphates, 1.5 mM $MgCl_2$, 0.63 units of AmpliTaq polymerase (Perkin-Elmer Corp., Foster City, CA), and HEPES buffer [10 mM HEPES and 50 mM KCl (pH 8.3)]. After the initial denaturation and the addition of Amplitaq, reaction products were subjected to 23 cycles of 94°C for 40 s, 55°C for 30 s, and 72°C for 30 s, with a final extension at 72°C for 2 min. Samples were then denatured and loaded on a 6% acrylamide gel with 33% formamide and 6 M urea. Electrophoresis was performed at 60 W for approximately 2–3 h. Subsequently, gels were vacuum-dried and exposed to autoradiography film overnight at room temperature.

RT-PCR. The RT reaction was performed using the Superscript Preamplification kit (Life Technologies, Inc.) and an oligodeoxythymidylic acid primer according to manufacturer's instructions. PCR amplifications for the *FHIT* gene were carried out in 500-μl microcentrifuge tubes containing 2 μl of RT reaction products, 1.5 mM $MgCl_2$, 0.2 μM of each primer [5′-TGAGGACATGTCGTTCAGATTTGG-3′ and 5′-CTGTGTCACTGAAAGTAGACC-3′, described by Ohta *et al.* (17)], 0.2 μM deoxynucleotide triphosphates, and 2.5 units of Amplitaq polymerase in a buffer [10 mM Tris-HCl (pH 8.3), 50 mM KCl, and 0.001% gelatin]. Thermal cycling consisted of an initial denaturation at 95°C for 5 min followed by 40 cycles of 94°C for 30 s, 55°C for 30 s, and 72°C for 45 s, with a final elongation at 72°C for 5 min. Samples were analyzed on 2% NuSieve agarose gels and visualized by ethidium bromide staining.

Results

Physical Mapping of the *NRC-1* Locus. To limit the region containing *NRC-1* in suppressed and unsuppressed clones, the following cell lines were analyzed by high-resolution cytogenetics as well as by microsatellite polymorphism analysis. The recipient cell line (SN12C.19) for these studies is a subcloned cell line of the original RCC cell line (SN12C) derived from a sporadic, mixed clear cell and granular cell, nonpapillary RCC. Cytogenetic analysis of this cell line indicated that it contains multiple copies of chromosome 3 as well as an unbalanced t(3;8) translocation,[4] resulting in a derivative chromosome composed of most of the p arm of chromosome 3 (3pter–3p14.3 or 3p14.2) fused to the centromere and q arm of chromosome 8 [der(8)(3pter→3p14.3 or 3p14.2::8cen→8qter)]. Also, nucleotide sequence analysis indicated that SN12C.19 is wild-type for VHL (data not shown).

One of the donor cell lines for microcell fusion into SN12C.19 was HA(3)IIaa, a microcell hybrid containing an introduced 3p centric fragment in the A9 mouse fibrosarcoma cell background. The original characterization of HA(3)IIaa by cytogenetic analysis was hampered because of the small size of the fragment. FISH studies using

[4] S. Pathak, personal communication.

Locus	Chromosomal Location	HA(3)BB	HA(3)IIaa	SN19(3)EEE
D3S1261	3p12-3p14.1	+	-	
D3S1210	3p12-3p14.1	+	-	
D3S1598	3p12	+	-	
D3S1284	3p12	+	-	
D3S2484	3p12	+	-	
D3S2563	3p12	+	-	
D3S2537	3p12	+	-	
D3S2540	3p12	+	-	
D3S1542	3p12	+	-	
D3S1757	3p12	+	-	
D3S1758	3p12	+	-	
D3S2375	3p12	+	-	
D3S2389	3p12	+	-	
GATA88E12	3p12	+	+	-
D3S2323	3p12	+	+	-
D3S2438	3p12	+	+	-
GATA67F08	3p12	+	+	-
D3S1577	3p12	+	+	NI
D3S1254	3p12	+	+	NI
D3S2555	3p12	+	+	NI
D3S2429	3p12	+	+	NI
D3S2560	3p12	+	+	NI
D3S2372	3p12	+	+	NI
D3S2451	3p11.2-3p12	+	+	NI
D3S1595	3p11.2-3p12	+	+	+

Fig. 2. Microsatellite marker analysis of the donor chromosome 3 [*HA(3)BB*], the donor centric fragment [*HA(3)IIaa*], and the unsuppressed SN12C.19 hybrid [*SN19(3)EEE*]. +, marker was present; −, marker was absent; *NI*, not informative.

HA(3)IIaa as a probe onto normal human metaphases indicated that the 3p fragment mapped exclusively to the centromeric regions of 3p and 3q. Estimation of the telomeric breakpoint of the centric fragment was based on positive FISH results using *D3S3* as a probe for 3p14 on the 3p centric fragment (18). However, the original map location for *D3S3* was incorrect, and *D3S3* has been physically mapped much more centromeric at 3p12 within the region shown to be homozygously deleted in the SCLC cell line U2020 (20, 21). This finding prompted a reexamination of the centric fragment using microsatellite markers to determine whether it encompassed the 3p14 fragile site or was smaller than originally estimated.

To examine the centric fragment in detail, high-resolution cytogenetic analysis was used. Detailed cytogenetic analysis of the 3p centric fragment, both in the donor line for microcell fusion [HA(3)IIaa, Fig. 1*a*] and after transfer into the SN12C.19 background, suggested a fragment of 15–20 Mb that was inclusive of the centromere.

To further characterize the centric fragment, detailed microsatellite polymorphism analysis was carried out on donor cell line HA(3)IIaa and hybrid cell line HA(3)BB containing an intact copy of chromosome 3 using 25 markers spanning the 3p11–13 region (Fig. 2). Of the 25 markers examined, 13 were missing in the HA(3)IIaa 3p fragment, limiting the telomeric boundary to within 3p12 between *GATA88E12* and *D3S2389*.

The *NRC-1* Critical Region Excludes *FRA3B* and *FHIT*. Because this data effectively eliminates the fragile site, the familial RCC translocation breakpoint, and the *FHIT* gene from the *NRC-1* critical region, we formally excluded this region from the 3p centric fragment. To definitively exclude the familial RCC translocation breakpoint region within microcell hybrid clones, microsatellite PCR was performed on HA(3)IIaa using primers for *D3S1480* and *D3S1481*, markers that flank the t(3;8) breakpoint with *D3S1480* centromeric and *D3S1481* telomeric to the break. Both markers were absent in the HA(3)IIaa centric fragment (Fig. 3*A*). *D3S1480* and *D3S1481* lie in the intron between exons 3 and 4 of the *FHIT* gene. The *FHIT* gene, which spans the translocation breakpoint region t(3;8) (3p14.2) associated with the familial form of RCC, is therefore not a part of the centric fragment (17). In addition, the expression of *FHIT* was determined by RT-PCR in SN12C.19 that contains a t(3;8) with a breakpoint within 3p14.2. Primers described by Ohta *et al.* (17) for the coding exons (exons 5–9) of the *FHIT* gene were used to amplify a 456-bp product in SN12C.19, which indicated that the gene was expressed with no aberrant transcripts detected (Fig. 3*B*). After PCR amplification, the band was excised and sequenced. Sequence analysis of exons 5–9 failed to detect a mutation in the coding region of the *FHIT* gene (data not shown).

***NRC-1* Maps within 3p12 and the U2020 Homozygous Deletion Region.** One of the dramatic results of previous studies was the finding that one microcell hybrid [SN19(3)EEE] suffered terminal deletions of the intact chromosome 3 after microcell fusion into SN12C.19 and as a result formed tumors in nude mice that were twice as large as those formed by parental RCC cells (18). Cytogenetic analysis of SN19(3)EEE indicated that the telomeric breakpoint resided within 3p12 (Fig. 1*b*). FISH analyses using *D3S3* as a probe failed to detect a signal on the introduced chromosome 3 fragment in SN19(3)EEE (data not shown). Twelve microsatellite markers spanning the 3p11–p13 region were then used to screen SN19(3)EEE (Fig. 2). The results indicate that the SN19(3)EEE break is in the 3p12

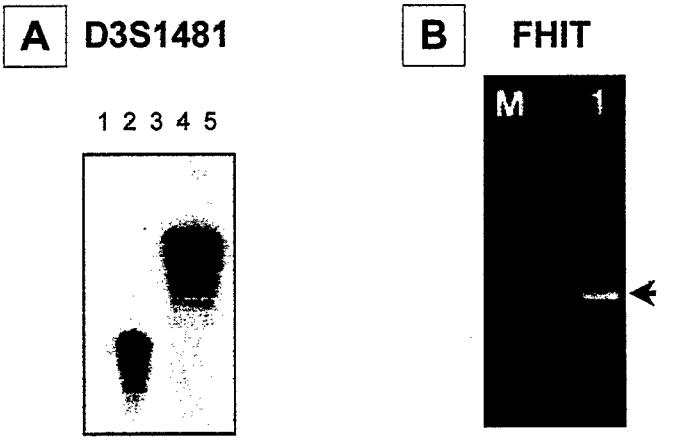

Fig. 3. *A*, the microsatellite locus *D3S1481*, which lies immediately telomeric to the t(3;8) translocation breakpoint in familial RCC, was amplified by PCR in the following cells: *Lane 1*, A9 (the mouse background line); *Lane 2*, HA(3)BB (monochromosomal hybrid with an intact human chromosome 3); *Lane 3*, HA(3)IIaa (monochromosomal hybrid with a 3p14–3q11 centric fragment of human chromosome 3); *Lane 4*, SN12C.19 (the RCC recipient cell line); and *Lane 5*, SN19(3)EEE (an SN12C.19 hybrid with an introduced 3p12–3q24 that was not suppressed for tumor formation). *B*, the *FHIT* gene was amplified by RT-PCR using primers that flank exons 5–9. Reaction products were electrophoresed on an agarose gel. A normal band of 456 bp was obtained. *M*, pBR322 *Hae*III digest molecular weight marker; *1*, SN12C.19 amplification products.

region. Because of the presence of several noninformative markers within the SN19(3)EEE 3p fragment, the exact 3p12 breakpoint could not be determined; however, the boundary lies distal to *D3S1595* (Fig. 2). Furthermore, these data map the *NRC-1* critical region within the 5–7-Mb homozygous deletion region described in the U2020 SCLC cell line (22). Thus, the region of nonoverlap between suppressed and unsuppressed clones lies within 3p12 and is a much smaller region of human chromosome 3p than originally estimated (Fig. 1*c*). Furthermore, these data provide the first functional evidence for a tumor suppressor locus within 3p12.

Discussion

At least three separate regions of chromosome 3p have been implicated by LOH studies and cytogenetics to contain possible tumor suppressor genes for RCC. The most distal region contains the *VHL* gene, which seems to play an integral role in the pathway to tumorigenesis in the kidney. The *FHIT* gene at 3p14.2, identified from the breakpoint region associated with familial RCC and containing the most common fragile site in the human genome, is also a candidate tumor suppressor gene. In this report, the first functional evidence to limit the region containing a tumor suppressor gene for RCC distinct from either *VHL* or *FHIT* is presented. Physical and functional mapping of the *NRC-1* locus places it within the most proximal region of high-frequency LOH within 3p and within a region of homozygous deletion in SCLC.

There are many questions to be answered with regard to the relationship between *VHL*, *NRC-1*, and other genes involved in kidney cancer that map to the short arm of chromosome 3. Clearly, mutation of the *VHL* gene is widespread in sporadic RCC, and the replacement of *VHL* in RCC cell lines suggests a function as a tumor suppressor. However, a major question arises with respect to the diversity of tumor types associated with *VHL* disease that do not appear in familial RCC. Is *VHL* the tumor suppressor gene for familial and sporadic RCC within 3p? If so, then what is the role for *NRC-1*?

Much information has accumulated recently that suggests a novel role for the *VHL* gene in the development of hyperplasia in a number of tissues, including the kidney. LOH of the *VHL* gene has been documented in the single cell lining of a benign renal cyst from a *VHL*-affected individual, suggesting that additional genetic alterations may occur that result in malignant conversion in *VHL* disease (23). In addition, binding of the *VHL/Elongin B, C* complex with *Hs-CUL-2*, a member of the *Cdc53* protein family, has been shown (24). The *Cdc53* gene in yeast has been implicated in the targeted degradation of cell cycle proteins and as a putative gatekeeper gene that carefully monitors the balance between controlled cell division and cell death (25). Null mutation of the *Ce-cul-1* homologue in *Caenorhabditis elegans* produced hyperplasia in all tissues (26). Support for the role of the *VHL* gene in the initiation of hyperplastic growth, rather than malignant conversion, is also indicated by the development of primarily benign tumors associated with *VHL*. Only a subset of tumor types, most commonly RCC and pancreatic islet cell tumors, progress to malignancy in VHL. Thus, for those tumor types that progress to malignancy, additional genetic alterations might be required for malignant conversion. We have recently shown that introduction of the 3p fragment containing *NRC-1* into histologically diverse RCC tumor lines with and without *VHL* mutation results in tumor suppression.[5] In addition, investigation of a *VHL* family with a preponderance of pancreatic islet cell tumors has shown high-frequency LOH for 3p loci distinct from *VHL* that correlated with conversion to malignancy and implicated a stepwise mutation mechanism for *VHL* tumorigenesis.[6]

Thus, *VHL* mutation could represent an initial hyperplastic event in *VHL* disease with subsequent 3p LOH or deletion events signaling malignant conversion in those tumor types that progress to malignancy. One candidate gene that could play a role in malignant RCC conversion in *VHL* and yet also be a component of an independent pathway to tumorigenesis in sporadic RCC is *NRC-1*. In this report, we present data that narrows the region on chromosome 3p containing *NRC-1* to within a 5–7-Mb region shown to be deleted in the SCLC cell line U2020. LOH of this region has also been observed in clear cell RCC by Lubinski *et al.* (27). In a study of 30 RCC tumors, a complex pattern of LOH in RCC tumors was observed, with LOH flanking the t(3;8) breakpoint, and with some tumors exhibiting additional losses within the U2020 region. Clearly, the location of *NRC-1* within a homozygous deletion region for SCLC might imply that this locus could function more broadly in a number of tumor types or that there are several very interesting genes in this 5–7-Mb interval. Definitive conclusions await the identification of *NRC-1* and the determination of its role in the genesis of kidney cancer.

References

1. Kovacs, G., Erlandsson, R., Boldog, F., Ingvarsson, S., Müller-Brechlin, R., Klein, G., and Sümegi, J. Consistent chromosome 3p deletion and loss of heterozygosity in renal cell carcinoma. Proc. Natl. Acad. Sci. USA, *85:* 1571–1575, 1988.
2. Kovacs, G., and Frisch, S. Clonal chromosome abnormalities in tumor cells from patients with sporadic renal cell carcinomas. Cancer Res., *49:* 651–659, 1989.
3. Ogawa, O., Kakehi, Y., Ogawa, K., Koshiba, M., Sugiyama, T., and Yoshida, O. Allelic loss at chromosome 3p characterizes clear cell phenotype of renal cell carcinoma. Cancer Res., *51:* 949–953, 1991.
4. Szucs, S., Müller-Brechlin, R., DeRiese, W., and Kovacs, G. Deletion of 3p: the only chromosome loss in a primary renal cell carcinoma. Cancer Genet. Cytogenet., *26:* 369–373, 1987.
5. Zbar, B., Brauch, H., Talmadge, C., and Linehan, M. Loss of alleles of loci on the short arm of chromosome 3 in renal cell carcinoma. Nature (Lond.), *327:* 721–724, 1987.
6. Latif, F., Tory, K., Gnarra, J., Yao, M., Duh, F-M., Orcutt, M. L., Stackhouse, T., Kuzmin, I., Modi, W., Geil, L., Schmidt, L., Zhou, F., Li, H., Wei, M. H., Chen, F., Glenn, G., Choyke, P., Walther, M. M., Weng, Y., Duan, D-S. R., Dean, M., Glavac, D., Richards, F. M., Crossey, P. A., Ferguson-Smith, M. A., LePaslier, D., Chumakov, I., Cohen, D., Chinault, A. C., Maher, E. R., Linehan, W. M., Zbar, B., and Lerman, M. I. Identification of the von Hippel-Lindau disease tumor suppressor gene. Science (Washington DC), *260:* 1317–1320, 1993.
7. Gnarra, J. R., Tory, K., Weng, Y., Schmidt, L., Wei, M. H., Li, H., Latif, F., Liu, S., Chen, F., Duh, F-M., Lubensky, I., Duan, D. R., Florence, C., Pozzatti, R., Walther, M. M., Bander, N. H., Grossman, H. B., Brauch, H., Pomer, S., Brooks, J. D., Isaacs, W. B., Lerman, M. I., Zbar, B., and Linehan, W. M. Mutations of the *VHL* tumour suppressor gene in renal carcinoma. Nat. Genet., *7:* 85–90, 1994.
8. Herman, J. G., Latif, F., Weng, Y., Lerman, M. I., Zbar, B., Liu, S., Samid, D., Duan, D. S., Gnarra, J. R., Linehan, W. M., and Baylin, S. B. Silencing of the *VHL* tumor-suppressor gene by DNA methylation in renal carcinoma. Proc. Natl. Acad. Sci. USA, *91:* 9700–9704, 1994.
9. Iliopoulos, O., Kibel, A., Gray, S., and Kaelin, W. G., Jr. Tumour suppression by the human von Hippel-Lindau gene product. Nat. Med., *1:* 822–826, 1995.
10. Naylor, S. L., Johnson, B. E., Minna, J. D., and Sakaguchi, A. Y. Loss of heterozygosity of chromosome 3p markers in small-cell lung cancer. Nature (Lond.), *329:* 451–454, 1987.
11. Ehlen, T., and Dubeau, L. Loss of heterozygosity of chromosomal segments 3p, 6q and 11p in human ovarian carcinomas. Oncogene, *5:* 219–223, 1990.
12. Killary, A. M., Wolf, M. E., Giambernardi, T. A., and Naylor, S. L. Definition of a tumor suppressor locus within human chromosome 3p21–p22. Proc. Natl. Acad. Sci. USA, *89:* 10877–10881, 1992.
13. Daly, M. C., Xiang, R-H., Buchhagen, D., Hensel, C. H., Garcia, D. K., Killary, A. M., Minna, J. D., and Naylor, S. L. A homozygous deletion on chromosome 3 in a small cell lung cancer cell line correlates with a region of tumor suppressor activity. Oncogene, *8:* 1721–1729, 1993.
14. Kok, K., van den Berg, A., Veldhuis, P. M., van der Veen, A. Y., Franke, M., Schoenmakers, E. F., Hulsbeek, M. M., van der Hout, A. H., de Leij, L., van de Ven, W., and Buys, C. H. C. M. A homozygous deletion in a small cell lung cancer cell line involving a 3p21 region with a marked instability in yeast artificial chromosomes. Cancer Res., *54:* 4183–4187, 1994.

[5] M. Lovell, S. T. Lott, P. Wong, and A. M. Killary. The genetic locus NRC-1 within chromosome 3p12 mediates tumor suppression in renal cell carcinoma independently of histologic type, tumor microenvironment, and VHL mutation, manuscript in preparation.

[6] S. T. Lott, S. Curley, M. Frazier, J. Luca, M. Lovell, and A. M. Killary. High frequency loss of heterozygosity for chromosome 3p proximal loci in VHL-associated and sporadic pancreatic islet cell tumors: evidence for a stepwise mechanism for malignant conversion in VHL tumorigenesis, manuscript in preparation.

21. Latif, F., Tory, K., Modi, W. S., Grazziano, S. L., Gamble, G., Douglas, J., Heppell-Parton, A. C., Rabbitts, P. H., Zbar, B., and Lerman, M. I. Molecular characterization of a large homozygous deletion in the small cell lung cancer cell line U2020: a strategy for cloning the putative tumor suppressor gene. Genes Chromosomes Cancer, *5:* 119–127, 1992.
22. Todd, S., Roche, J., Hahner, L., Bolin, R., Drabkin, H. A., and Gemmill, R. M. YAC contigs covering an 8-megabase region of 3p deleted in the small-cell lung cancer cell line U2020. Genomics, *25:* 19–28, 1995.
23. Lubensky, I. A., Gnarra, J. R., Bertheau, P., Walther, M. M., Linehan, W. M., and Zhuang, Z. Allelic deletions of the *VHL* gene detected in multiple microscopic clear cell renal lesions in von Hippel-Lindau disease patients. Am. J. Pathol., *149:* 2089–2094, 1996.
24. Pause, A., Lee, S., Worrell, R. A., Chen, D. Y., and Burgess, W. H. The von Hippel-Lindau tumor-suppressor gene product forms a stable complex with human CUL-2, a member of the Cdc53 family of proteins. Proc. Natl. Acad. Sci. USA, *94:* 2156–2161, 1997.
25. King, R. W., Deshaies, R. J., Peters, J. M., and Kirschner, M. W. How proteolysis drives the cell cycle. Science (Washington DC), *274:* 1652–1659, 1996.
26. Kipreos, E. T., Lander, L. E., Wing, J. P., He, W. W., and Hedgecock, E. M. Cul-1 is required for cell cycle exit in *C. elegans* and identifies a novel gene family. Cell, *85:* 829–839, 1996.
27. Lubinski, J., Hadaczek, P., Podoiski, J., Toloczko, A., Sikorski, A., McCue, P., Druck, T., and Huebner, K. Common regions of deletion in chromosome regions 3p12 and 3p14.2 in primary clear cell renal carcinomas. Cancer Res., *54:* 3710–3713, 1994.

METHODS: A Companion to Methods in Enzymology 8, 234–246 (1995)

Functional Studies to Identify Tumor Suppressor Genes

Ann McNeill Killary, Steven T. Lott, and Yolanda Sanchez

Division of Laboratory Medicine, The University of Texas M. D. Anderson Cancer Center, 1515 Holcombe Boulevard, Box 72, Houston, Texas 77030-4095

Techniques in somatic cell genetics have proven to be very important in the elucidation of genetic mechanisms in cancer and, in particular, the functional definition of tumor suppressor genes. Genetic complementation studies using microcell fusion have allowed the identification of specific chromosomes and particular chromosome regions that contain functional tumor suppressor genes for a variety of human cancers. In this article, the basic strategy for insertion of dominant selectable markers into human chromosomes is described, as are the methods for microcell fusion of tagged chromosomes into malignant cell lines. Molecular cytogenetic characterization protocols for microcell hybrids generated by such strategies are outlined. Finally, novel approaches to the isolation of dominantly tagged subchromosomal fragments for functional assays as well as to the isolation of new tumor suppressor genes are also described.

The existence of tumor suppressor genes was first demonstrated by early somatic cell hybridization experiments performed over 25 years ago (for review see 1, 2). Cell–cell hybridization or fusion of highly malignant mouse cells to cells of normal growth potential (mouse embryo fibroblasts) resulted in hybrid clones that failed to form tumors when injected into nude or immunocompromised mice. With time in culture, these hybrids lost chromosomes, usually from the normal parent in the cross. Phenotypic changes accompanied this preferential chromosome loss, which resulted in hybrid clones that regained the ability to form progressive tumors in nude mice. Thus, early somatic cell hybridization experiments indicated that malignancy behaved as a recessive trait. As long as the normal genome was represented in the hybrid background, suppression of the malignant phenotype was observed. Reversion to the malignant phenotype was observed following segregation of normal genetic information. Many studies were subsequently performed in an attempt to identify the normal chromosomes that were essential for tumor suppression; however, limited information was obtained because of the karyotypic heterogeneity and complexity of whole-cell hybrid genomes (3, 4).

The utility of somatic cell hybrids for the definition of tumor suppressor genes was contingent on the development of microcell fusion, a technology that allows the transfer of single, intact chromosomes from one cell to another. In 1977, Fournier and Ruddle first described the technology for the transfer of murine chromosomes from one cell to another (5). Later, this method was expanded by McNeill and Brown (1980) to include the transfer of single human chromosomes into recipient mouse cells (6). Chromosomes transferred via microcell fusion can be stably retained in the recipient cell background under dominant selective pressure. This type of monochromosomal hybrid has several advantages over whole cell hybrid clones. Monochromosomal microcell hybrids necessarily contain only the introduced chromosome, whereas, in segregating whole cell hybrids, other chromosomes and, potentially, translocations and chromosomal fragments could be present and difficult to detect. Also, if a dominant selectable marker is inserted into the donor population prior to microcell fusion, then microcell hybrids that stably maintain the introduced chromosome at high frequency in the recipient cell background can be selected, resulting in a nearly homogeneous hybrid population for genetic analysis.

One of the important applications of microcell fusion has been in the functional identification of novel tumor suppressor loci. Cytogenetic analysis and loss of heterozygosity (LOH) studies can point to regions of the human genome that could encode tumor suppressor loci. However, functional evidence is further required to substantiate that a particular chromosome or chromosomal region contains a tumor suppressor locus. The basic strategy is similar to traditional somatic cell hybridization experiments; however, instead of introduc-

1046-2023/95 $12.00

ing the entire genome from the normal cell into the malignant partner, a single chromosome containing a deletion or high-frequency LOH is introduced into the malignant cell. If the introduced chromosome can complement the genetic defect in the cancer cell, then a more normal phenotype should be restored in the complemented hybrid. Studies such as these have been fruitful for the functional identification of tumor suppressor loci for a variety of tumor types (Table 1). More recently, it has been possible to push the system even further, to transfer subchromosomal fragments via microcell fusion (Table 1). The microcell fusion of a defined chromosomal region not only provides valuable information to narrow the region containing the locus, but also allows utilization of the fragment-containing clones for the isolation of new tumor suppressor genes.

In this article the technology for the microcell fusion of dominantly marked human chromosomes is described. Methods for characterization of hybrid clones as well as isolation of fragment-containing microcell clones are also included.

INSERTION OF DOMINANT SELECTABLE MARKERS INTO DONOR HUMAN CELLS

In the 1980 article describing human microcell fusion, the feasibility of the generation of a library of human microcell clones containing individual dominantly tagged human chromosomes was discussed (6). Since that time, several different protocols have described the introduction of dominant selectable markers into human cells and the subsequent microcell fusion of the tagged human chromosomes into recipient cells. In this section, the published techniques for marker insertion will be outlined and discussed.

Calcium Phosphate Coprecipitation

Several different reports have documented the calcium phosphate transfection (7) of the dominant marker *gpt* (8) into donor human chromosomes for microcell fusion experiments (9, 10). Although these experimental strategies produced dominantly tagged human chromosomes that were transferred into recipient cells, there are some distinct disadvantages to this system. Calcium phosphate coprecipitation often results in concatamers of transferred DNA integrated in the donor genome in multiple locations. Also, most diploid human donor cells are not efficiently transfected using calcium phosphate (11, 12). Saxon and co-workers transfected HeLa and HT1080 cells with *gpt* and used those cells as donors for microcell fusion (10). Athwal and co-workers also used an established tumor line, MGH-1, as a source of *gpt*-marked human chromosomes (9). These cells are aneuploid, transformed cell lines that contain detectable and probably undetectable human chromosome rearrangements. Cell lines such as these might be easily transfected and micronucleated; however, they have limited usefulness for functional studies to define tumor suppressor loci. Therefore, methods for the selective marking of normal human cells are preferable and are described in this article.

Retroviral Infection

Retroviral vectors have been successfully used to introduce selectable markers into diploid human cells. The defective retrovirus pZIP-*neo*-SV(X) was used by Lugo and co-workers to introduce the bacterial gene *neo* into human diploid fibroblasts (14). In the presence of *neo,* cells gain resistance to the antibiotic G418, which is the basis for selection of viable microcell hybrid clones containing dominantly tagged human chromosomes. Retroviral transfer has the advantage that the vector can be inserted into a single site per cell. Moreover, the multiplicity of infection can be determined such that high-frequency transfer in virtually 100% of cells is possible.

Electroporation

Electroporation is a simple gene transfer technique that is based on the exposure of cell membranes to a high-voltage electric discharge (15). Neumann and co-workers first subjected mouse L cells in an isotonic salt solution to a series of electric impulses of high field strength and were able to show that the electric discharges destabilized or permeabilized the membrane such that DNA was transferred into the L cells (16). Potter and co-workers modified the existing electroporation protocols by using a single electric pulse of lower field strength, which resulted in the transfer of DNA into a variety of cell types (17). Electroporation is an excellent method because it affords a simple, straightforward way of introducing a dominant selectable marker into cells that are more difficult to transfect using calcium phosphate, such as human fibroblasts (12). Electroporation also has distinct advantages in that the transferred DNA is very low copy number, the integration sites are limited, and the procedure can be used without the biosafety concerns associated with the use of retroviral vectors.

Electroporation has been successfully used for the transfection of primary human fetal fibroblasts (18). Fountain and co-workers also transfected primary human skin fibroblasts by electroporation in both transient and stable transfection assays (12). To tag normal diploid human fibroblasts for use as donors for microcell fusion, we have used the technique of electroporation to introduce pSV2*neo* into normal diploid human

TABLE 1

Year	Tumor	Chromosome transferred	Tumor suppression	Reference
1992	Bladder carcinoma	13	+	Banerjee *et al.* (52)
1992	Breast carcinoma	11	+	Negrini *et al.* (53)
1993	Breast carcinoma	17	+	Casey *et al.* (54)
		13	−	
1994	Breast carcinoma	6q	+	Negrini *et al.* (55)
		11q	+	
1986	Cervical carcinoma	11	+	Saxon *et al.* (56)
1989	Cervical tumor	11	+	Koi *et al.* (41)
		12	−	
1990	Cervical carcinoma	11	+	Oshimura *et al.* (57)
1991	Colorectal carcinoma	5	+	Tanaka *et al.* (58)
		18	+	
		11 (control)	−	
1992	Colorectal carcinoma	4	+	Goyette *et al.* (59)
		17	+	
		18	+	
		15 (control)	−	
1993	Colon carcinoma	1p36	+	Tanaka *et al.* (60)
1990	Endometrial carcinoma	1	+	Yamada *et al.* (61)
		6	+	
		9	+	
		11	+/−	
		19	−	
1990	Fibrosarcoma (HT1080	1	+	Kugoh *et al.* (62)
		11	+	
		2 (control)	−	
		7 (control)	−	
		12 (control)	−	
1992	Fibrosarcoma (mouse, A9)	3p21–p22	+	Killary *et al.* (23)
		2 (control)	−	
		X (control)	−	
1994	Fibrosarcoma (HT1080)	13	−	Anderson *et al.* (63)
1994	Fibrosarcoma	1	−	Anerson *et al.* (64)
		11	−	
1994	Fibrosarcoma	1q23–qter	+	Klein *et al.* (65)
1993	Glioblastoma	10	+	Pershouse *et al.* (38)
		2	−	
1986	HeLa	t(X;11)	+	Saxon *et al.* (56)
		X (control)	−	
1993	Lung adenocarcinoma	3	+	Satoh *et al.* (66)
		7 (control)	−	
		11	+	
1990	Melanoma	6	+	Trent *et al.* (67)
1989	Neuroblastoma	1	+	Oshimura *et al.* (68)
		11	−	
1991	Neuroblastoma	1p	+	Bader *et al.* (69)
		17	+	
		11	−	
1994	Ovarian carcinoma	3	+	Rimessi *et al.* (70)
		11	−	
1992	Prostate	13	+	Banerjee *et al.* (52)
1994	Prostate carcinoma	12pter–q13	+	Bérubé *et al.* (71)
		3	−	
1995	Prostate carcinoma	10pter–q11	+	Sanchez *et al.* (77)
1990	Renal cell carcinoma	3p	(+)	Shimizu *et al.* (72)
1992	Renal cell carcinoma	3p14–q11	+	Sanchez *et al.* (25)
1990	Rhabdomyosarcoma	11	+	Oshimura *et al.* (57)

TABLE 1—*Continued*

Year	Tumor	Chromosome transferred	Tumor suppression	Reference
1994	Teratocarcinoma	4	+	McGowan-Jordan *et al.* (73)
		der7	−	
		der12	−	
1994	Thyroid carcinoma	11	−	Yoshida *et al.* (74)
		10	−	
1987	Wilms tumor	t(X;11)	+	Weissman *et al.* (75)
		X	−	
		t(X;13)	−	
1991	Wilms tumor	11p15.5–p14.1	+	Dowdy *et al.* (40)
		11p13	−	

fibroblasts (19). For our experiments, the method of Potter and co-workers was modified for human foreskin fibroblasts and for use with a commercial electroporator (Bio-Rad gene pulser). For these experiments human diploid fibroblasts (1×10^7 cells) are mixed with linearized plasmid DNA (10 μg pSV2*neo*) in phosphate-buffered saline solution and incubated on ice for 10 min. A 2000-V electrical pulse is applied to the cell–DNA suspension, and cells are incubated for 10 min (0–4°C) and replated in complete nonselective medium at 5×10^5 cells per T25 tissue culture flask. After a 48-h incubation at 37°C, selective medium containing 750 μg/ml G418 is added to each flask. Cloning should be observed 10 days postelectroporation.

HUMAN MICROCELL-MEDIATED CHROMOSOME TRANSFER

Following insertion of a dominant selectable marker, normal human cells can be used as donors for microcell fusion into any recipient cell background. Microcell fusion, as diagrammed in Fig. 1, consists of five essential steps: (1) micronucleation of donor cells; (2) enucleation of the micronucleate cell population; (3) isolation of microcells; (4) fusion of microcells to recipient cells; and (5) selection of viable microcell hybrid clones. Briefly, donor cells are exposed to the mitotic inhibitor Colcemid for a prolonged arrest. This aberrant mitotic arrest induces the formation of micronuclei containing single or small numbers of chromosomes. Micronuclei can then be separated from the cytoplasm using the technique of enucleation, in which micronuclei are extruded from the cytoplasm by centrifugation in the presence of cytochalasin B. This treatment results in isolated microcells as well as contaminating nuclei (karyoplasts) from enucleated whole cells, whole cells, and cytoplasmic vesicles. Microcells are then purified away from other cell particles and can then be fused to recipient cells. Viable microcell hybrid clones can be isolated by selection for the dominant marker transfected into random donor chromosomes.

In the following section, a detailed protocol for microcell fusion of dominantly tagged human chromosomes is described.

MICRONUCLEATION

The technology of microcell fusion is centered around the induction of micronuclei formed by prolonged treatment of growing cells with the mitotic inhibitor Colcemid (20). In the presence of this microtubule polymerization inhibitor, cells form no functional mitotic spindle. In a Colcemid-induced mitotic arrest, chromosomes appear scattered throughout the cell. During prolonged Colcemid arrest, some proportion of cells within the population will attempt to divide. The nuclear membrane will reform around single or small clusters of chromosomes, forming micronuclei. Micronucleation of rodent cells is quite easily accomplished using concentrations of Colcemid in the range 0.01–0.1 μg/ml for 48 h (5, 21). Optimal conditions, however, should be determined for each cell line by performing 48- and 72-h concentration curves. Human cell lines are much more difficult to micronucleate. An effective strategy for the preparation of micronucleate human cells is outlined in the following section.

Micronucleation of Normal Diploid Human Fibroblasts

Human foreskin fibroblasts have been successfully micronucleated (40–60%) using a prolonged 48-h Colcemid arrest (6, 22–25). For micronucleation and subsequent enucleation, donor human cells are plated onto thin plastic sheets or "bullets" cut from the bottoms of T75 or T150 tissue culture flasks. These bullets are cut

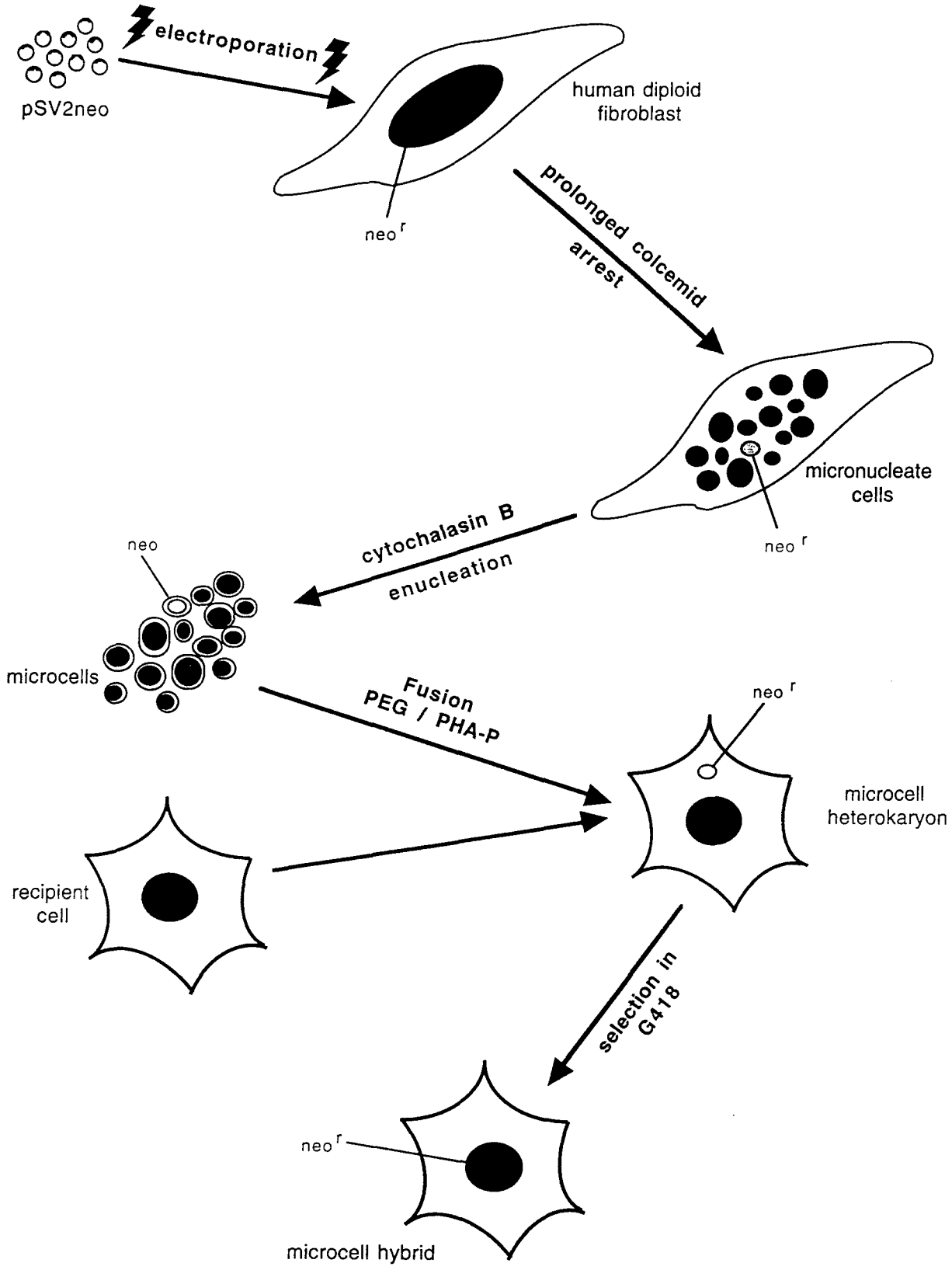

FIG. 1. Microcell-mediated chromosome transfer.

using a hot wire cutter to an approximate size of 25 × 90 mm with one end rounded at the bottom so as to fit into Nalgene 50-ml conical centrifuge tubes for enucleation. Prior to setting up the experiment, bullets should be washed in glassware detergent, rinsed thoroughly in water, and placed in 95% ethanol for 17–24 h prior to cell plating. Before cell plating, bullets are removed from ethanol using sterile forceps, placed in T150 tissue culture dishes (four bullets per dish), and left in the tissue culture hood to dry. Following the enucleation procedure, bullets are left in a 3% solution of bleach overnight, washed with detergent, and rinsed in water. Bullets can be stored and reused until cracking occurs from excessive usage.

The number of bullets used per experiment is dependent on the percentage of cells in the population that micronucleate. Rodent cells easily micronucleate (90–95% of the cell population); therefore, 8 bullets per fusion are adequate (usually two fusions per experiment are performed). For human fibroblasts (40–60% micronucleate), twice that number of bullets are used. Sixteen bullets per fusion or 32 bullets per experiment are adequate.

Four T150 tissue culture flasks containing logarithmically growing human foreskin fibroblasts at 80–90% confluence are seeded (1:2) in eight 150-mm tissue culture dishes, each containing four bullets in complete medium containing 50 μg/ml gentamycin. Tissue culture dishes containing cells are incubated at 37°C for at least 3–4 h to allow for cell attachment prior to Colcemid addition. Colcemid is added (10 μg/ml) to each dish, and cells are incubated at 37°C for 48 h to induce micronucleation. Following micronucleation, the percentage of cells containing micronuclei is quantitated. One simple way to determine the percentage of micronucleate cells is to first fix one bullet in a 1:1 mixture of 95% methanol for 10 min. followed by a second fixation in 95% methanol (10 min), and, finally, staining in a 10-μg/ml solution of acridine orange prepared in water or normal saline. Acridine orange is a fluorochrome that stains the nucleus and cytoplasm differentially. Nuclei and micronuclei appear green, whereas the cytoplasm stains red using fluorescence microscopy. Bullets should be stained with acridine orange solution for 30–60 s, rinsed twice in deionized water, and coverslipped using 0.05 M citrate phosphate-mounting buffer (pH 4.1). Bullets can be viewed by fluorescence microscopy using a barrier filter that excites in the 500-nm range. This stain is excellent for the quantitation of micronucleation, enucleation efficiency, or microcell yield. Acridine orange is a carcinogen, however, and should be handled with caution.

Induction of micronucleate populations of human fibroblasts is critically dependent on the concentration of mitotic inhibitor and the absolute passage number of the donor cells (6). The concentration of Colcemid required to induce micronucleation of normal foreskin fibroblasts is in the range 10–20 μg/ml. Higher concentrations of the mitotic inhibitor result in increased cell toxicity and decreased yield of micronucleated cells (6). Micronuclei obtained by this procedure have been carefully analyzed for the number of micronuclei per cell as a function of Colcemid concentration and length of mitotic arrest. Antikinetochore antibody staining has also been used to determine that the smallest of micronuclei contain single human chromosomes (A. McNeill Killary, R. L. Brown, S. Brinner, B. Brinkley, and E. Stubblefield, unpublished results). Another important variable is the culture age. Cells of early passage micronucleate optimally; however, after a population doubling of 17–18, the percentage of micronucleate cells decreases dramatically (6). Another variable to be determined for each human cell line or strain is the length of Colcemid-induced mitotic arrest. The period of Colcemid block required to induce optimal micronucleation varies depending on the doubling time of the particular donor cell line. Human foreskin fibroblasts optimally micronucleate following incubation in 10 μg/ml Colcemid for 48 h. Slower-growing cell lines may require longer arrest times. Also, we have observed that recovery of viable microcell hybrid clones containing intact donor chromosomes is greater in incubations of shorter duration (48 h). In general, the longer the incubation time in Colcemid, the greater the frequency of fragmented donor chromosomes.

The procedure as outlined should result in the generation of large numbers of cells containing micronuclei. A technique has also been described for micronucleation of human lymphoblastoid cells in culture (26).

ENUCLEATION OF MICRONUCLEATE CELL POPULATIONS

Micronucleate cell populations can be enucleated by centrifugation in the presence of cytochalasin B. Cytochalasin B is a fungal metabolite that interferes with microfilament attachment to the cell membrane (27). A proportion of cells exposed to this drug in high concentrations (5–10 μg/ml) will extrude their nuclei. The first large-scale enucleation of whole cells was performed by incubation in cytochalasin B in the presence of centrifugal force (28–30). In the presence of cytochalasin B and centrifugation, nuclei protrude on thin cytoplasmic stalks and pellet in the bottom of the centrifuge tube. The cytoplasm of enucleate cells remains attached to the surface on which the cells are plated.

Enucleation of micronucleate cells to form microcells was first performed by Ege and Ringertz in 1974 (31).

Each microcell consists of a single micronucleus containing approximately one to five chromosomes surrounded by a small amount of cytoplasm and an intact plasma membrane. Following enucleation, the pellet in each centrifuge tube contains microcells of various sizes, enucleated whole cells, whole cells that (have been) stripped off prior to enucleation, and cytoplasmic particles. A detailed protocol for enucleation of human diploid fibroblasts as well as methods for quantitation of microcell yield and enucleation conditions for other cell lines is described in the next section.

Enucleation of Human Diploid Fibroblasts

Each bullet containing micronucleate human cells is placed back-to-back inside a Nalgene 50-ml conical centrifuge tube in serum-free medium containing 5 μg/ml cytochalasin B. Tubes are immediately placed inside a prewarmed superspeed centrifuge (28–33°C) in a fixed angle rotor such that bullets are parallel to rotor radii. Tubes are centrifuged at 18,800*g* for 35 min to induce enucleation. The number of cells enucleated should be >90–95% and can be determined by staining with acridine orange as described for quantitation of micronucleation efficiency.

Enucleation for Nonadherent Cells

For cells that grow in suspension, or cells that do not adhere well to the substratum, bullets can be treated prior to cell plating with concanavalin A to allow for firm attachment (21, 32). Concanavalin A (Sigma) (15 mg/ml solution in 0.9% saline) can be cross-linked to bullets using a cross-linking agent (1-cyclohexyl-3-(2-morpholinoethyl) carbodiimide metho-*p*-toluenesulfonate water-soluble carbodiimide (Sigma, 75 mg/ml prepared in 0.9% saline). Micronucleate cells (generated by prolonged arrest) are trypsinized and resuspended in phosphate-buffered saline at 10^6 cells/ml. Cell suspension is added to each bullet (1.2 ml/bullet), and cells are allowed to attach for 10–15 min at room temperature. Complete medium is added and cells are incubated for 30–60 min at 37°C to allow cells to flatten and spread. Bullets can then be used for enucleation as described.

Suspension Enucleation

Protocols have been described elsewhere for suspension enucleation through Ficoll (33) or Percoll (26) gradients and have been successfully used for cell lines that are nonadherent, such as lymphoblastoid cells. Gradient separation is based on differences in buoyant densities of nucleoplasm versus cytoplasm in a centrifugal force. This type of approach is useful, for example, in lymphoblastoid cell lines in which the frequency of micronucleation is low; yet, because large numbers of cells can be processed by gradient separation, these types of cell lines can still be used as donors for microcell fusion. Enucleation is often incomplete, however, in these gradients, and many partially enucleated cells will be lost because they partition away from isolated microcells. Nevertheless, gradient enucleation provides a way to enucleate cell lines that cannot be enucleated on bullets.

MICROCELL ISOLATION

The cell pellet recovered following enucleation consists of a variety of cell particles including microcells of various sizes, usually containing one to five interphase chromosomes, intact nuclei resulting from enucleation of whole cells, whole cells that stripped off the bullet prior to enucleation, and cytoplasmic particles. A hemocytometer can be used to rapidly determine the number of total particles per experiment. To determine the percentage of microcells in the total particle count, microcells are quantitated using aceto-orcein staining and bright-field microscopy or using acridine orange staining and fluorescence microscopy. For acridine orange staining, a drop of microcell preparation before and after filtration is placed on a microscope slide. To that drop, one drop of 10 μg/ml acridine orange solution is added, and a coverslip is placed on top of the slide. After a 30- to 60-s incubation, particles are counted using fluorescence microscopy.

Aceto-orcein will also differentially stain the nucleus from the cytoplasm and is the method of choice when fluorescence microscopy is not readily available (32). Using this stain, nuclei appear red and cytoplasm pink. The procedure is similar to that described for acridine orange. A solution of aceto-orcein, made by mixing 0.5% orcein solution (Sigma) in 50% acetic acid, is refluxed for several hours. To one drop of microcell preparation, one drop of aceto-orcein stain is added and incubated for 2–5 min with coverslip. The particles can then be viewed by bright-field microscopy. If the stain is allowed to incubate for 5–10 min, all particles will appear red; therefore, care must be taken to limit staining time (21, 32).

PURIFICATION OF MICROCELL PREPARATION

The generation of microcell hybrid clones containing single human chromosomes requires that the microcell preparation be purified to select for the smallest of microcells that most probably contain single human chromosomes. Originally, microcell preparations were separated by size using unit gravity sedimentation (5). This technique has been described in detail elsewhere

and is an efficient way to select for the smallest microcells in the donor population (34). A simple and rapid separation based on size can also be accomplished by filtration through nuclepore filters of different sizes (6). For this procedure, Swinnex filter units (Swinnex, 25 mm) containing 8-, 5-, or 3-μm Nuclepore filters (VWR Scientific) are used. Filter units are autoclaved and attached to sterile 10-cc syringes. The microcell preparation is passed through one to two 5-μm filters followed by filtration through 3-μm filters. Filtration through 5-μm filters effectively eliminates karyoplasts and whole cells, and subsequent passage through 3-μm filters selects for the smallest of the microcells. Preparations containing large numbers of intact cells should be passed through 8-μm filters prior to 5-μm filtration. The microcell preparation should be monitored at each step by staining with acridine orange or aceto-orcein.

Purification of the crude microcell population is an important step in the procedure of microcell-mediated chromosome transfer. Without this step, the microcell hybrid clones isolated from a typical experiment would contain a number of whole cell hybrids or hybrids containing large numbers of transferred chromosomes. The relative proportion of whole cell hybrids to microcell hybrids recovered per experiment is related to the percentage of micronucleate cells in the population. For human microcell fusion, in which the frequency of micronucleation is much lower than in rodent cells, filtration is an essential step. However, A9 hybrids containing single human chromosomes micronucleate very well (>95% of cells contain micronuclei). In this case, the numbers of whole-cell hybrids recovered are very small. Purification of the donor microcell population also has the advantage that it increases the probability of recovering monochromosomal hybrids or hybrids containing fragments of the donor chromosome.

MICROCELL FUSION

Microcells can be fused to recipient cells using any of several experimental strategies. Initially, microcells were fused to recipient cells using inactivated Sendai virus (5). Human microcells have also been fused to recipient mouse cells using a protocol that combined microcells with phytohemagglutinin-P (PHA-P; Difco) to adhere microcells to recipient cells in suspension, followed by fusion using polyethylene glycol (PEG) (6). Subsequent protocols modified this approach by adhering microcells in PHA-P to a monolayer of recipient cells (22, 32). This combined PHA-P/PEG (Koch Chemical United, MW 1540) monolayer fusion protocol is the most efficient approach for microcell fusion. For this technique, the filtered microcell preparation is centrifuged at 2000*g* for 10 min (37°C). The microcell pellet is then resuspended well (to disperse clumps of agglutinating microcells) in 4 ml PHA-P solution (100 μg/ml, absolute concentration) and added to three T25 flasks of recipient cells (70–80% confluent). Two of these flasks are used for fusion, and one flask serves as the unfused control. The T25s are then incubated at 37°C until microcells have agglutinated to the monolayer (usually 10–20 min).

For microcell fusion, the PHA-P solution is carefully aspirated off the monolayer and to each of two T25s, 0.5 ml PEG (44–50% w/w) is added, and the flasks are rocked gently for 1 min. The PEG solution is quickly removed and the monolayers rinsed three times with 4 ml serum-free medium. Complete nonselective medium is then added to each flask, and flasks are incubated at 37°C for 16–24 h.

Suspension Microcell Fusion

Microcells can be fused to recipient cells in suspension (77). This procedure does not require PHA-P and is useful for cell lines that grow in suspension or for which PHA-P is cytotoxic. Isolated microcells are combined with 1×10^6 recipient cells in serum-free medium and centrifuged at 2000*g* for 15 min at 37°C. The pellet is resuspended well and 0.5 ml PEG (44–50% w/w) is added dropwise while the pellet is gently dispersed for 1 min. Serum-free medium (9.5 ml) is quickly added over 1 min with gentle swirling. Next, 0.5 ml of fusion mixture is added to each of 20 T25s containing complete nonselective medium. Flasks are then incubated overnight (17–24 h) at 37°C prior to addition of selective medium.

Two critical variables must be analyzed for each recipient cell line prior to microcell fusion. It is very important that optimal concentrations of fusogen and agglutinin be used; this results in fusion of microcells to recipient cells with the least amount of cell toxicity. A concentration curve can be easily performed with the recipient cell line alone to quantitate the numbers of binucleate heterokaryons postfusion with increasing concentrations of PEG (ranging usually from 44 to 50%). At higher concentrations of PEG, increased cell toxicity will be observed as well as fusion of large numbers of recipient cells *en masse*. The same type of concentration curve should be performed with PHA-P. We have found that absolute concentrations in the range 50–200 μg/ml are effective at agglutinating microcells to a variety of recipient cells. PHA-P is cytotoxic to some cell lines at the higher end of this range; it is important to perform concentration curves with the recipient line and monitor agglutination by phase micros-

copy. Trypan blue can be used to measure the degree of cell toxicity.

SELECTION OF *neo*-MARKED HUMAN CHROMOSOMES

The procedure as outlined should allow isolation of dominantly tagged human chromosomes for use in functional assays to identify tumor suppressor loci. The insertion of the selectable marker, however, is a random event in donor human chromosomes. Therefore, one must first identify which chromosomes of the normal diploid complement contain selectable marker insertions. One way to determine the integration site in individual electroporated clones is to perform fluorescence *in situ* hybridization using the selectable marker DNA as a probe on metaphase spreads from the individual electroporated clones. G-banding in combination with FISH can precisely locate the integrated marker to within a chromosome band.

A second approach to finding the human chromosomes carrying selectable marker insertions is to transfer pools of electroporated clones containing a number of different tagged human chromosomes into a recipient cell line whose chromosome constitution is easily distinguishable from that of the transferred human chromosome. This recipient cell line should also be efficient at micronucleation such that once characterized, the donor chromosome could be transferred from this background into a human tumor line showing LOH or cytogenetic deletion involving that chromosome. The mouse L-cell line, A9 (36, 76), is an excellent choice for the recipient cell line because it has a rapid doubling time and is easily maintained *in vitro*. A9 is also extremely efficient at micronucleation (>95%) (23). Thus, if pSV2*neo* is the dominant marker inserted into the human genome, then microcell fusion into A9 and selection in the presence of G418 should result in a variety of hybrid clones containing different *neo*-tagged chromosomes in the mouse cell background generated from one fusion experiment. Metaphase spreads from hybrid clones can be quickly screened by G-11 analysis, a cytogenetic stain that differentially stains human and mouse chromosomes at an alkaline pH (37). Monochromosomal hybrids can be further characterized by G-banding and DNA marker analysis. Using this kind of approach, we have generated panels of hybrid clones containing dominantly marked normal human chromosomes (23–25, 38, 39) in the A9 cell background.

FUNCTIONAL STUDIES TO IDENTIFY TUMOR SUPPRESSOR GENES

Monochromosomal microcell hybrids have proven to be valuable reagents for the functional definition of tumor suppressor loci. High-frequency LOH and cytogenetic analysis may point to regions of the human genome that may encode tumor suppressor genes; however, there may be many regions of high-frequency LOH associated with a particular tumor. It is important to be able to determine which of these losses correspond to early events in the genesis of the cancer. Functional studies are very important to define those early events. The basic strategy for this approach is genetic complementation. If high-frequency LOH or cytogenetic rearrangements or deletions are associated with a particular neoplasia, then it should be possible to complement the loss in the tumor by the introduction of normal genetic information using microcell fusion of these dominantly tagged human chromosomes. These complemented hybrids can be tested for growth both *in vitro* and *in vivo* to determine if the introduced chromosome can restore a more normal phenotype to the malignant cell.

The *in vivo* assay involves the injection of hybrid cells either subcutaneously or orthotopically into athymic nude mice. If hybrid cells either fail to form tumors *in vivo* or show a much greater latency period for tumor formation relative to control hybrids containing different human chromosomes, then it can be concluded that the introduced chromosomes contain a genetic locus or loci capable of suppressing the malignant phenotype. The introduced human chromosome, therefore, must contain an important tumor suppressor gene(s) involved in the genesis of the tumor, because if the genetic alterations were much later in the pathway to malignant growth or metastasis, one would not expect complementation to suppress tumor formation. In recent years, it has become possible to use microcell fusion to limit the region within a particular chromosome containing functional tumor suppressor genes (23, 25, 40, 41). In the following section, techniques of microcell fusion for the definition of tumor suppressor loci will be discussed as well as methods for the generation of defined deletion microcell hybrids for tumor suppression assays.

Microcell Fusion Using Monochromosomal Hybrids as Donors

For microcell fusion, monochromosomal hybrids containing dominantly tagged human chromosomes are used as donors for microcell fusion into a malignant cell line. Because the human chromosome is in a mouse background, micronucleation is quite easily accomplished. For micronucleation and enucleation, one T150 flask of monochromosomal hybrids (in A9 background) (80–90% confluent) is trypsinized and replated into four 150-mm plates, each containing four bullets in complete medium. Following incubation at 37°C for at least 3–4 h, Colcemid is added at 0.06 μg/ml to each

dish, and cells are incubated again for 48 h to induce micronucleation in the range 90–95%. For enucleation, the steps are the same as outlined in the section pertaining to enucleation of human fibroblasts with the exception that for monochromosomal hybrids in the A9 background, 10 μg/ml cytochalasin B is used to induce enucleation with a centrifugation speed of 27,000*g* for 70 min. Isolation of microcells and fusion of microcells to recipient cells follows directly from the outlined procedure for human microcell fusion.

Isolation of Fragment-Containing Microcell Hybrids

Microcell hybrids generated from the outlined procedures should be extremely valuable to determine if a tumor suppressor locus resides on the introduced human chromosome. In addition to this information, however, monochromosomal microcell hybrids have proven to be very important for the regional localization of functional tumor suppressor loci. This strategy makes use of fragments of the donor chromosome that can be introduced in a manner similar to that described for the intact chromosome, to address whether the tumor suppressor activity can be narrowed to a region within the chromosome. Microcell hybrids generated in a single experiment typically yield clones containing intact donor chromosomes as well as clones containing fragments of the introduced chromosome (42–44). The number of fragment-containing clones isolated from a single experiment seems to be partially dependent on the length of Colcemid-induced mitotic arrest and also a function of the stability of the introduced chromosome in the particular recipient cell background. The utility of the technology for generation of fragment-containing clones is very much dependent on the ease with which hybrid clones can be screened for fragments. For this reason, interspecific microcell hybrids have been extremely valuable because they can be screened rapidly with cytogenetics (G-11 staining) and DNA marker analysis.

Using this kind of strategy, two novel tumor suppressor loci have been functionally identified on the short arm of human chromosome 3 and mapped to an interval of 2 Mb within 3p21–p22 (23) and 10–15 Mb within 3p12–p14 (25). A limitation of this approach is that fragments must contain selectable marker insertions for them to be useful for microcell fusion studies. It is therefore easy to isolate large fragments with this approach. Smaller fragments that flank the selectable marker insertion are also quite possible to attain with this approach. However, if the region of interest is far away from the selectable marker integration site, then other strategies for generating small fragments can be used, including the targeting of the selectable marker to a precise region within the chromosome of interest.

Another strategy involves the use of radiation microcell fusion (40, 45, 46). Using this technique, microcells are gamma-irradiated and rescued by fusion to a recipient cell. Using radiation microcell hybrids, a high-resolution physical map may be generated; the extent of chromosome fragmentation becomes a function of the dosage of radiation. Fragment-containing hybrids generated by either route are useful sources of molecular probes for defined chromosomal segments and have been instrumental in the position cloning of several important human genes (47–49).

Characterization of Intraspecific Microcell Hybrids

To define novel tumor suppressor loci using functional assays, most investigations have transferred *neo*- or *gpt*-tagged human chromosomes into recipient human tumor lines. Characterization of intraspecific hybrids is much more difficult than that described previously for transfer of human chromosomes into a mouse cell background (interspecific crosses). One must have a definitive way to identify the introduced human chromosome in the tumor cell background. Our laboratory uses chromosome painting as the first step in the characterization of each hybrid using chromosome-specific probes. This technique allows a rapid quantification of the frequency with which the introduced fragment is present in the hybrid cell population as well as determination of any karyotypic changes in the recipient cell genome for that chromosome of interest.

For these experiments, human DNA is amplified using polymerase chain reaction (PCR) from a monochromosomal hybrid containing the *neo*-tagged human chromosome and used as probe for *in situ* hybridization onto metaphase spreads from the parental tumor cell line. Chromosome-specific probes are prepared, as described by Sanchez and co-workers (25), by PCR amplifying the human-specific DNA from each monochromosomal hybrid using inter-*Alu* primers (50). For each reaction, 100 ng of hybrid DNA is incubated with 50 pmol of each of the *Alu* primers in buffer containing 15 mM magnesium and 1.25 units of AmpliTaq polymerase (Perkin–Elmer/Cetus). The DNA is denatured at 94°C for 5 min followed by five cycles of 1 min at 94°C, 1 min at 65°C, and 3 min at 72°C. An elongation step of 10 min at 72°C is then performed; samples of the PCR products are run on a 2% agarose gel. The primers are then removed from the remaining PCR product using Centricon-100 columns. Chromosome-specific DNA is then labeled with biotin-14–dATP using nick-translation. For hybridization, the biotinylated probe and 50× COT 1 (GIBCO) unlabeled DNA and 10% dextran sulfate, 2× SSC, and 50% formamide are denatured at 75°C for 10 min. The DNA is allowed to reanneal at 37°C for 20 min and is hybridized to processed metaphases from the tumor cell lines. Hybridization is de-

tected using fluorescein–avidin conjugate and amplified using biotinylated anti-avidin antibody.

In addition to chromosome painting experiments, hybrid clones can be analyzed with fluorescence *in situ* hybridization using pSV2*neo* as a probe to unambiguously identify the introduced chromosome in the recipient cell background. This procedure, in combination with G-banding analysis, should document the presence of the introduced chromosome in hybrid cells. For FISH using pSV2*neo* as probe (25), chromosome preparations are treated with RNase A and denatured with 70% formamide/2× SSC at 71°C. Slides are then hybridized with biotinylated probe in 2× SSC, 50% formamide, and sonicated salmon sperm DNA. Hybridization is carried out for 16 h at 37°C. Slides are then washed in 50% formamide/2× SSC at 37°C, and hybridization is detected by incubating slides in a fluorescein–avidin conjugate followed by amplification using a biotinylated anti-avidin antibody. Preparations are mounted in antifade containing propidium iodide as a counterstain.

Using molecular cytogenetic analyses, hybrid clones can be carefully characterized and monitored during all phases of investigation. This type of analysis is imperative for somatic cell hybrid analysis of complex phenotypes. For example, hybrid cells should be screened at the time of injection into nude mice using FISH to determine the fraction of cells in the hybrid population that retain the intact chromosome. Likewise, if tumors form following an increased latency period *in vivo*, explants from these tumors should be examined for loss of the introduced chromosome. In addition to molecular cytogenetic analysis, microsatellite marker analysis is helpful to screen for regions of the introduced chromosome present in the recipient cell background.

In Vivo Growth Assays

Once hybrid lines have been characterized, they can be injected into athymic nude mice to determine if the introduced chromosome restores a more normal growth to the malignant cell. For these experiments, hybrid cells, parental tumor cells, and control hybrids containing a different region of the chromosome or an entirely different chromosome can be injected into athymic nude mice. Procedures for injection of nude mice have been described elsewhere in detail for both subcutaneous and orthotopic injections (51). Briefly, in our experiments (23, 25) hybrid cells (5×10^6 or 1×10^7 cells per injection site) are injected in triplicate into 4- to 6-week-old athymic nude mice. Cell suspensions for injection are washed two times in serum-free medium, and cell counts and viabilities are determined using trypan blue exclusion. No suspension having less than 95% viability should be used for *in vivo* studies. Cells are maintained at 37°C in medium at pH 7.4 until injection time. A 0.2-ml cell suspension containing 5×10^6–1×10^7 viable cells is drawn into a tuberculin syringe using an 18-gauge needle. Immediately prior to injection, the cell suspension in the syringe should be resuspended well. A vehicle-only control of 50 μl of medium is included with each experimental series. Injected mice are monitored, and tumor volumes determined biweekly. In addition to tumor volumes, it is advisable to also determine tumor wet weights at the end of the experiment.

FUNCTIONAL ASSAYS AND TUMOR SUPPRESSOR GENES

The experimental protocols outlined in this article provide a methodology with which functional tumor suppressor loci can be defined. High-frequency LOH and cytogenetic analysis may point to regions of the human genome that may encode tumor suppressor genes; however, there may be many regions of high-frequency LOH associated with a particular tumor. It is important to be able to determine which of these losses correspond to early events in the genesis of the cancer. Microcell hybrid clones generated using these kinds of approaches should be extremely useful not only for definition and regional mapping of novel loci, but also as valuable reagents to isolate new tumor suppressor genes.

REFERENCES

1. Sager, R. (1989) *Science* **246,** 1406–1412.
2. Anderson, M. J., and Stanbridge, E. J. (1993) *FASEB J.* **7,** 826–833.
3. Jonasson, J., Povey, S., and Harris, H. (1977) *J. Cell Sci.* **24,** 217–254.
4. Harris, H. (1986) *J. Cell Sci.* **4**(Suppl.), 431–444.
5. Fournier, R. E. K., and Ruddle, F. H. (1977) *Proc. Natl. Acad. Sci. USA* **74,** 319–323.
6. McNeill, C. A., and Brown, R. L. (1980) *Proc. Natl. Acad. Sci. USA* **77(9),** 5394–5398.
7. Gorman, C. M., Padmanabhan, R., and Howard, B. (1983) *Science* **221,** 551–553.
8. Mulligan, C., and Berg, P. (1980) *Science* **209,** 1422–1427.
9. Athwal, R., Smarsh, M., Searle, B. M., and Surinder, S. D. (1985) *Somatic Cell Mol. Genet.* **11,** 177–187.
10. Saxon, P. J., Srivatsan, E. S., Leipzig, G. V., Sameshima, J. H., and Stanbridge, E. J. (1985) *Mol. Cell. Biol.* **5,** 140–146.
11. Cananni, D., Naiman, T., Teitz, T., and Berg, P. (1986) *Somatic Cell Mol. Genet.* **12,** 13–20.
12. Fountain, J. W., Lockwood, W. K., and Collins, F. S. (1988) *Gene* **68,** 167–172.

13. Deleted in proof.
14. Lugo, T. G., Handelin, B., Killary, A. M., Houseman, D. E., and Fournier, R. E. K. (1987) *Mol. Cell. Biol.* **7,** 2814–2820.
15. Zimmerman, U., and Vienken, J. (1982) *J. Membr. Biol.* **67,** 165–182.
16. Neumann, E., Schaefer-Ridder, M., Wang, Y., and Hofschneider, P. H. (1982) *EMBO J.* **1,** 841–845.
17. Potter, H., Weir, L., and Leder, P. (1984) *Proc. Natl. Acad. Sci. USA* **81,** 7161–7165.
18. Chu, G., Hayakawa, H., and Berg, P. (1987) *Nucleic Acids Res.* **15,** 1311–1326.
19. Killary, A. M., Wolf, E., Lovell, M., Giambernardi, T., and Sanchez, Y. (1995), in preparation.
20. Stubblefield, E. (1964) (Harris, R. J. C., Ed.), pp. 223–298, Academic Press, New York.
21. Killary, A. M., and Fournier, R. E. K. (1995) *Methods Enzymol.* **254,** 133–152.
22. Killary, A. M., and Fournier, R. E. K. (1984) *Cell* **38,** 523–534.
23. Killary, A. M., Wolf, M. E., Giambernardi, T. A., and Naylor, S. L. (1992) *Proc. Natl. Acad. Sci. USA* **89,** 10877–10881.
24. Ning, Y., Weber, J. L., Killary, A. M., Ledbetter, D. H., Smith, J. R., and Pereira-Smith, O. M. (1991) *Proc. Natl. Acad. Sci. USA* **88,** 5635–5639.
25. Sanchez, Y., El-Naggar, A., Pathak, S., and Killary, A. M. (1994) *Proc. Natl. Acad. Sci. USA* **91,** 3383–3387.
26. Sanford, J. A., and Stubblefield, E. (1987) *Somatic Cell Mol. Genet.* **13,** 279.
27. Carter, S. B. (1967) *Nature* **213,** 261–264.
28. Prescott, D. M., Myerson, D., and Wallace, J. (1972) *Exp. Cell Res.* **71,** 480–485.
29. Poste, G., and Reeve, P. (1972) *Exp. Cell Res.* **73,** 287–294.
30. Wright, W. E., and Hayflick, L. (1972) *Exp. Cell Res.* **74,** 187–194.
31. Ege, T., and Ringertz, N. R. (1974) *Exp. Cell Res.* **87,** 378–382.
32. Fournier, R. E. K. (1981) *Proc. Natl. Acad. Sci. USA* **78(10),** 6349–6353.
33. Wigler, M. H., and Weinstein, I. B. (1975) *Biochem. Biophys. Res. Commun.* **63,** 669–674.
34. Fournier, R. E. K. (1982) *in* Techniques in Somatic Cell Genetics (Shay, J., Ed.), pp. 309–327, Plenum, New York.
35. Deleted in proof.
36. Littlefield, J. W. (1964) *Science* **145,** 709–710.
37. Friend, K. K., Dorman, B. P., Kucherlapati, R. S., and Ruddle, F. H. (1976) *Exp. Cell Res.* **99,** 31–36.
38. Pershouse, M. A., Stubblefield, E., Hadi, A., Killary, A. M., Yung, W. K. A., and Steck, P. A. (1993) *Cancer Res.* **53,** 5043–5053.
39. Sanchez, Y., Garcia-Heras, M., Giambernardi, T., Wolf, M. E., Banks, A. U., and Killary, A. M. (1995), in preparation.
40. Dowdy, S. F., Fasching, C. L., Araujo, D., Lai, K.-M., Livanos, E., Weissman, B. E., and Stanbridge, E. J. (1991) *Science* **254,** 293–295.
41. Koi, M., Morita, H., Yamada, H., Satoh, H., Barrett, J. C., and Oshimura, M. (1989) *Mol. Carcinog.* **2,** 12–21.
42. Fournier, R. E. K., and Frelinger, J. A. (1982) *Mol. Cell. Biol.* **2,** 526–534.
43. Fournier, R. E. K., and Moran, R. G. (1983) *Somatic Cell Mol. Genet.* **9,** 69–84.
44. Leach, R. J., Thayer, M. J., Schafer, A. J., and Fournier, R. E. K. (1989) *Genomics* **5,** 167–176.
45. Goss, S. J., and Harris, H. (1975) *Nature* **255,** 1445.
46. Koi, M., Johnson, L. A., Kalikin, L. M., Little, P. F. R., Nakamura, Y., and Feinberg, A. P. (1993) *Science* **260,** 361–364.
47. Jones, K. W., Shapero, M. H., Chevrette, M., and Fournier, R. E. K. (1991) *Cell* **66,** 861–872.
48. Fountain, J. W., Wallace, M. R., Bereretón, A. M., O'Connell, P., White, R. L., Rich, D. C., Ledbetter, D. H., Leach, R. J., Fournier, R. E. K., Menon, A. G., Gusella, J. F., Barker, D., Stephens, K., and Collins, F. S. (1989) *Am. J. Hum. Genet.* **44,** 58–67.
49. Leach, F. S., Nicolaides, N. C., Papadopoulos, N., Liu, B., Jen, J., Parsons, R., Peltomäki, P., Sistonen, P., Aaltonen, L. A., Nyström-Lahti, M., Guan, X.-Y., Zhang, J., Meltzer, P. S., Yu, J.-W., Kao, F.-T., Chen, D. J., Cerosaletti, K. M., Fournier, R. E. K., Todd, S., Lewis, T., Leach, R. J., Naylor, S. L., Weissenbach, J., Mecklin, J.-P., Järvinen, H., Petersen, G. M., Hamilton, S. R., Green, J., Jass, J., Watson, P., Lynch, H. T., Trent, J. M., de la Chapelle, A., Kinzler, K. W., and Vogelstein, B. (1993) *Cell* **75,** 1215–1225.
50. Liu, P., Siciliano, J., Seong, D., Craig, J., Zhao, U., de Jong, P. J., and Siciliano, M. J. (1995) *Cancer Genet. Cytogenet.,* in press.
51. Fidler, I. J., Naito, S., and Pathak, S. (1990) *Cancer Metast. Rev.* **9,** 149–165.
52. Banerjee, A., Xu, H.-J., Hu, S.-X., Araujo, D., Takahashi, R., Stanbridge, E. J., and Benedict, W. F. (1992) *Cancer Res.* **52,** 6297–6304.
53. Negrini, M., Castagnoli, A., Sabbioni, S., Recanatini, E., Giovannini, G., Possati, L., Stanbridge, E. J., Nenci, I., and Barbanti-Brodano, G. (1992) *Oncogene* **7,** 2013–2018.
54. Casey, G., Plummer, S., Hoeltge, G., Scanlon, D., Fasching, C., and Stanbridge, E. J. (1993) *Hum. Mol. Genet.* **2,** 1921–1927.
55. Negrini, M., Sabbioni, S., Possati, L., Rattan, S., Corallini, A., Barbanti-Brodano, G., and Croce, C. M. (1994) *Cancer Res.* **54,** 1331–1336.
56. Saxon, P. J., Srivatsan, E. S., and Stanbridge, E. J. (1986) *EMBO J.* **5(13),** 3461–3466.
57. Oshimura, M., Kugoh, H., Koi, M., Shimizu, M., Yamada, H., Satoh, H., and Barrett, J. C. (1990) *J. Cell. Biochem.* **42,** 135–142.
58. Tanaka, K., Oshimura, M., Kikuchi, R., Seki, M., Hayashi, T., and Miyaki, M. (1991) *Nature* **349,** 340–342.
59. Goyette, M. C., Cho, K., Fasching, C. L., Levy, D. B., Kinzler, K. W., Paraskeva, C., Vogelstein, B., and Stanbridge, E. J. (1992) *Mol. Cell. Biol.* **12,** 1387–1395.
60. Tanaka, K., Yanoshita, R., Konishi, M., Oshimura, M., Maeda, Y., Mori, T., and Miyaki, M. (1993) *Oncogene* **8,** 2253–2258.
61. Yamada, H., Wake, N., Fujimoto, S., Barrett, J. C., and Oshimura, M. (1990) *Oncogene* **5,** 1141–1147.
62. Kugoh, H. M., Hashiba, H., Shimizu, M., and Oshimura, M. (1990) *Oncogene* **5,** 1637–1644.
63. Anderson, M. J., Fasching, C. L., Xu, H.-J., Benedict, W. F., and Stanbridge, E. J. (1994) *Genes Chrom. Cancer* **9,** 251–260.
64. Anderson, M. J., Casey, G., Fasching, C. L., and Stanbridge, E. J. (1994) *Genes Chrom. Cancer* **9,** 266–281.
65. Klein, K. G., and Bouck, N. P. (1994) *Cancer Genet. Cytogenet.* **73,** 109–121.
66. Satoh, H., Lamb, P. W., Dong, J.-T., Everitt, J., Boreiko, C., Oshimura, M., and Barrett, J. C. (1993) *Mol. Carcinog.* **7,** 157–164.
67. Trent, J. M., Stanbridge, E. J., McBride, H. L., Meese, E. U., Casey, G., Araujo, D. E., Witkowski, C. M., and Nagle, R. B. (1990) *Science* **247,** 568–571.

68. Oshimura, M., Koi, M., Morita, H., Yamada, H., Shimizu, M., and Ono, T. (1989) *Proc. Am. Assoc. Cancer Res.* **30,** 786.

69. Bader, S. A., Fasching, C., Brodeur, G. M., and Stanbridge, E. J. (1991) *Cell Growth Differ.* **2,** 245–255.

70. Rimessi, P., Gualandi, F., Morelli, C., Trabanelli, C., Wu, Q., Possati, L., Montesi, M., Barrett, J. C., and Barbanti-Brodano, G. (1994) *Oncogene* **9,** 3467–3474.

71. Bérubé, N. G., Speevak, M. D., and Chevrette, M. (1994) *Cancer Res.* **54,** 3077–3081.

72. Shimizu, M., Yokota, J., Mori, N., Shuin, T., Shinoda, M., Terada, M., and Oshimura, M. (1990) *Oncogene* **5,** 185–194.

73. McGowan-Jordan, I. J., Speevak, M. D., Blakey, D., and Chevrette, M. (1994) *Cancer Res.* **54,** 2568–2572.

74. Yoshida, A., Asaga, T., Masuzawa, C., and Kawahara, S. (1994) *J. Surg. Oncol.* **55,** 170–174.

75. Weissman, B. E., Saxon, P. J., Pasquale, S. R., Jones, G. R., Geiser, A. G., and Stanbridge, E. J. (1987) *Science* **236,** 175–180.

76. Cos, R. P., Drauss, M. R., Balis, M. E., and Dancis, J. (1974) *Amer. J. Human Genet.* **26,** 272–273.

77. Sanchez, Y., Lovell, M., Marin, M. C., Wong, P., Wolf, M. E. L., McDonnell, T. J., and Killary, A. M., *Proc. Natl. Acad. Sci. USA* in press.

Proc. Natl. Acad. Sci. USA
Vol. 93, pp. 2551–2556, March 1996

Tumor suppression and apoptosis of human prostate carcinoma mediated by a genetic locus within human chromosome 10pter–q11

YOLANDA SANCHEZ*†, MERCEDES LOVELL*, MARIA C. MARIN‡, PATRICIA E. WONG*, M. ELIZABETH WOLF-LEDBETTER*§, TIMOTHY J. MCDONNELL‡, AND ANN MCNEILL KILLARY*¶

*Division of Laboratory Medicine, and ‡Division of Pathology, Department of Molecular Pathology, The University of Texas M. D. Anderson Cancer Center, Houston, TX 77030-4095

Communicated by Frank H. Ruddle, Yale University, New Haven, CT, November 13, 1995

ABSTRACT **Prostate cancer is the second leading cause of male cancer deaths in the United States. Yet, despite a large international effort, little is known about the molecular mechanisms that underlie this devastating disease. Prostate secretory epithelial cells and androgen-dependent prostate carcinomas undergo apoptosis in response to androgen deprivation and, furthermore, most prostate carcinomas become androgen independent and refractory to further therapeutic manipulations during disease progression. Definition of the genetic events that trigger apoptosis in the prostate could provide important insights into critical pathways in normal development as well as elucidate the perturbations of those key pathways in neoplastic transformation. We report the functional definition of a novel genetic locus within human chromosome 10pter–q11 that mediates both *in vivo* tumor suppression and *in vitro* apoptosis of prostatic adenocarcinoma cells. A defined fragment of human chromosome 10 was transferred via microcell fusion into a prostate adenocarcinoma cell line. Microcell hybrids containing only the region 10pter–q11 were suppressed for tumorigenicity following injection of microcell hybrids into nude mice. Furthermore, the complemented hybrids undergo programmed cell death *in vitro* via a mechanism that does not require nuclear localization of p53. These data functionally define a novel genetic locus, designated *PAC1*, for *prostate adenocarcinoma 1*, involved in tumor suppression of human prostate carcinoma and furthermore strongly suggest that the cell death pathway can be functionally restored in prostatic adenocarcinoma.**

The initiation and progression of human cancer is a multistep process that must involve genetic alterations of critical genes controlling the destiny of defined cell lineages with regard to cellular proliferation, differentiation, or death. Elucidation of the genetic mechanisms underlying these growth control processes is crucial to understanding the origins of the malignant state. Prostate cancer is the most common cancer in men and, with rising incidence, is the second leading cause of male cancer deaths in the United States (1, 2). The search for specific genetic changes associated with prostate cancer has failed to uncover a single high-frequency event (with the exception of overproduction of prostate-specific antigen).

Cytogenetic and loss of heterozygosity studies, however, have pointed to several regions of the human genome that could contain tumor suppressor genes involved in the etiology of prostate cancer (3–8). Allelotyping studies such as that of Kunimi *et al.* (4) in prostate adenocarcinoma indicate candidate regions to include chromosome 8p(50–65%), 10p(55%), 10q(30%), 16q(55–60%), and 18q(43%) (4). High-frequency loss of heterozygosity and homozygous deletion have been observed within chromosome 8p22 at the MSR locus in a prostate tumor (9). Recently, a candidate tumor suppressor gene *MXI1* was identified within 10q24 (10). Mutation of the *MXI1* gene, a negative regulator of the MYC oncoprotein, was found in 4 of 10 primary prostate tumors examined (10).

Cytogenetic analyses of human prostatic adenocarcinoma have also implicated nonrandom aberrations of several different human chromosomes. A recent study by Lundgren *et al.* (11) indicated consistent aberrations of chromosomes 1, 7, 8, and 10. Breakpoints were identified at 7q22 and 10q24. The cumulative findings of cytogenetic analysis and allele loss studies suggest a consistent association with genetic loci on a subset of human chromosomes, the most consistent correlations being with chromosomes 8 and 10 and prostate carcinoma.

For our experiments, a functional genetic approach was taken to identify tumor suppressor loci involved in prostate cancer. Previous studies have shown that it is possible to complement the genetic defect in particular human cancers, which show high-frequency allele loss on a defined chromosome, by the microcell fusion (12, 13) of a normal copy of that chromosome containing a putative tumor suppressor gene (14–21). We report that the introduction of human chromosome 10 or a subchromosomal fragment of 10 (encompassing 10pter–q11) into a prostate adenocarcinoma cell line resulted in a dramatic suppression of tumor formation following injection of hybrid clones into nude mice. Furthermore, we provide evidence that complemented hybrid clones undergo programmed cell death *in vitro* via a mechanism of apoptosis that does not require nuclear localization of p53. Induction of phagocytosis of apoptotic cells by neighboring prostate cells was observed *in vitro*, a process reminiscent of prostatic involution in response to androgen withdrawal (22, 23).

MATERIALS AND METHODS

Cell Lines and Construction of Hybrids. The prostatic adenocarcinoma cell line PC-3 was established from the poorly differentiated adenocarcinoma from a vertebral body metastasis in a patient with hormone-insensitive prostate cancer (24). The PC-3 cell line, obtained from the American Tissue Culture Collection, clearly contained two subpopulations of cells: one population containing a modal number of 60 and a second tetraploid population. PC-3 contained no recognizable chromosome 10 by G-banding analysis. A subcloned line (PC-3H) was isolated for these studies that contained a modal

The publication costs of this article were defrayed in part by page charge payment. This article must therefore be hereby marked "*advertisement*" in accordance with 18 U.S.C. §1734 solely to indicate this fact.

†Present address: Department of Biochemistry, Baylor College of Medicine, Houston, TX 77030.
§Present address: National Institutes of Health, National Center for Human Genome Research, Bethesda, MD 20892.
¶To whom reprint requests should be addressed at: Division of Laboratory Medicine, The University of Texas M. D. Anderson Cancer Center, 1515 Holcombe Boulevard, Box 72, Houston, TX 77030-4095.

number of 60 chromosomes and served as recipient for the transfer of human chromosome 10 or a defined region of chromosome 10 via microcell fusion.

The following microcell hybrids were used as donor lines for microcell transfer into PC-3H: HA(10)A, which contains an intact *neo*-marked human chromosome 10 in the A9 mouse cell background: HA(10p)A, which contains the region 10pter–q11 in the mouse A9 cell background. The centric fragment is dominantly marked with *neo*, which is integrated near the centromere on the long arm of chromosome 10: HA(8)A, a monochromosomal hybrid containing a *neo*-marked human chromosome 8 in the A9 cell background.

Microcell-Mediated Chromosome Transfer. Conditions for efficient micronucleation of A9-based hybrids and subsequent enucleation have been previously outlined (for review, see ref. 25). Fusion of HA(10)A or HA(10p)A microcells to recipient PC-3H cells was accomplished by a suspension microcell fusion technique (13, 25).

Characterization of Microcell Hybrid Clones. For chromosome painting, human chromosome 10-specific DNA from HA(10)A was amplified by PCR using inter-Alu primers (26). Hybridization and detection was carried out as described (21).

Tumorigenicity Assays. The PC-3H line and PC(10) series hybrids were injected at 5×10^6 cells into each of three 6- to 8-week-old athymic nude mice (Harlan). Injections were performed subcutaneously and tumor volumes were monitored biweekly using calipers as described (21).

Apoptosis Assays. The DNA laddering protocol was that of Fernandez *et al.* (27). Detection of DNA fragmentation *in situ* followed the procedure of Gavrieli *et al.* (28).

p53 Immunostaining and Western Blot Analysis. Immunostaining of p53 in PC-3H and PC(10) hybrids was accomplished using a mouse monoclonal antibody against human p53 (D01) (Santa Cruz Biotechnology). The bound antibody was detected with an anti-mouse antibody conjugated to horseradish peroxidase, according to the manufacturer's directions. BCL-2 protein levels were detected in parental and microcell hybrid clones by Western blot analysis as described by Hockenbery *et al.* (29).

RESULTS

Construction and Characterization of Monochromosomal Microcell Hybrid Clones. A subcloned line of the prostatic adenocarcinoma PC-3 was chosen as recipient for microcell fusion of human chromosome 10. PC-3H contained no intact copies of human chromosome 10; however, small fragments of chromosome 10 interspersed throughout the genome were apparent by chromosome painting using chromosome 10-specific DNA as a probe (Fig. 1*A*).

HA(10)A was used as a donor cell line for microcell fusion into PC-3H [PC(10) series hybrids]. Twenty hybrid clones isolated from a single microcell fusion experiment were examined by high-resolution cytogenetics for the presence of an intact chromosome 10. Twelve of 20 clones contained an intact human chromosome 10 (Fig. 1*B*).

Introduction of Human Chromosome 10 Results in Prostate Carcinoma Tumor Suppression. To test the effect of the introduced chromosome on the tumorigenic potential of the PC-3H cells, three PC(10) hybrids and parental PC-3H cells were injected subcutaneously in triplicate (at 5×10^6 cells per animal) into 6- to 8-week-old athymic nude mice. Tumor volumes were followed weekly and the tumors were excised 8 weeks postinjection and established in culture. The first of three separate nude mice experiments is illustrated in Table 1. Tumor volumes and tumor wet weights were calculated from an average of three animals injected per cell line tested. In the first series of injections, the parental subcloned line PC-3H was injected subcutaneously into each of six animals with an average tumor wet weight at the end of 65 days equal to 0.61 g.

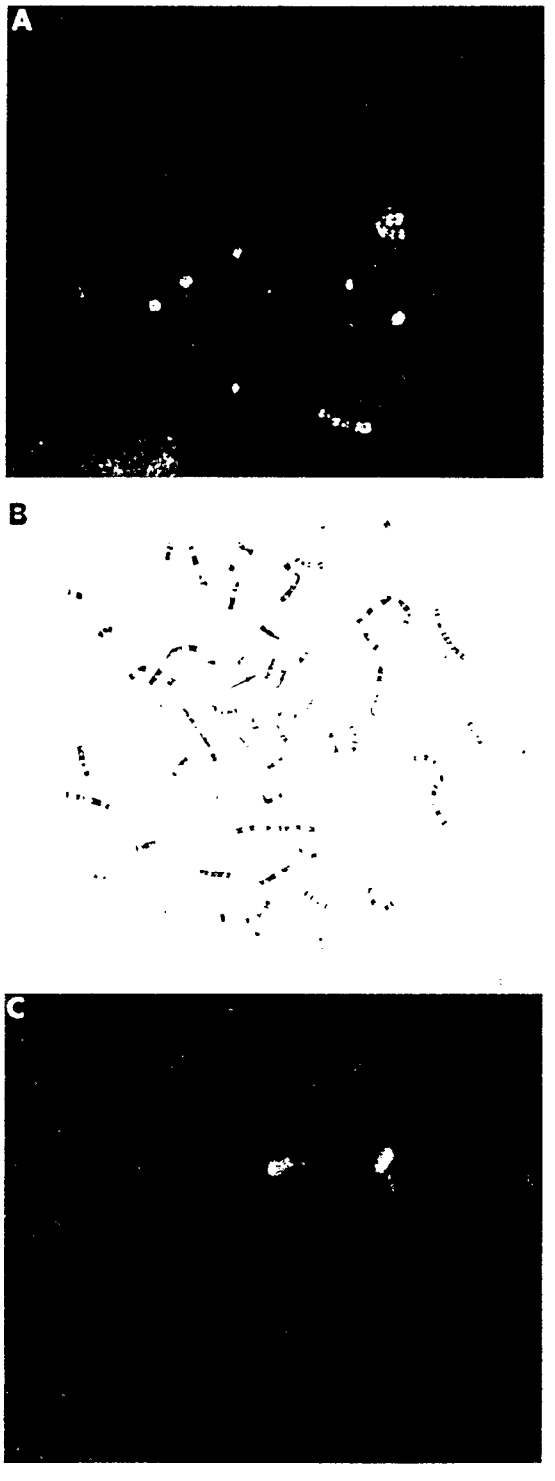

FIG. 1. Classical and molecular cytogenetic characterization of PC-3H cells and PC(10) series hybrids. (*A*) Chromosome 10-specific DNA used as a probe for the presence *in situ* hybridization on PC-3H. (*B*) High-resolution G-banding analysis of PC(10)7; arrow indicates human chromosome 10 in the PC-3H background. (*C*) Human DNA amplified using inter-Alu PCR from HA(10p)A used as probe onto normal human metaphases indicating the presence of 10pter–q11 in HA(10p)A.

In total, PC-3H was injected into 12 mice. Only 1 of the 12 mice injected failed to form any tumor. Eleven of the 12 mice injected consistently formed large tumors with average tumor wet weights in the range of 0.61–1.3 g (56–65 days postinjection). Injection of monochromosomal hybrids containing an intact chromosome 10 into athymic nude mice, however, showed dramatic tumor sup-

Table 1. Tumor incidence in PC hybrids 65 days postinjection

Cell line	Tumor vol. mm^3 (average ± SD)	Tumor wet weight, g (average ± SD)
PC-3H	730.79 ± 179.05	0.61 ± 0.17
PC-3H*	655.38 ± 86.61	0.62 ± 0.05
PC(10)1	413.40 ± 191.89	0.42 ± 0.17
PC(10)2	60.83 ± 93.92	0.06 ± 0.07
PC(10)7	70.83 ± 14.43	0.05 ± 0.04
PC(10p)C	119.42 ± 111.51	0.08 ± 0.09
PC(10p)D*	24.22 ± 3.93	0.01 ± 0.02

*One of three mice injected died postinjection. Average is based on two animals.

pression (Fig. 2 and Table 1). Two of three PC(10) hybrids (PC(10)2 and PC(10)7) showed >10-fold suppression of tumor formation relative to parental PC-3H cells. The average tumor wet weights of three animals injected per cell line were 0.06 and 0.05 g, respectively (Table 1). The remaining PC(10)1 hybrid formed tumors of intermediate size between PC-3H and the suppressed PC(10) clones. PC(10)1 contained an intact chromosome 10 at the time of injection. However, an increase in chromosome instability was clearly evident in this clonal population. Fourteen percent of metaphases examined in PC(10)1 showed evidence of chromosome breakage compared with 4% in PC(10)2 and 2% in PC(10)7. Thus, an increased chromosome instability, leading to a more rapid loss of the introduced chromosome from the cells *in vivo*, could potentially explain the intermediate tumor suppression observed in PC(10)1. Cytogenetic analysis performed on tumors from hybrid clones explanted on day 65 indicated loss of the introduced chromosome 10 in 100% of metaphases examined in each of three PC(10) clones (data not shown). In fact, in one experiment, tumor volumes for PC(10)7 increased from 54.1 mm^3 at day 51 to 228 mm^3 at day 58, indicating a more rapid expansion of the hybrid population *in vivo* at the end of the experiment concomitant with loss of the introduced chromosome. Thus, introduction of chromosome 10 into PC-3H resulted in a suppression of the malignant phenotype *in vivo*; furthermore, loss of the introduced chromosome was found in all hybrid metaphases derived from the explanted tumors, indicating that tumor suppression was dependent on retention of the normal copy of chromosome 10. These data define a functional tumor suppressor locus within chromosome 10 involved in the etiology of human prostate cancer.

Fragment-Containing Microcell Hybrids Used to Limit the Region Within Chromosome 10 Containing a Functional Tumor Suppressor Gene. To regionally localize the tumor suppressor gene within chromosome 10, microcell hybrid clones were first constructed in the A9 cell background carrying a deletion of the introduced chromosome 10. The HA(10) series hybrids were first rescreened to detect any clones that might contain a deletion of the introduced chromosome in the A9 cell background. One hybrid clone, HA(10p)A, was obtained that contains a large terminal deletion of most of the long arm of chromosome 10 and retains only the region 10pter–q11 by high-resolution cytogenetics as well as by chromosome painting using HA(10p)A as a probe onto normal human metaphases (Fig. 1*C*). HA(10p)A was then used as a donor cell line to transfer this small *neo*-marked centric fragment of chromosome 10 into PC-3H [PC(10p) series hybrids].

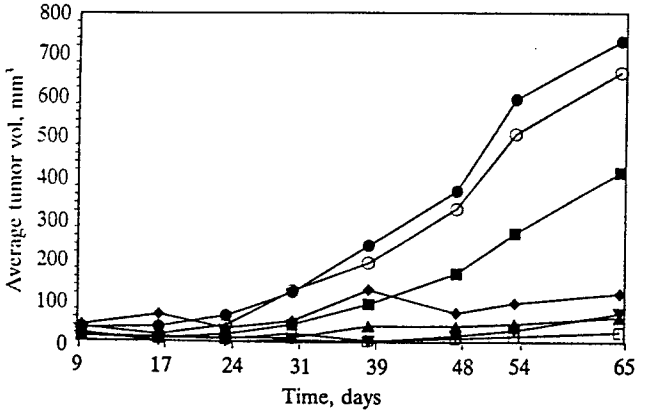

FIG. 2. Tumor volumes postinjection of hybrid and parental lines into nude mice. ●, PC-3H; ○, PC-3H; ■, PC(10)1; ▲, PC(10)2; ▼, PC(10)7; ◆, PC(10p)C; □, PC(10p)D.

Two PC(10p) hybrid clones containing the introduced region 10pter–q11 in the PC-3H background were each injected into three athymic nude mice along with PC(10)7 and PC-3H cells. As illustrated in Fig. 2 and Table 1, the introduction of the region 10pter–q11 mediated tumor suppression equivalent to that observed with the introduction of the intact chromosome 10. This experiment was repeated using PC(10p)C and PC(10p)D for a total of six mice injected and PC(10)7 for a total of nine mice injected. Consistent tumor suppression was observed following introduction of chromosome 10 and chromosome 10pter–q11. These results regionally define a genetic locus within human chromosome 10 involved in the etiology of prostate cancer. We have designated this genetic locus *PAC1*, for prostatic adenocarcinoma 1.

A Genetic Locus Within Chromosome 10pter–q11 Restores the Programmed Cell Death Pathway in Prostate Carcinoma Cells. In addition to the functional studies *in vivo*, we further examined the PC(10) and PC(10p) series hybrids for growth *in vitro* in an attempt to provide insight into the mechanism of action of *PAC1*. The first clues to the phenotypic changes in PC-3H growth *in vitro* were evident upon clonal expansion of PC(10) hybrids. Nine of 17 PC(10) clones died following expansion from six-well plates at one to three absolute passages *in vitro*. We hypothesized that both *in vitro* cell death and *in vivo* tumor suppression could be explained if the genetic complementation in the PC(10) series clones was the result of activation of a cell death program. In this regard, prostatic secretory epithelial cells and androgen-dependent prostate carcinomas undergo apoptosis in response to androgen deprivation (22, 23). Furthermore, during disease progression most prostate carcinomas become androgen independent and refractory to further therapeutic manipulations (30). To test whether genes on chromosome 10 could restore the cell death pathway in PC-3H, three PC(10) clones and two fragment-containing clones PC(10pter–q11) clones were expanded for *in vitro* apoptosis assays. As a control, a hybrid was also constructed containing an intact *neo*-marked human chromosome 8 in the PC-3H background [PC(8)B]. DNAs isolated from these hybrids and PC-3H were analyzed by agarose gel electrophoresis for the presence of the characteristic DNA ladder indicative of apoptosis. All hybrids containing chromosome 10 as well as all fragment-containing hybrids displayed the typical endonuclease-induced DNA fragmentation often seen in cells undergoing apoptosis (30, 31). DNA ladders were observed in all hybrids even in 10% serum, whereas no laddering was observed in PC-3H or PC(8)B using the same conditions (Fig. 3).

Hybrid clones were also analyzed by the TUNEL technique to visualize DNA fragmentation *in situ*. Significantly, all PC(10) and PC(10p) hybrids examined showed positive staining that indicated not only the presence of fragmented chromatin but also of apoptotic bodies (Fig. 4 *A* and *B*). TUNEL staining detected fragmented chromatin and apoptotic bodies in the cytoplasm of hybrid cells with intact nuclei, suggesting that cells undergoing apoptosis were being phagocytized by neighboring cells with intact nuclei (Fig. 4 *A* and *B*). Phagocytosis of apoptotic cells has been commonly observed *in vivo*.

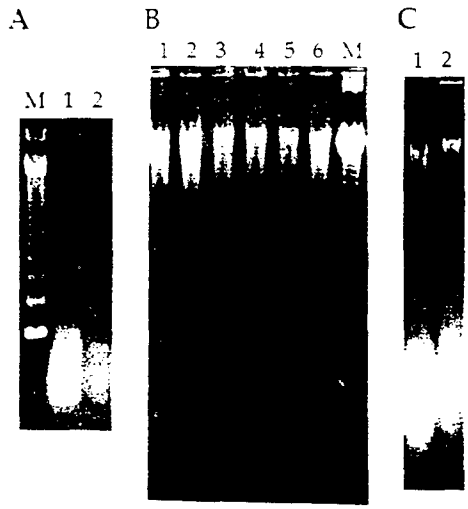

FIG. 3. Induction of apoptosis in PC(10) and PC(10p) microcell hybrids. (*A*) PC-3H (lanes 1 and 2). (*B*) PC(10)7 (lanes 1 and 2), PC(10p)D (lanes 3 and 4), and PC(10p)C (lanes 5 and 6). (*C*) PC(8)B (lanes 1 and 2). Growth conditions were in either 10% fetal bovine serum (odd-numbered lanes) or 0.1% fetal bovine serum (even-numbered lanes). Lanes M, size markers.

and it is thought to be an efficient clearing mechanism to rid the developing tissue of large numbers of dying cells (22, 23, 31, 32). Electron microscopic analysis confirmed TUNEL studies and indicated apoptosis and phagocytosis in PC(10) and PC(10p) series hybrids (data not shown). These data functionally define a genetic locus within human chromosome 10pter–q11 that directs the programmed cell death of prostatic carcinoma cell line PC-3H. Furthermore, results from these studies strongly suggest that one mechanism of *PAC1*-mediated tumor suppression could be by induction of apoptosis. Finally, by analyses of these defined microcell hybrids, we have shown that the cell death pathway can be functionally restored in prostatic adenocarcinoma.

Apoptosis in PC(10) Series Hybrids Is Independent of Nuclear Localization of p53 or Downregulation of *BCL2*. The protein product of the tumor suppressor gene p53 has been shown to have a major role in regulation of apoptosis in other systems (33). Alterations in the p53 gene and aberrant expression of p53 protein have been associated with poorly differentiated, metastatic, androgen-independent prostatic tumors (34–37). For these reasons, hybrid clones were examined for changes in levels of p53 protein coincident with the introduction of the region 10pter–q11 into PC-3H cells. Immunohistochemistry was carried out to detect p53 protein in the PC-3H and PC(10) hybrid clones. Cells were cultured *in vitro* using conditions similar to those used to detect DNA fragmentation and then incubated with a monoclonal antibody against p53 (DO1) and a secondary antibody conjugated to horseradish peroxidase. No detectable p53 protein was observed in PC-3H cells (Fig. 5*A*) when cells were grown in 10% or 0.1% fetal bovine serum. However, clearly detectable p53 protein was observed in hybrids containing either the intact human chromosome 10 or the 10pter–q11 region (Fig. 5 *C* and *D*). These data suggest that either the transcription of p53 is upregulated or the p53 protein is stabilized in response to introduction of a genetic locus within chromosome 10. p53 protein, however, fails to localize to the nucleus in hybrid cells.

In addition to its role in induction of apoptosis, wild-type p53 seems to be required for induction of G_1 arrest in the mammalian cell cycle. Rapid induction of stable p53 protein following UV irradiation of cells has been documented and suggests that the p53 pathway is required as a checkpoint in G_1 to prevent entry into S phase until UV-damaged DNA can be repaired (38). To determine whether p53 in PC-3H cells is capable of nuclear localization, UV was used to induce up-

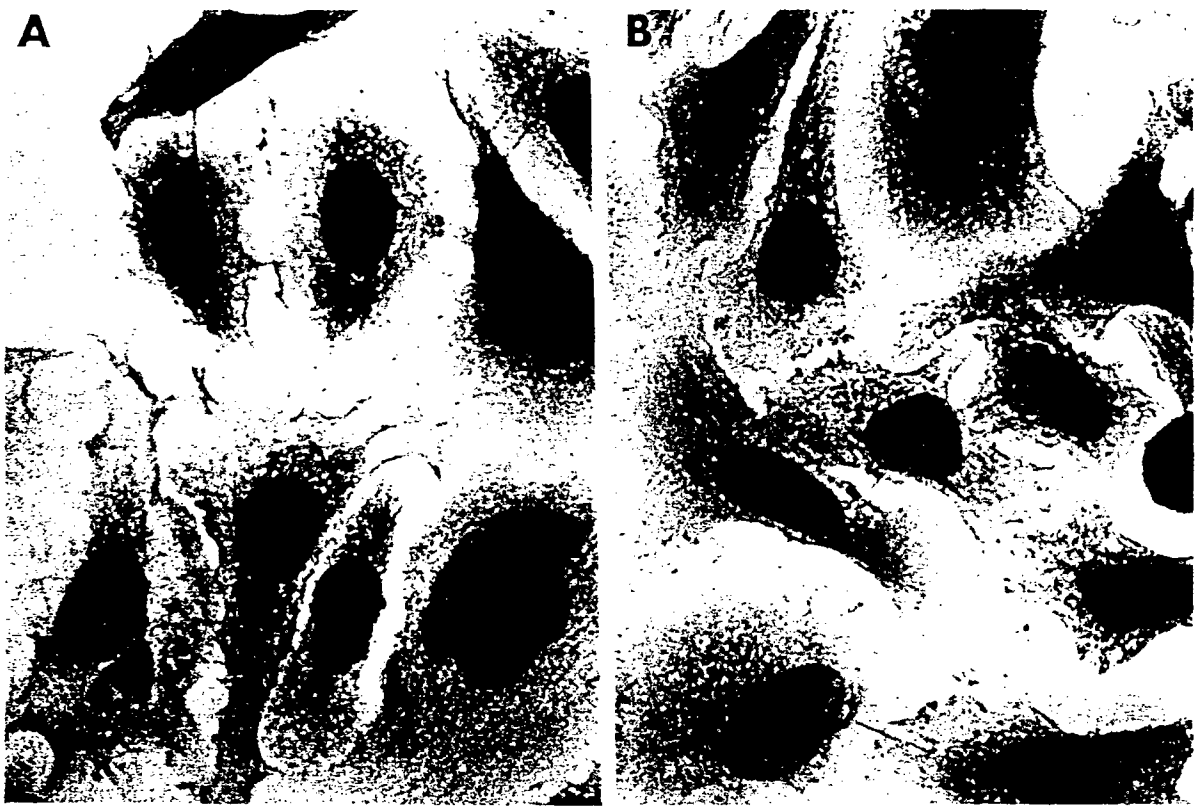

FIG. 4. Detection of DNA fragmentation *in situ* and phagocytosis in prostate hybrid cells. (*A* and *B*) Presence of apoptotic bodies and phagocytosis in PC(10) series hybrids.

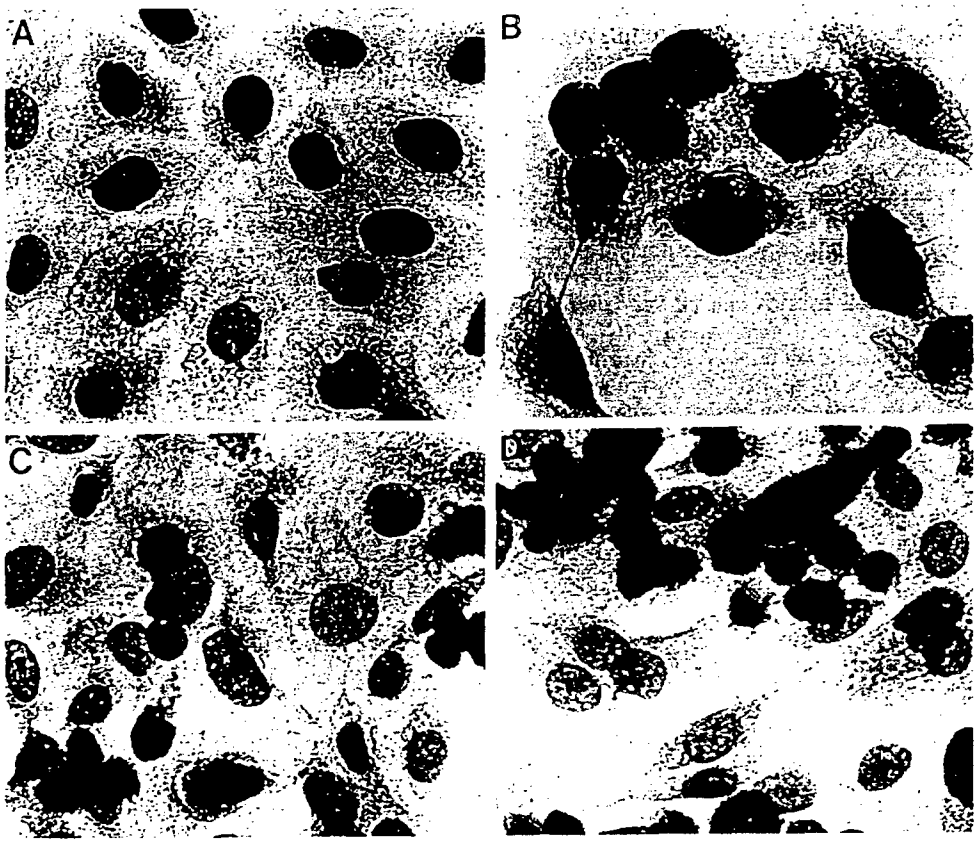

FIG. 5. Immunostaining of p53 in prostate and hybrid cells. (*A*) PC-3H. (*B*) PC-3H 6 hr post-UV irradiation with 50 J/m^2. (*C*) Microcell hybrid PC(10)2. (*D*) PC(10p)C.

regulation of p53 in PC-3H cells. PC-3H cells were irradiated with UV radiation (50 J m^{-2}). As a control, LNCaP cells, another prostatic adenocarcinoma line, and early passage human fibroblasts were also irradiated under the same conditions. Six hours post-UV irradiation, p53 protein was detected in the nuclei of primary human fibroblasts and LNCaP cells as expected for wild-type p53 (data not shown); however, in PC-3H cells, p53 protein was highly expressed only in the cytoplasm (Fig. 5*B*). Thus, p53 protein in PC-3H cells is upregulated by introduction of chromosome 10, chromosome 10pter–q11, and presumably *PAC1*; however, the p53 protein localizes to the cytoplasm.

Apoptotic cell death in PC(10) and PC(10p) hybrids could also be the result of *PAC1*-directed downregulation of *BCL2*, a protooncogene that has been shown to rescue certain cell types from apoptotic death (34, 35). Previous work has shown that *BCL2* is not expressed in normal prostate secretory epithelial cells. However, *BCL2* is highly expressed in relapsed, androgen-independent prostate cancers (30). To address the involvement of *BCL2* in this system, levels of BCL2 protein in PC-3H and PC(10) hybrids were studied by Western blot analysis (data not shown). Results indicated that BCL2 protein is expressed at basal levels in PC-3H and hybrid cells. These data indicate that PC-3H cells are not refractory to apoptosis due to upregulation of *BCL2* and that the induction of a cell death pathway in PC(10) and PC(10p) hybrids does not involve downregulation of *BCL2*.

DISCUSSION

Our studies indicate the involvement of the genetic locus *PAC1* in the tumor suppression and induction of apoptosis in the prostate adenocarcinoma cell line PC-3H. This study provides functional evidence for a tumor suppressor gene within human chromosome 10 involved in prostate cancer. We furthermore show that the pathway to programmed cell death can be functionally restored in PC-3H and implicate a novel mechanism that does not require nuclear localization of p53. A previous report documented that PC-3 contains an exon 5 mutation in p53 that would cause a frameshift in the amino acid sequence (39). Sequence analysis in our laboratory has confirmed the exon 5 mutation in codon 138 in the subcloned line PC-3H. The frameshift mutation generates a premature stop codon in exon 5, well before the nuclear localization signal in exon 10 (A.M.K., unpublished results). The consequence of this mutation would then be a truncated p53 protein that localizes to the cytoplasm. We furthermore report upregulation of p53 protein in PC-3H in response to UV and following the introduction of *PAC1*, although the p53 protein remains in the cytoplasm. One possible explanation for these results could be that p53 has a nontranscriptional activation-dependent role in apoptosis as proposed by Caelles and coworkers (40), perhaps in a cytoplasmic signaling pathway. An alternative explanation is that the tumor suppression and apoptosis in PC-3H cells does not require wild-type p53. In this regard, previous work has shown that the programmed cell death of murine androgen-dependent prostatic glandular cells *in vivo* following androgen ablation does not require wild-type p53 (41). However, the apoptosis observed in these *in vivo* studies was the result of growth factor withdrawal; the cell death phenotype in the PC(10) and PC(10p) hybrids does not require an inducing agent. These results, then, taken together would suggest that the tumor suppressor locus within 10pter–q11 mediates its effect on apoptosis either independently or upstream of p53. Supportive of these data is the finding that p53 mutations in prostate cancer have been found in the later stages of disease (35–36).

Definition of *PAC1* was made possible by the use of genetic complementation via microcell fusion experiments. Although allele loss studies and cytogenetic analysis can

implicate specific chromosomal regions as sites for putative tumor suppressor loci. these studies point to multiple regions on different chromosomes that are potentially involved in prostate cancer. Microcell fusion of defined chromosomal regions can functionally define the region containing tumor suppressor genes important in the genesis of this cancer. In addition. these studies and others indicate that complemented microcell hybrid clones are valuable to gain insight into the phenotypic changes *in vitro* and *in vivo* that accompany the introduction of a single copy of the normal genetic locus.

Defined deletion microcell hybrids can be very useful as starting materials for the physical mapping of *P4C1* and to determine whether subsequent deletions in PC hybrids allow separation of the phenotypes of tumor suppression and apoptosis or indicate single gene involvement. Such deletion hybrids should be extremely valuable in combination with functional assays to isolate candidate tumor suppressor genes involved in prostate cancer.

A.M.K. is supported by grants from the National Institutes of Health and The University of Texas M. D. Anderson Physicians Referral Service. Y.S. was supported by National Institutes of Health Postdoctoral Fellowship CA09299. T.J.M. is a Pew Scholar in the Biomedical Sciences and is supported by CAPCURE. The Association for the Cure of Cancer of the Prostate. M.C.M. is supported by National Institutes of Health Predoctoral Fellowship CA09255.

1. Boring. C. C.. Squires. T. S. & Tong. T. (1991) *Cancer J. Clin.* **41.** 19–36.
2. Isaacs. J. T. (1993) *Cancer Metast. Rev.* **12.** 1–2.
3. Bergerheim. U. S. R.. Kunimi. K.. Collins. V. P. & Ekman. P. (1991) *Genes Chromosomes Cancer* **3.** 215–220.
4. Kunimi. K., Bergerheim. U. S. R., Larsson. I.-L.. Ekman. P. & Collins. V. P. (1991) *Genomics* **11.** 530–536.
5. Brothman. A. R.. Peehl. D. M.. Patel. A. M. & McNeal. J. E. (1990) *Cancer Res.* **50.** 3795–3803.
6. Brothman. A. R.. Peehl. D. M.. Patel. A. M.. MacDonald. G. R., McNeal. J. E.. Ladaga. L. E. & Schellhammer. P. F. (1991) *Cancer Genet. Cytogenet.* **55.** 79–84.
7. Carter. B. S.. Ewing. C. M.. Ward. W. S.. Treiger. B. F., Aalders. T. W.. Schalken. J. A.. Epstein. J. I. & Isaacs. W. B. (1990) *Proc. Natl. Acad. Sci. USA* **87.** 8751–8755.
8. Micale. M. A.. Mohamed. A.. Sakr. W.. Powell. I. J. & Wolman. S. R. (1992) *Cancer Genet. Cytogenet.* **61.** 165–173.
9. Bova. G. S.. Carter. B. S.. Bussemakers. M. J. G.. Emi. M.. Fujiwara. Y.. Kyprianou. N.. Jacobs. S. C.. Robinson. J. C., Epstein. J. I.. Walsh. P. C. & Isaacs. W. B. (1993) *Cancer Res.* **53.** 3869–3873.
10. Eagle. L. R.. Yin. X.. Brothman. A. R.. Williams. B. J.. Atkin. N. B. & Prochownik. E. V. (1995) *Nature Genet.* **9.** 249–255.
11. Lundgren. R.. Mandahl. N.. Heim. S.. Limon. J.. Henrikson. H. & Mitelman. F. (1992) *Genes Chromosomes Cancer* **4.** 16–24.
12. Fournier. R. E. K. & Ruddle. F. H. (1977) *Proc. Natl. Acad. Sci. USA* **74.** 319–323.
13. McNeill. C. A. & Brown. R. L. (1980) *Proc. Natl. Acad. Sci. USA* **77.** 5394–5398.
14. Saxon. P. J.. Srivatsan. E. S. & Stanbridge. E. J. (1986) *EMBO J.* **5.** 3461–3466.
15. Oshimura. M.. Kugoh. H.. Koi. M.. Shimizu. M.. Yamada. H.. Satoh. H. & Barrett. J. C. (1990) *J. Cell. Biochem.* **42.** 135–142.
16. Weissman. B. E.. Saxon. P. J.. Pasquale. S. R.. Jones. G. R.. Geiser. A. G. & Stanbridge. E. J. (1987) *Science* **236.** 175–180.
17. Trent. J. M.. Stanbridge. E. J.. McBride. H. L.. Meese. E. U.. Casey. G.. Araujo. D. E.. Witkowski. C. M. & Nagle. R. B. (1990) *Science* **247.** 568–571.
18. Tanaka. K.. Oshimura. M.. Kikuchi. R.. Seki. M.. Hayashi. T. & Miyaki. M. (1991) *Nature (London)* **349.** 340–342.
19. Shimizu. M.. Yokota. J.. Mori. N.. Shuin. T.. Shinoda. M.. Terada. M. & Oshimura. M. (1990) *Oncogene* **5.** 185–194.
20. Killary. A. M.. Wolf. M. E.. Giambernardi. T. A. & Naylor. S. L. (1992) *Proc. Natl. Acad. Sci. USA* **89.** 10877–10881.
21. Sanchez. Y.. El-Naggar. A.. Pathak. S. & Killary. A. M. (1994) *Proc. Natl. Acad. Sci. USA* **91.** 3383–3387.
22. Kerr. J. F. R. & Searle. J. (1973) *Virchows Arch. Abt. B. Zellpath.* **13.** 87–102.
23. Helminen. H. J. & Ericsson. J. L. E. (1972) *J. Ultrastruct. Res.* **39.** 443–455.
24. Kaighn. M. E.. Narayan. K. S.. Ohnuki. Y.. Lechner. J. F. & Jones. L. W. (1979) *Invest. Urol.* **17.** 16–23.
25. Killary. A. M. & Fournier. R. E. K. (1995) *Methods Enzymol.* **254.** 133–152.
26. Liu. P.. Siciliano. J.. Seong. D.. Craig. J.. Zhao. U.. deJong. P. J. & Siciliano. M. J. (1993) *Cancer Genet. Cytogenet.* **65.** 93–99.
27. Fernandez. A.. Marin. M. C.. McDonnell. T. J. & Ananthaswamy. H. N. (1994) *Oncogene* **9.** 2009–2017.
28. Gavrieli. Y.. Sherman. Y. & Ben-Sasson. S. A. (1992) *J. Cell Biol.* **119.** 493–501.
29. Hockenbery. D.. Nunez. G.. Milliman. C.. Schreiber. R. D. & Korsmeyer. S. J. (1990) *Nature (London)* **348.** 334–336.
30. McDonnell. T. J.. Troncoso. P.. Brisbay. S. M.. Logothetis. C.. Chung. L. W.. Hsieh. J. T.. Tu. S. M. & Campbell. M. L. (1992) *Cancer Res.* **52.** 6940–6944.
31. Wyllie. A. H.. Kerr. J. F. R. & Currie. A. R. (1980) *Int. Rev. Cytol.* **68.** 251–306.
32. Ellis. R. E.. Yuan. J. & Horvitz. H. R. (1991) *Annu. Rev. Cell Biol.* **7.** 663–698.
33. Yonish-Rouach. E.. Resnitzky. D.. Lotem. J.. Sachs. L.. Kimchi. A. & Oren. M. (1991) *Nature (London)* **352.** 345–347.
34. Navone. N. M.. Troncoso. P.. Pisters. L. L.. Goodrow. T. L.. Palmer. J. L.. Nichols. W. W.. Von Eschenbach. A. C. & Conti. C. J. (1993) *J. Natl. Cancer Inst.* **85.** 1657–1665.
35. Bookstein. R.. MacGrogan. D.. Hilsenbeck. S. G.. Sharkey. F. & Allred. D. C. (1993) *Cancer Res.* **53.** 3369–3373.
36. Bookstein. R. & Allred. D. C. (1993) *Cancer* **71.** Suppl.. 1179–1186.
37. Effert. P. J.. Neubauer. A.. Walther. P. J. & Liu. E. T. (1992) *J. Urol.* **147.** 789–793.
38. Lu. X. & Lane. D. P. (1993) *Cell* **75.** 765–778.
39. Isaacs. W. B.. Carter. B. S. & Ewing. C. M. (1991) *Cancer Res.* **51.** 4716–4720.
40. Caelles. C.. Helmberg. A. & Karin. M. (1994) *Nature (London)* **370.** 220–223.
41. Berges. R. R.. Furuya. Y.. Remington. L.. English. H. F.. Jacks. T. & Isaacs. J. T. (1993) *Proc. Natl. Acad. Sci. USA* **90.** 8910–8914.

[CANCER RESEARCH 59, 2182–2189, May 1, 1999]

The Genetic Locus *NRC-1* within Chromosome 3p12 Mediates Tumor Suppression in Renal Cell Carcinoma Independently of Histological Type, Tumor Microenvironment, and *VHL* Mutation[1]

Mercedes Lovell, Steven Trent Lott, Patricia Wong, Adel El-Naggar, Susan Tucker, and Ann McNeill Killary[2]

Section of Experimental Laboratory Medicine, Departments of Laboratory Medicine [M. L., S. T. L., P. W., A. M. K.] and Pathology [A. E-N.], Division of Pathology and Laboratory Medicine and Department of Biomathematics [S. T.], The University of Texas M. D. Anderson Cancer Center, Houston, Texas 77030-4095

ABSTRACT

Human chromosome 3p cytogenetic abnormalities and loss of heterozygosity have been observed at high frequency in the nonpapillary form of sporadic renal cell carcinoma (RCC). The *von Hippel-Lindau (VHL)* gene has been identified as a tumor suppressor gene for RCC at 3p25, and functional studies as well as molecular genetic and cytogenetic analyses have suggested as many as two or three additional regions of 3p that could harbor tumor suppressor genes for sporadic RCC. We have previously functionally defined a novel genetic locus *nonpapillary renal carcinoma-1 (NRC-1)* within chromosome 3p12, distinct from the *VHL* gene, that mediates tumor suppression and rapid cell death of RCC cells *in vivo*. We now report the suppression of tumorigenicity of RCC cells *in vivo* after the transfer of a defined centric 3p fragment into different histological types of RCC. Results document the functional involvement of *NRC-1* in not only different cell types of RCC (*i.e.*, clear cell, mixed granular cell/clear cell, and sarcomatoid types) but also in papillary RCC, a less frequent histological type of RCC for which chromosome 3p LOH and genetic aberrations have only rarely been observed. We also report that the tumor suppression observed in functional genetic screens was independent of the microenvironment of the tumor, further supporting a role for *NRC-1* as a more general mediator of *in vivo* growth control. Furthermore, this report demonstrates the first functional evidence for a *VHL*-independent pathway to tumorigenesis in the kidney via the genetic locus *NRC-1*.

INTRODUCTION

Genetic abnormalities in RCC[3] have indicated a consistent involvement of chromosome 3 loci in the genesis of the disease. High frequency LOH as well as cytogenetic aberrations involving the short arm of human chromosome 3 have been observed in the vast majority of sporadic RCCs (1, 2). The familial form of RCC involves defined translocation events with breakpoints in 3p (3). These types of analyses in combination with functional genetic approaches have suggested as many as three separate regions within 3p that could harbor tumor suppressor genes for RCC.

The most distal region of 3p (3p25) contains the *VHL* gene. Inheritance of the *VHL* gene predisposes to the development of a number of different tumor types including spinal hemangioblastomas, retinal angiomas, pheochromocytomas, as well as renal and pancreatic cysts (4). The *VHL* gene is mutated in 57% of sporadic RCC, suggesting an important role for *VHL* in the sporadic form of RCC as well (5). Introduction of the *VHL* cDNA into RCC cell lines has functionally indicated that *VHL* is a tumor suppressor gene for RCC (6).

Genetic alterations in lung cancer, as well as renal cell, ovarian, uterine cervical, and testicular carcinoma, implicate a 3p region more proximal than 3p25 to contain a putative tumor suppressor gene. High frequency LOH has been reported in SCLC (100%), RCC (95–100%), and ovarian carcinoma (57%) in the 3p21.1–3 region (1–2, 7–10). Functional genetic screens developed in our laboratory were used to identify regions of 3p with tumor suppressor functional activity. For these experiments, a defined fragment of 3p was identified in microcell hybrids generated in the A9 fibrosarcoma background which suppressed tumor formation in athymic nude mice (11). The region of functional tumor suppressor activity was first limited to a 2-Mb region within 3p21-p22 (11) and later refined by Daly (12) and others (13) within 3p21.3 by detection of homozygous deletion in SCLC.

In addition to the 3p21.3 region, high frequency LOH in the region 3p13–14.2 has also been documented (14, 15). Furthermore, the breakpoint region in familial RCC lies within 3p14. Recently, the *FHIT* gene was isolated from the breakpoint region in familial RCC and includes the FRA-3B region, which is the most common fragile site in the human genome (16). Multiple deletions and alternative transcripts have been observed in a number of different tumor types.

Evidence for a tumor suppressor gene in the 3p region proximal to FHIT has been shown by our previous functional studies in which we transferred an intact human chromosome 3 and subsequently a centric fragment of 3p (encompassing the 3p14–q11 region by cytogenetic analysis) into a nonpapillary RCC line SN12C.19 (17). In all experiments, the 3p centric fragment mediated a dramatic tumor suppression and rapid induction of tumor cell death after s.c. injection of microcell hybrids in athymic nude mice (17). Physical mapping of suppressed and unsuppressed fragment-containing microcell hybrids limited the region containing the tumor suppressor locus *NRC-1* to within 3p12 and distinct from the *VHL* gene (18). The *NRC-1* critical region directly overlaps a 5–7-Mb homozygous deletion region observed in the SCLC line U2020 (19). Thus, either the most proximal region of 3p contains multiple genes, each involved in different tumor types, or there is a more general tumor suppressor gene in this interval.

One of the critical questions to be addressed regarding the putative 3p tumor suppressor genes, then, is whether there is a cell type specificity to their involvement in the kidney and more broadly within the diverse histological tumors for which 3p LOH has been documented. The criteria for classification of renal cell tumors is based largely on histopathological parameters and does not seem to correlate directly with clinical outcome. Renal cell tumors are classified by histological observation as either papillary or nonpapillary (including tumors of solid, alveolar, tubular, or cystic) origin (20). Cell types of RCC include clear cell, granular cell, mixed (clear and granular) cell, pleomorphic, and spindle type (20). Most reports of LOH and cytogenetic alterations within 3p in sporadic RCC have involved the more common nonpapillary form. Few reports have indicated an association between 3p cytogenetic aberrations or high frequency LOH and the papillary form, indicating a possible cell type specificity for the 3p genes in RCC. Additional support for cell type specificity in different

Received 8/6/98; accepted 3/4/99.

The costs of publication of this article were defrayed in part by the payment of page charges. This article must therefore be hereby marked *advertisement* in accordance with 18 U.S.C. Section 1734 solely to indicate this fact.

[1] This work was supported by NIH Grant CA62027 (to A. M. K.). S. T. L. was supported by National Cancer Institute Training Grant 5 T32 CA-09299-18.

[2] To whom requests for reprints should be addressed, at Section of Experimental Laboratory Medicine, Box 54, Division of Pathology and Laboratory Medicine, University of Texas M. D. Anderson Cancer Center, 1515 Holcombe Boulevard, Houston, TX 77030-4095. Phone: (713) 792-7833; Fax: (713) 794-1294; E-mail: akillary@odin.utmdacc.tmc.edu.

[3] The abbreviations used are: RCC, renal cell carcinoma; LOH, loss of heterozygosity; VHL, von Hippel-Lindau; NRC-1, nonpapillary renal carcinoma-1; SCLC, small cell lung carcinoma; SSCP, single strand conformational polymorphism.

histological RCCs has been shown in that an inherited form of papillary RCC has been characterized that involves a t(X;1) translocation as well as an t(X;17) translocation, unlike the nonpapillary familial form, which has been characterized by 3p translocation events (21). Kovacs (22), in fact, has proposed a new classification system for renal tumors based on cytogenetics and LOH indicating that 3p cytogenetic aberrations are consistent only with the nonpapillary form and not the papillary. The implications of this system would be toward the use of LOH for diagnosis of RCC and classification of tumors by histological type.

Thus, much evidence supports a cell type specificity to the RCC tumor suppressor genes on 3p. However, more recent reports document 3p LOH in papillary RCC (two of seven; Ref. 23). One allelotyping study indicated that although no 3p LOH was observed in papillary RCC, that the remainder of genome wide losses on chromosomes 6q, 8p, 9p, 9q, and 14q were found in both papillary and nonpapillary RCCs (24). These data suggest that, other than chromosome 3 involvement, the remainder of high frequency losses suggest a common pathway to tumorigenesis in papillary and nonpapillary RCC. However, only three markers on 3p were tested in this allelotyping study, none of which mapped into the most proximal 3p region. Although no high frequency cytogenetic alteration within 3p has been observed in papillary RCC, Hughson *et al.* (25) reported a papillary RCC with two normal copies of 3 that showed significant 3p LOH by RFLP analysis. Their data indicated that one copy of chromosome 3 was lost, followed by a nondisjunction event that placed two copies of the remaining chromosome in the tumor. Thus, two apparently normal copies of 3 were observed cytogenetically, with LOH observed in 3p and 3q. These data suggest that chromosome 3 loss/nondisjunction events could be a mechanism involved in the genesis of papillary RCC. It therefore remains to be definitively determined whether chromosome 3p loci play a role in all types of kidney cancer.

We now present extensive data to document that the chromosome 3p12 locus *NRC-1* functionally suppresses tumors in RCC regardless of the histological type of RCC or the microenvironment of the tumor. Furthermore, because *NRC-1* maps within the 3p12 homozygous deletion region in SCLC, these functional studies predict the potential involvement of *NRC-1* in different histological cancers as well. Results from this study, furthermore, provide evidence that *NRC-1* suppresses tumor formation of RCC in the presence of a *VHL* mutation and thus provide the first functional evidence for a *VHL*-independent pathway to renal tumorigenesis via *NRC-1*.

MATERIALS AND METHODS

Cell Lines. The A498 cell line was isolated from the primary kidney tumor of a 52-year-old female (26). The KRC-7 line was established in our laboratory from a primary kidney tumor and is a nonpapillary RCC of sarcomatoid origin.[4] The SN12C.19 line is a subcloned line of SN12C, derived from a mixed clear cell, granular cell nonpapillary RCC (27). The HA(3)IIaa cell line contains the introduced 3p centric fragment in the A9 mouse fibrosarcoma cell background (17). Cell lines were maintained in DMEM (high glucose)/F12 medium containing 10% fetal bovine serum. In addition, HA(3)IIaa and all microcell hybrids derived from the transfer of the 3p centric fragment were cultured in 500 μg/ml G418.

Microcell Fusion. Microcell fusion using A9-based microcell hybrids containing single neo-tagged human chromosomes has been described previously (28). Briefly, micronucleation of donor HA(3)IIaa was accomplished by 48-h mitotic arrest using 0.06 μg/ml Colcemid. Enucleation of micronucleate populations was accomplished using 10 μg/ml cytochalasin B and centrifugation (27,000 × *g* for 70 min). Microcells were filtered through 5- and 3-μm nucleopore filters to eliminate whole cells and enucleated whole cells and to select for the smallest of the microcells, corresponding to the transfer of single chromosomes.

Cytogenetic Analysis. G-11 analysis of hybrid lines followed the protocol of Bobrow (29). G-banding analysis was performed as described (30).

Microsatellite Analysis. Microsatellite polymorphism analysis followed the method of Lott *et al.* (18). Microsatellite PCR was performed using primers synthesized by Research Genetics (Huntsville, AL). Before amplification, the forward primer was end labeled with ^{32}P by T4 polynucleotide kinase (Promega, Madison, WI). PCR amplification was performed in a 25-μl reaction volume containing: 0.63 μM concentration of forward and reverse primers, 100 ng of template DNA, 0.2 mM deoxynucleotide triphosphates, 1.5 mM $MgCl_2$, 0.63 unit AmpliTaq polymerase (Perkin-Elmer, Foster City, CA), and HEPES buffer (10 mM HEPES, 50 mM KCl, pH 8.3). After initial denaturation and addition of Amplitaq, reaction products were subjected to 23 cycles of 94°C for 40 s, 55°C for 30 s, and 72°C for 30 s, with a final extension at 72°C for 2 min. Samples were then denatured and loaded on a 6% acrylamide gel with 33% formamide and 6 M urea. Electrophoresis was performed at 60 W for ~2–3 h. Subsequently, gels were vacuum dried and exposed to autoradiography film overnight at room temperature.

***In Vivo* Assays for Tumor Suppression.** Cells (5×10^6) of hybrid or parental origin were injected s.c. into athymic nude mice (5–7 weeks of age) as described previously (17). Cell viabilities were performed using trypan blue exclusion immediately before and after injections. For renal subcapsular injection, the protocol of Fidler *et al.* (31) was followed. Athymic nude mice were anesthetized with methoxyflurane. After a left subcostal incision, made to allow access to the left kidney, a tuberculin syringe with 30-gauge needle was inserted from the lower pole to just below the renal capsule on the superior pole of the kidney. Then 0.05 ml, containing 1×10^6 cells, was slowly injected, resulting in a subcapsular bleb. The incision was closed with a single layer of wound clips.

SSCP Analysis and DNA Sequence Analysis. SSCP and DNA sequencing were performed as described previously (18).

RESULTS

***NRC-1* Mediates Tumor Suppression in Papillary as well as Nonpapillary RCC.** We previously reported tumor suppression and rapid cell death of RCC *in vivo* after introduction of the 3p centric fragment into a nonpapillary RCC line SN12C.19 (17). To test the role of *NRC-1* in papillary RCC, we transferred the 3p centric fragment from HA(3)IIaa (an A9 microcell hybrid containing the pSV2neo-tagged subchromosomal region 3p12–q11; Fig. 1) into a papillary RCC cell line A498 (Fig. 2*a*; Ref. 26). The A498 cell line was obtained from the American Tissue Culture Association, where it had

Fig. 1. Cytogenetic analysis of HA(3)IIaa, the donor line for microcell fusion into RCC lines. G-banded metaphase spread shows the presence of the 3p12–q11 fragment in the A9 mouse fibrosarcoma cell background. *Arrows*, the 3p fragment in HA(3)IIaa.

[4] M. Lovell, S. T. Lott, A. El-Naggar, and A. M. Killary. Establishment of renal cell carcinoma cell lines of different histologic origin, manuscript in preparation.

a

b

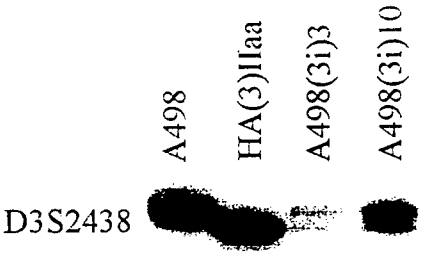

Locus	Number of Alleles
D3S1254	1
D3S2372	1
D3S2438	1
GATA67F08	1

c

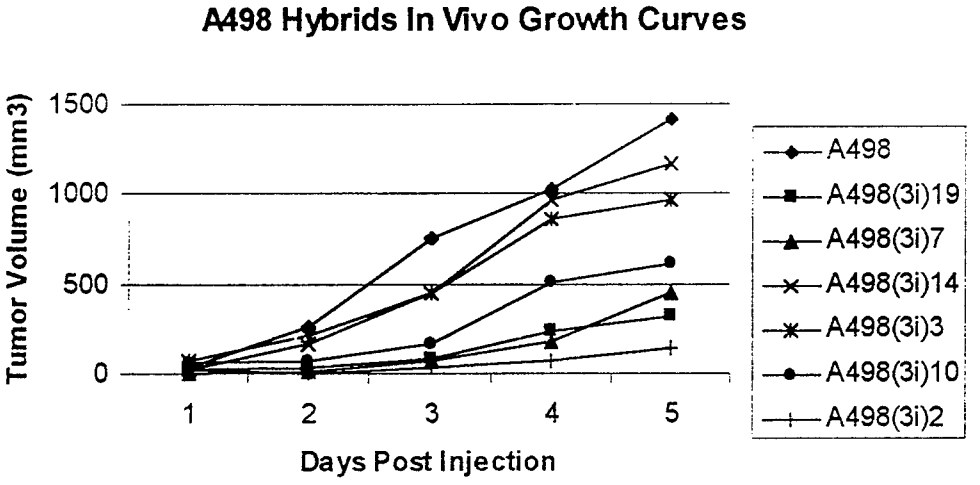

d

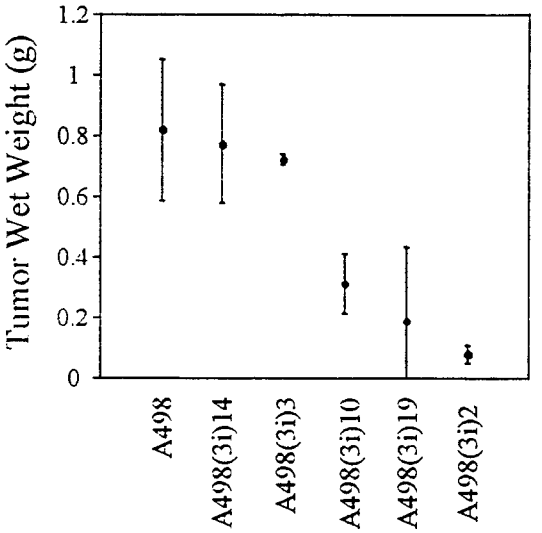

e

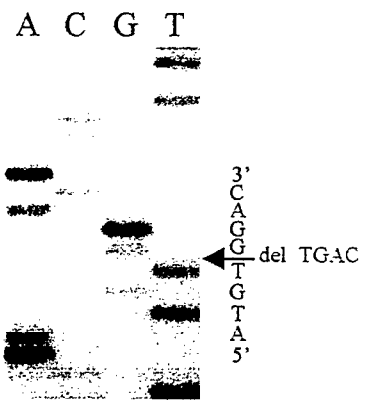

Fig. 2. Microcell fusion experiments into the A498 RCC cell line. *a*, G-banded metaphase spread of A498(3i) series microcell hybrid; *b*, microsatellite analysis of A498 indicating homozygosity for four of four markers in the 3p12 region; *c*, tumor volumes of A498 hybrids in the second experiment after injection into athymic nude mice; *d*, wet weights from the second experiment in which A498(3i) series hybrids were injected into nude mice (graph indicates mean kidney wet weights; *bars*, 95% confidence intervals; *e*, mutation screening for *VHL* in A498 (*arrow*, mutation).

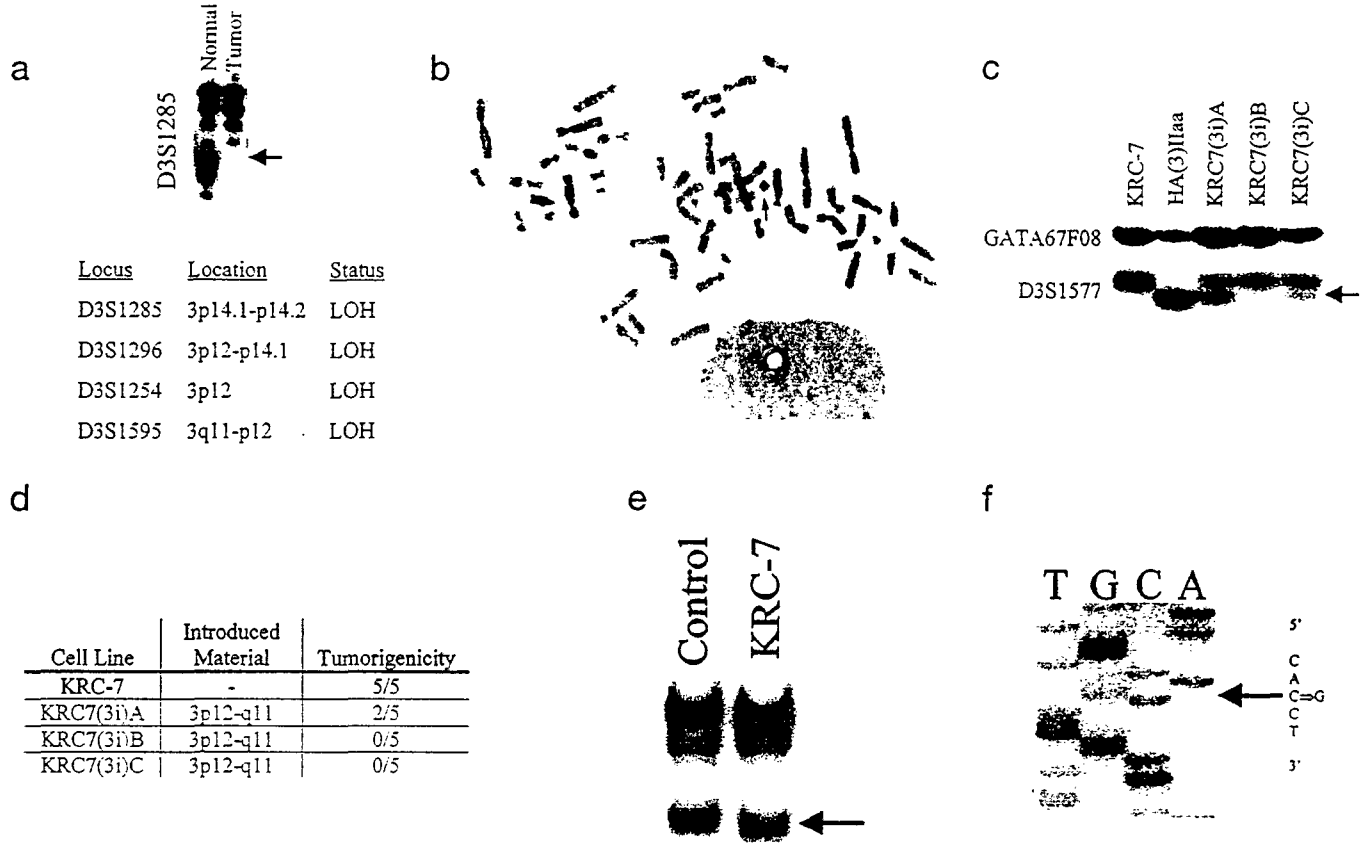

Locus	Location	Status
D3S1285	3p14.1-p14.2	LOH
D3S1296	3p12-p14.1	LOH
D3S1254	3p12	LOH
D3S1595	3q11-p12	LOH

Cell Line	Introduced Material	Tumorigenicity
KRC-7	-	5/5
KRC7(3i)A	3p12-q11	2/5
KRC7(3i)B	3p12-q11	0/5
KRC7(3i)C	3p12-q11	0/5

Fig. 3. Microcell fusion experiments into the KRC-7 RCC cell line. *a*, LOH analysis of tumor cell line/normal tissue in KRC-7; *b*, G-banded metaphase spread indicating the presence of the 3p centric fragment in the KRC-7 sarcomatoid hybrid KRC-7(3i)B; *c*, microsatellite analysis using markers in the distal region of the introduced fragment indicating retention of the region in the transferred fragment in wo of three hybrids; *d*, *in vivo* summary of injections of KRC-7 series hybrids in athymic nude mice; *e*, SSCP analysis (*arrow*, shift); DNA sequencing of the *VHL* gene (*arrow*, mutation) in KRC-7.

been classified as being of papillary origin. Confirmation of papillary histology was obtained by histological examination of A498 tumors formed after injection into athymic nude mice. Results indicated that histologically, tumor nodules manifested papillary and solid areas. The papillary component comprised the majority of the histological patterns and showed fronds and rosettes formed of central fibrovascular core lined by cuboidal tumor cells. Tumor cells were cytomorphologically similar in both the solid and the papillary patterns. This cell line was also examined cytogenetically and found to contain two normal copies of chromosome 3; however, microsatellite screening of A498 indicated homozygosity for four of four markers tested in the 3p12 interval containing *NRC-1* (Fig. 2*b*). Given the high degree of heterozygosity for the microsatellite markers tested (>75–85%), results suggest that A498 may be hemizygous for this region of 3p. Twelve microcell hybrid clones were generated in the A498 background after transfer of the 3p centric fragment via microcell fusion using HA(3)IIaa as the donor line. All clones were extensively characterized by G-11 analysis for the presence of any donor mouse chromosomes and by classical cytogenetics. Results indicated the presence of the centric fragment at high frequency (89–95%) in all hybrid clones examined.

Five microcell hybrid clones [A498(3i) series] as well as parental A498 controls were injected s.c. at 5×10^6 cells in the right flank of each of three athymic nude mice. Tumor volumes were measured biweekly for 2 months, after which time the tumors were excised and wet weights were determined. Four of the five hybrid clones demonstrated a dramatic tumor suppression ranging from 2- to 5-fold relative to parental controls (data not shown). Clone A498(3i)14 formed tumors of equivalent or slightly smaller size than parental controls, whereas A498(3i)3 formed tumors larger than A498. This experiment was repeated with an additional microcell hybrid clone for a total of six microcell hybrids containing the introduced 3p fragment. Tumor volumes were calculated again biweekly (Fig. 2*c*), and final tumor wet weights were determined (Fig. 2*d*). At the end of 47 days after injection, the parental A498 line formed tumors of 1417 mm^3, which required that the experiment be terminated. In this experiment, tumor volumes for A498(3i)2, A498(3i)19, and A498(3i)7 all ranged from 138–444 mm^3, again resulting in a greater than 3–10-fold suppression of tumor formation ($P = 0.0495$ for each hybrid clone). A(3i)10 was also suppressed as in the first experiment in the range of 617 mm^3. In the second experiment, A498(3i)14 and A498(3i)3 hybrids were intermediate in tumor formation ($P = 0.827$ and $P = 0.513$, respectively) relative to parental controls with no obvious deletions observed by microsatellite analysis. Thus, in two separate experiments, comparison between wet weights and tumor volumes indicated a dramatic suppression of tumorigenicity. As in previous experiments, complete suppression of tumorigenicity mediated by the chromosome 3p fragment was not observed, with outgrowth of tumors at the end of the experiment. Explants derived from tumors formed at the end of the experiment were cultured *in vitro* and examined by G-banding for the presence of the 3p fragment. Results indicated a loss of the introduced fragment in tumor explants in the range of 32–98% in hybrid clones, with the least suppressed clone A498(3i)14 retaining the fragment in only 2% of the population. These results indicate the involvement of the tumor suppressor locus *NRC-1* in not only nonpapillary RCC but

also the papillary form of the disease as well, which confirm and extend our previous findings that the 3p12–q11 fragment of <20 Mb, inclusive of the centromeric region, mediates tumor suppression in two different RCC cell lines.

***NRC-1* Mediates Tumor Suppression in Different Cell Types of Nonpapillary RCC.** Initial studies which defined the tumor suppressor locus *NRC-1* were performed by the transfer of the 3p centric fragment region into a nonpapillary RCC cell line SN12C.19, which is of mixed granular cell, clear cell origin. To study the involvement of the *NRC-1* locus in different cell types of nonpapillary RCC, we established over 20 new cell lines of different histological origin.[4] KRC-7 represents a rare sarcomatoid variant of RCC, the karyotype of which contains two normal copies of chromosome 3 and two copies of a chromosome 3 with a cytogenetic deletion of 3p12–3pter. LOH studies were performed for the 3p12 interval in the KRC-7 cell line *versus* adjacent normal tissue from the tumor originating KRC-7 (Fig. 3*a*). Results indicated LOH for four of four 3p markers tested. Thus, although KRC-7 contains multiple copies of chromosome 3, the 3p12 region is hemizygous, indicative that nondisjunction/loss may have occurred. Microcell hybrids were then constructed by transfer of the 3p12–q11 region from HA(3)IIaa into KRC-7. Unlike fusions in SN12C.19, which generated 30–40 hybrids/fusion, three microcell fusions were attempted in KRC-7, and only three hybrids in the KRC-7 background were obtained from one experiment. In all hybrids, however, the centric fragment was represented at high frequency (85–90%; Fig. 3*b*). Microsatellite analysis conducted on the KRC (7) series hybrids indicated that two of three hybrids retained distal marker *D351577* in the *NRC-1* critical region (Fig. 3*c*). One hybrid, KRC-7(3i)B, retained the introduced 3p fragment at high frequency by cytogenetic analysis; however, a deletion of *D351577* (additional markers examined were uninformative) was found upon microsatellite screening. KRC-7 hybrids were injected at 5×10^6 cells s.c. into athymic nude mice (five mice per hybrid line tested). Tumors were visible in the KRC-7 parental line injected at 6 weeks after injection. Wet weights of the KRC-7 line averaged 0.1 g 9 months after injection. Two of the three KRC-7 hybrids [KRC-7(3i)B and KRC-7(3i)C] failed to form any tumors during the 9-month study (Fig. 3*d*). The third clone [KRC-7(3i)A] was also completely suppressed for tumorigenicity in three of five mice injected. The remaining two mice, however, formed tumors larger than parental controls (Fig. 3*d*). Thus, although the parental line was not as aggressive as SN12C.19 or A498 in forming tumors *in vivo*, detection of 2–10-fold differences in hybrid tumor wet weights were possible and representative of previous experiments. Furthermore, because KRC-7(3i)B contained a deletion of 3p12 sequences as well as failed to form tumors *in vivo*, this microcell hybrid deletion clone may prove valuable to further limit the *NRC-1* critical region. KRC-7 is the only RCC line under study for which complete suppression of tumorigenicity was observed; because it is a newly established line, it may be more representative of the original tumor than the other lines under investigation that have been in culture for prolonged periods and perhaps acquired additional genetic aberrations. The combined results of the A498 and the KRC-7 study (Table 1) indicate that the *NRC-1* locus mediates tumor suppression independently of histological type and cell type of RCC and perhaps represents a more general tumor suppressor gene in the 3p12 region involved in diverse histological tumors.

Orthotopic Injection of Microcell Hybrids Containing the 3p Centric Fragment Indicates That Tumor Suppression via *NRC-1* Is Independent of the Microenvironment of the Tumor Cells. To determine whether the microenvironment of the tumor would affect hybrid growth rates *in vivo*, the same series of microcell hybrids previously reported by s.c. injection in the SN12C.19 background (17) were also injected orthotopically into the kidney of athymic nude mice. SN12C.19 contains multiple copies of chromosome 3, as well as an unbalanced t(3;8) translocation,[5] resulting in a derivative chromosome composed of most of the 3p arm of chromosome 3 (3pter–3p14.3 or 3p14.2) fused to the centromere and long arm of chromosome 8. For this experiment, two hybrids containing the introduced centric fragment and which were suppressed in s.c. injections were used [SN19(3i)YY and SN19(3i)FF]. A G-banded metaphase of SN19(3i)YY is shown in Fig. 4*a*. One hybrid containing two copies of an intact chromosome 3 [SN19(3)WW] was also injected; for controls, one 3p centric fragment-containing hybrid [SN19(3i)KK] that had a longer latency period for tumor formation, but eventually formed large tumors in s.c. injections, was also used. Microsatellite screening of hybrid clones indicated that all retained the distal markers in the *NRC-1* critical region (Fig. 4*b*). Parental controls and an irrelevant chromosome 2 microcell hybrid, SN19(2)L, were also injected. Each line was injected into the kidneys of 10 athymic nude mice. Kidneys were excised 60 days after injection and weighed. Results (Fig. 4*c*) directly correlated with data obtained from s.c. injections. The average wet weight of parental SN12C.19 injected kidneys was 2.2 g; injections with a control chromosome 2 microcell hybrid showed a slight decrease in growth (1.8 g) that was not statistically significant as compared with parental controls ($P = 0.221$) using a Mann-Whitney statistical analysis. However, orthotopic growth of the two hybrids, SN19(3i)FF (0.7 g, $P = 0.007$) and SN19(3i)YY (0.8 g, $P = 0.007$) was suppressed significantly. SN19(3)WW, which contained two copies of the introduced chromosome 3, was the most suppressed for tumor formation with an average kidney wet weight of 0.6 g ($P = 0.002$). Hybrid SN19(3i)KK, which formed intermediate tumors between suppressed and parental cells in s.c. injections, again demonstrated an intermediate level of tumor suppression (1.6 g, $P = 0.125$) which was not significantly different from parental controls. Thus, tumor suppression via *NRC-1* is independent of the tissue-specific controls in the kidney and supports the role of *NRC-1* in different histological and cell types of RCC.

Table 1 *Summary of in vivo growth by histological type*

Cell line	RCC histological type	Donor chromosome introduced	Tumor suppressor phenotype
A498	Papillary	–	–
A(3i)2	Papillary	3p12–q11	–
A(3i)7	Papillary	3p12–q11	–
A(3i)19	Papillary	3p12–q11	–
A(3i)10	Papillary	3p12–q11	–
A(3i)14	Papillary	3q12–q11	–
A(3i)3	Papillary	3p12–q11	–
KRC-7	Nonpapillary sarcomatoid	–	–
KRC-7(3i)A	Nonpapillary sarcomatoid	3p12–q11	–/–
KRC-7(3i)B	Nonpapillary sarcomatoid	3p12–q11	–
KRC-7(3i)C	Nonpapillary sarcomatoid	3p12–q11	–
SN12C.19	Nonpapillary mixed clear cell/granular cell	–	–
SN19(3i)YY	Nonpapillary mixed clear cell/granular cell	3p12–q11	–
SN19(3i)FF	Nonpapillary mixed clear cell/granular cell	3p12–q11	–
SN19(3)WW	Nonpapillary mixed clear cell/granular cell	2 copies of intact chromosome 3	–
SN19(3i)KK	Nonpapillary mixed clear cell/granular cell	3p12–q11	–/–

Tumor Suppression via 3p12 Locus *NRC-1* Is Independent of VHL Mutation. We next tested whether a requirement for tumor suppression via *NRC-1* is a wild-type *VHL* gene. Given that both *NRC-1* and *VHL* are tumor suppressor genes for RCC, then if *NRC-1* was in fact upstream of *VHL* in the same pathway, tumor suppression

[5] S. Pathak, personal communication.

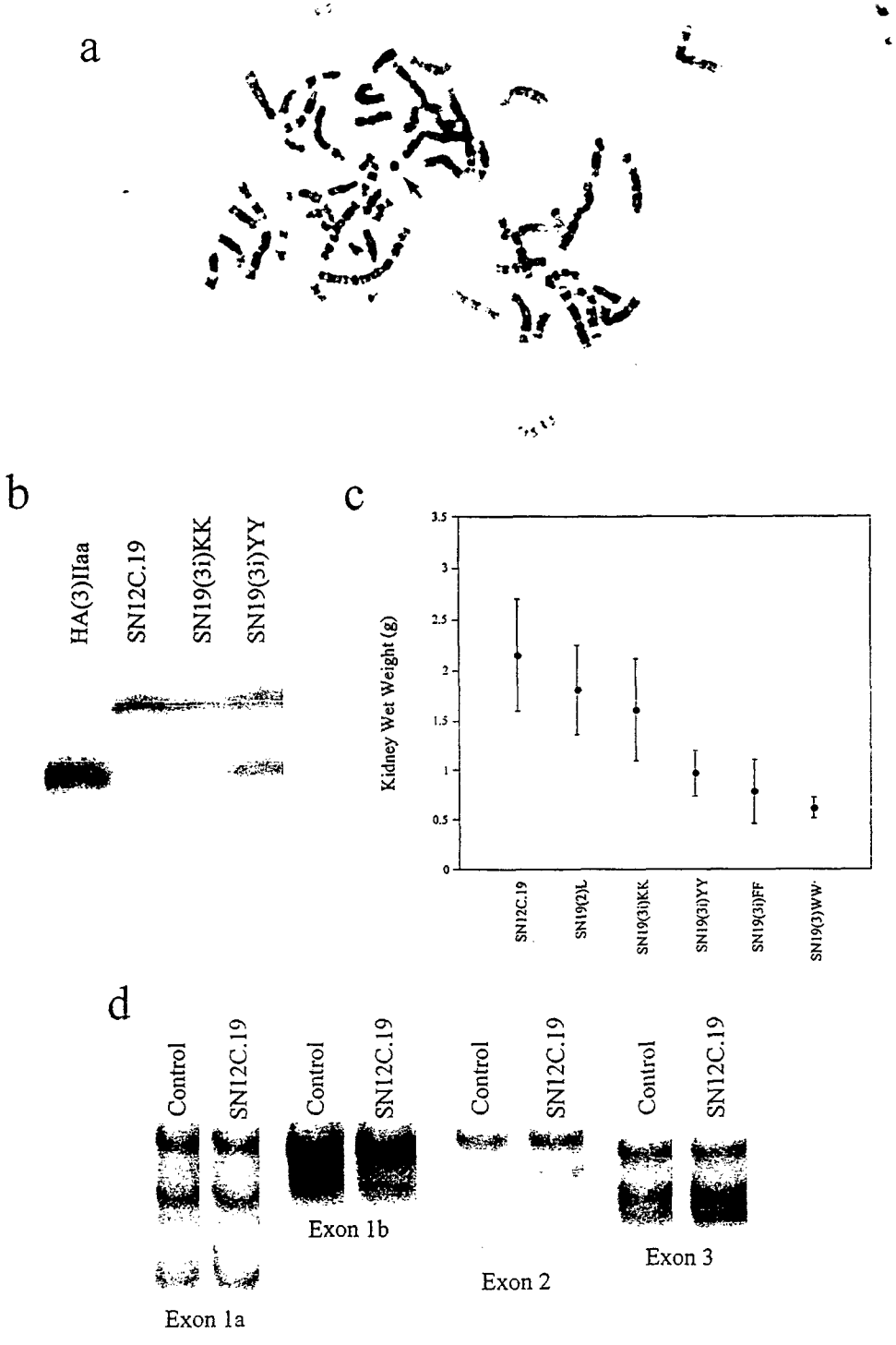

Fig. 4. Microcell fusion experiments into the SN12C.19 cell line. *a*, G-banded metaphase of SN12C.19 series hybrid SN19(3i)YY (*arrow*, presence of the 3p centric fragment); *b*, microsatellite analysis of SN12C.19 hybrids indicating the presence of the introduced 3p12 region in hybrid clones; *c*, wet weights of tumors after injection of SN12C.19 hybrids orthotopically into the kidney of athymic nude mice (graph denotes mean kidney wet weights; *bars*, 95% confidence intervals); *d*, SSCP analysis of SN12C.19 for the *VHL* gene. Control DNA was obtained from normal male lymphocytes.

might be abrogated in the presence of an inactivating mutation in *VHL*. If, on the contrary, *NRC-1* is either downstream of *VHL* or in an independent pathway, then *NRC-1* would be expected to mediate tumor suppression regardless of the absence of *VHL*.

To test the requirement of *VHL* for tumor suppression via *NRC-1*, we examined the status of *VHL* in the RCC cell lines under study. SN12C.19 is wild type for *VHL* by SSCP analysis (Fig. 4*d*). However, A498 and KRC-7 contain mutations in *VHL*. SSCP analysis of KRC-7 indicated a slight shift in one band relative to the normal tissue control (Fig. 3*e*). Sequence analysis indicated a C-G transition mutation in exon 2 at amino acid 186 in KRC-7 (Fig. 3*e*). A498 was previously used as recipient for transfection of wild-type *VHL* cDNA in experiments to document *in vitro* growth control via *VHL* in RCC (6). The cell line contains a previously reported 4-base deletion at nucleotides 639–642, resulting in a frameshift and lack of normal expression of the VHL protein (6). Sequencing of the *VHL* gene in the A498 line in our laboratory confirmed these data (Fig. 2*e*). Results clearly indicate that hybrids in the A498 and KRC-7 background (with *VHL* mutation), when injected s.c. into athymic nude mice, were suppressed for tumor formation as were hybrids in the SN12C.19 background (without *VHL* mutation), both in s.c. and orthotopic injections. We conclude that the *NRC-1*-mediated pathway to tumorigenesis is function-

ally independent of *VHL*, either downstream from *VHL* in the same pathway or in a completely independent pathway from *VHL*. Complementation of the pathway to tumorigenesis in the kidney, therefore, can be accomplished via *NRC-1*, even in a background of *VHL* mutation.

DISCUSSION

The critical events underlying the genesis of sporadic RCCs are not well understood. Clearly, the *VHL* gene is mutated at high frequency in sporadic RCCs, and replacement of *VHL* into RCC cell lines suggests a function as a tumor suppresser gene. However, inheritance of the *VHL* gene results in a diversity of tumor types and not just RCC, and the generation of these different tumor types is not easily explained by a strict genotype/phenotype relationship. Given this wide spectrum of primarily benign tumors that develop in *VHL*-affected individuals, one must consider the possible interactions of other genes that might influence the progression of *VHL*-associated malignancies. Binding of the *VHL*/Elongin B,C complex with Hs-CUL-2, a member of the Cdc53 protein family, has been shown (32). The *Cdc53* gene in yeast has been implicated in the targeted degradation of cell cycle proteins and acts as a putative "gatekeeper" gene that monitors the balance between controlled cell division and cell death. Null mutation of the Ce-cul-1 homologue in *Caenorhabditis elegans* produced increased cell numbers in many cell lineages examined (33). Studies on *VHL*-associated RCCs have documented, by both cytogenetic and LOH analyses, that losses occur commonly along the whole 3p arm. A likely mechanism for malignant conversion in *VHL*-associated tumorigenesis involves not only inheritance of a gatekeeper gene such as the *VHL* gene, which may predispose to the hyperplastic state, but also the loss of additional genes, such as *NRC-1*, which may be critical for malignant progression in RCC.

The results of this study indicate that the genetic locus *NRC-1*, syntenic to *VHL* on chromosome 3p, can function independently of *VHL* to suppress tumors in sporadic RCC. The exact role that *NRC-1* plays in the genesis of kidney cancer will await the identification of the tumor suppressor gene in this region. In our previous functional studies in which the 3p centric fragment was introduced into the RCC cell line SN12C.19, cell death was observed in the smallest tumors at week 1 after injection of hybrid cells in nude mice, and there was no evidence of angiogenesis in tumors at later stages based on morphology. At the periphery of the dead core of the tumor, there was an interface of cells actively undergoing apoptosis.[6] The formal possibility exists that *NRC-1* may play a critical role in the regulation of angiogenesis, downstream of *VHL*, and that loss of angiogenesis may result in induction of apoptosis as seen in our functional model. Thus, we can begin by addressing the role of *NRC-1* in a programmed cell death pathway in the kidney and the possible interrelatedness of a programmed cell death pathway and the *VHL* pathway associated with angiogenesis regulation and entrance into G_0. Mutations of the *VHL* gene have been shown to result in up-regulation of vascular endothelial growth factor and angiogenesis (34). Hanahan and Folkman (35), in a transgenic model for pancreatic islet cell tumors (one of two tumor types in *VHL* that progress to malignancy, RCC is the other), have shown that apoptosis in islet cell tumors in mice is highly dependent on persistent angiogenesis. When transgenic mice were treated with angiogenesis inhibitors, tumor growth was impaired and vessel density was reduced. The S-phase cell fraction remained high, whereas the apoptotic incidence increased significantly in the small tumors arising in mice treated with angiogenesis inhibitors. These results imply that the vasculature of the tumors may be a paracrine regulator of apoptosis and that inadequate vascularization can also cause tumor cell apoptosis.

In this report, we have also documented that introduction of *NRC-1* into histologically diverse RCC tumor lines results in tumor suppression and that this tumor suppression is independent of the microenvironment of the tumor. These data suggest that the tumor suppression mediated by *NRC-1* is independent of potential differential gene expression in the different cell types of RCC. These data also call into question the histological classification of RCC tumors based on presence or absence of 3p LOH. LOH is only as accurate as the markers available. Previous allelotyping studies excluded 3p12 loci in the region of *NRC-1* in their analysis. As documented in this report, the 3p12 region is important in different histological types of RCC and potentially other malignancies involving 3p aberrations. Only when the syntenic loci on 3p are isolated, however, can the formal definition of the selectivity and generality of these important tumor suppresser genes be elucidated.

[6] Sanchez and A. M. Killary, unpublished observations.

ACKNOWLEDGMENTS

We are grateful to Dr. I. J. Fidler and Mike Wilson for conducting orthotopic injections and James Luca for technical assistance.

REFERENCES

1. Zbar, B., Brauch, H., Talmadge, C., and Linehan, M. Loss of alleles of loci on the short arm of chromosome 3 in renal cell carcinoma. Nature (Lond.), *327:* 721–724, 1987.
2. Kovacs, G., Erlandsson, R., Boldog, F., Ingvarsson, S., Muller-Brechlin, R., Klein, G., and Sumegi, J. Consistent chromosome 3p deletion and loss of heterozygosity in renal cell carcinoma. Proc. Natl. Acad. Sci. USA, *85:* 1571–1575, 1988.
3. Cohen, A. J., Li, F. P., Berg, S., Marchetto, D. J., Tsai, S., Jacobs, S. C., and Brown, R. S. Hereditary renal-cell carcinoma associated with a chromosomal translocation. N. Engl. J. Med., *301:* 592–595, 1979.
4. Latif, F., Tory, K., Gnarra, J., Yao, M., Duh, F. M., Orcutt, M. L., Stackhouse, T., Kuzmin, I., Modi, W., Geil, L., *et al.* Identification of the von Hippel-Lindau disease tumor suppressor gene [see comments]. Science (Washington DC), *260:* 1317–1320, 1993.
5. Crossey, P. A., Richards, F. M., Foster, K., Green, J. S., Prowse, A., Latif, F., Lerman, M. I., Zbar, B., Affara, N. A., Ferguson-Smith, M. A., *et al.* Identification of intragenic mutations in the von Hippel-Lindau disease tumour suppressor gene and correlation with disease phenotype. Hum. Mol. Genet., *3:* 1303–1308, 1994.
6. Chen, F., Kishida, T., Duh, F. M., Renbaum, P., Orcutt, M. L., Schmidt, L., and Zbar, B. Suppression of growth of renal carcinoma cells by the von Hippel-Lindau tumor suppressor gene. Cancer Res., *55:* 4804–4807, 1995.
7. Naylor, S. L., Johnson, B. E., Minna, J. D., and Sakaguchi, A. Y. Loss of heterozygosity of chromosome 3p markers in small-cell lung cancer. Nature (Lond.), *329:* 451–454, 1987.
8. Brauch, H., Johnson, B., Hovis, J., Yano, T., Gazdar, A., Pettengill, O. S., Graziano, S., Sorenson, G. D., Poiesz, B. J., Minna, J., *et al.* Molecular analysis of the short arm of chromosome 3 in small-cell and non-small-cell carcinoma of the lung. N. Engl. J. Med., *317:* 1109–1113, 1987.
9. Yokota, J., Wada, M., Shimosato, Y., Terada, M., and Sugimura, T. Loss of heterozygosity on chromosomes 3, 13, and 17 in small-cell carcinoma and on chromosome 3 in adenocarcinoma of the lung. Proc. Natl. Acad. Sci. USA, *84:* 9252–9256, 1987.
10. Ehlen, T., and Dubeau, L. Loss of heterozygosity on chromosomal segments 3p, 6q and 11p in human ovarian carcinomas. Oncogene, *5:* 219–223, 1990.
11. Killary, A. M., Wolf, M. E., Giambernardi, T. A., and Naylor, S. L. Definition of a tumor suppressor locus within human chromosome 3p21–p22. Proc. Natl. Acad. Sci. USA, *89:* 10877–10881, 1992.
12. Daly, M. C., Xiang, R. H., Buchhagen, D., Hensel, C. H., Garcia, D. K., Killary, A. M., Minna, J. D., and Naylor, S. L. A homozygous deletion on chromosome 3 in a small cell lung cancer cell line correlates with a region of tumor suppressor activity. Oncogene, *8:* 1721–1729, 1993.
13. Kok, K., van den Berg, A., Veldhuis, P. M., van der Veen, A. Y., Franke, M., Schoenmakers, E. F., Hulsbeek, M. M., van der Hout, A. H., de Leij, L., van de Ven, W., *et al.* A homozygous deletion in a small cell lung cancer cell line involving a 3p21 region with a marked instability in yeast artificial chromosomes. Cancer Res., *54:* 4183–4187, 1994.
14. Yamakawa, K., Morita, R., Takahashi, E., Hori, T., Ishikawa, J., and Nakamura, Y. A detailed deletion mapping of the short arm of chromosome 3 in sporadic renal cell carcinoma. Cancer Res., *51:* 4707–4711, 1991.
15. Lubinski, J., Hadaczek, P., Podolski, J., Toloczko, A., Sikorski, A., McCue, P., Druck, T., and Huebner, K. Common regions of deletion in chromosome regions 3p12 and 3p14.2 in primary clear cell renal carcinomas. Cancer Res., *54:* 3710–3713, 1994.

16. Ohta, M., Inoue, H., Cotticelli, M. G., Kastury, K., Baffa, R., Palazzo, J., Siprashvili, Z., Mori, M., McCue, P., Druck, T., *et al.* The *FHIT* gene, spanning the chromosome 3p14.2 fragile site and renal carcinoma-associated t(3;8) breakpoint, is abnormal in digestive tract cancers. Cell, *84:* 587–597, 1996.
17. Sanchez, Y., el-Naggar, A., Pathak, S., and Killary, A. M. A tumor suppressor locus within 3p14–p12 mediates rapid cell death of renal cell carcinoma *in vivo*. Proc. Natl. Acad. Sci. USA, *91:* 3383–3387, 1994.
18. Lott, S. T., Lovell, M., Naylor, S. L., and Killary, A. M. Physical and functional mapping of a tumor suppressor locus for renal cell carcinoma within chromosome 3p12. Cancer Res., *58:* 3533–3537, 1998.
19. Latif, F., Tory, K., Modi, W. S., Graziano, S. L., Gamble, G., Douglas, J., Heppell-Parton, A. C., Rabbitts, P. H., Zbar, B., and Lerman, M. I. Molecular characterization of a large homozygous deletion in the small cell lung cancer cell line U2020: a strategy for cloning the putative tumor suppressor gene. Genes Chromosomes Cancer, *5:* 119–127, 1992.
20. Mostofi, F. K. (ed.). Histological typing of kidney tumours. International Histological Classification of Tumours, No. 25, pp. 1–23. Geneva, Switzerland: World Health Organization, 1981.
21. Zbar, B., Tory, K., Merino, M., Schmidt, L., Glenn, G., Choyke, P., Walther, M. M., Lerman, M., and Linehan, W. M. Hereditary papillary renal cell carcinoma [see comments]. J. Urol., *151:* 561–566, 1994.
22. Kovacs, G. The value of molecular genetic analysis in the diagnosis and prognosis of renal cell tumours. World J. Urol., *12:* 64–68, 1994.
23. Presti, J. C., Jr., Reuter, V. E., Cordon-Cardo, C., Mazumdar, M., Fair, W. R., and Jhanwar, S. C. Allelic deletions in renal tumors: histopathological correlations. Cancer Res., *52:* 5780–5782, 1992.
24. Thrash-Bingham, C. A., Greenberg, R. E., Howard, S., Bruzel, A., Bremer, M., Goll, A., Salazar, H., Freed, J. J., and Tartof, K. D. Comprehensive allelotyping of human renal cell carcinomas using microsatellite DNA probes. Proc. Natl. Acad. Sci. USA, *92:* 2854–2858, 1995.
25. Hughson, M. D., Meloni, A., Dougherty, S., Silva, F. G., and Sandberg, A. A. Analysis of 3p allelic loss in papillary and nonpapillary renal cell carcinomas. Correlation with tumor karyotypes. Cancer Genet. Cytogenet., *87:* 133–139, 1996.
26. Giard, D. J., Aaronson, S. A., Todaro, G. J., Arnstein, P., Kersey, J. H., Dosik, H., and Parks, W. P. *In vitro* cultivation of human tumors: establishment of cell lines derived from a series of solid tumors. J. Natl. Cancer Inst., *51:* 1417–1423, 1973.
27. Naito, S., von Eschenbach, A. C., Giavazzi, R., and Fidler, I. J. Growth and metastasis of tumor cells isolated from a human renal cell carcinoma implanted into different organs of nude mice. Cancer Res., *46:* 4109–4115, 1986.
28. Killary, A. M., and Lott, S. T. Production of microcell hybrids. Methods, *9:* 3–17, 1996.
29. Bobrow, M., and Cross, J. Differential staining of human and mouse chromosomes in interspecific cell hybrids. Nature (Lond.), *251:* 77–79, 1974.
30. ISCN. An International System for Human Cytogenetics Nomenclature: Birth Defects. Original Article Series, March of Dimes Birth Defects Foundation, 21(1). New York: 1985.
31. Fidler, I. J., Naito, S., and Pathak, S. Orthotopic implantation is essential for the selection, growth and metastasis of human renal cell cancer in nude mice [published erratum appears in Cancer Metastasis Rev., *10:* 79, 1991]. Cancer Metastasis Rev., *9:* 149–165, 1990.
32. Pause, A., Lee, S., Worrell, R. A., Chen, D. Y., Burgess, W. H., Linehan, W. M., and Klausner, R. D. The von Hippel-Lindau tumor-suppressor gene product forms a stable complex with human CUL-2, a member of the Cdc53 family of proteins. Proc. Natl. Acad. Sci. USA, *94:* 2156–2161, 1997.
33. Goebl, M. G., Yochem, J., Jentsch, S., McGrath, J. P., Varshavsky, A., and Byers, B. The yeast cell cycle gene CDC34 encodes a ubiquitin-conjugating enzyme. Science (Washington DC), *241:* 1331–1335, 1988.
34. Siemeister, G., Weindel, K., Mohrs, K., Barleon, B., Martiny-Baron, G., and Marme, D. Reversion of deregulated expression of vascular endothelial growth factor in human renal carcinoma cells by von Hippel-Lindau tumor suppressor protein. Cancer Res., *56:* 2299–2301, 1996.
35. Hanahan, D., and Folkman, J. Patterns and emerging mechanisms of the angiogenic switch during tumorigenesis. Cell, *86:* 353–364, 1996.

Other posters in each topic are scheduled for 4-day (W/T/F/S) or 2-day (W/T) display. See p. A-1 for complete listings.

1859

A Functional Genomic Approach for the Identification of *PAC-1*, a Novel Chromosome 10 Tumor Suppressor Gene. *P.E. Wong, M.M. Lovell, A. Goodacre, A.M. Killary.* Pathology and Laboratory Medicine, UT M.D. Anderson Cancer Center, Houston, TX.

A major goal of our laboratory's research is to use a functional genomic approach to define and isolate tumor suppressor genes involved in prostatic adenocarcinoma. Previously, we have defined a novel tumor suppressor locus *PAC-1* within chromosome 10p. Introduction of the short arm of chromosome 10 into a prostatic adenocarcinoma cell line PC-3H resulted in dramatic tumor suppression and restoration of a programmed cell death pathway. To functionally dissect the region within 10p containing *PAC-1*, we developed the novel strategy of serial microcell fusion, a technology that would allow the transfer of defined fragments of chromosome 10p into PC-3H and the rapid *in vivo* assay for functional tumor suppressor activity. Serial microcell fusion was used to transfer defined 10p fragments into a mouse A9 fibrosarcoma cell line. Once characterized by FISH and microsatellite analyses, the 10p fragments were subsequently transferred into PC-3H to generate a panel of microcell hybrid clones containing overlapping deletions of chromosome 10p. Additionally, comparative genomic hybridization was used to identify regions of loss in PC-3H. Extensive characterization of 10p deletion hybrids by microsatellite analysis and FISH allowed the exclusion of two separate candidate tumor suppressor regions within chromosome 10p implicated by LOH in gliomas and prostate tumors. Furthermore, these data limited the region for *PAC-1* from approximately 65 Mb to less than 10 Mb. These studies demonstrate the utility of this approach as a powerful tool to limit regions of functional tumor suppressor activity. In addition, the 10p deletion hybrid panel will be a critical resource for the physical mapping of 10p, as well as for the isolation of the important tumor suppressor gene *PAC-1*.

1860

Tumour Formation in Neurofibromatosis 2 (NF2): a test of fit for a "two-hit" hypothesis. *R. Woods[1,5], D.G.R. Evans[2], H. Joe[1,5], M.E. Baser[3], J.M. Friedman[1,4].* 1 University of British Columbia,Vancouver, British Columbia, Canada; 2) St. Mary's Hospital, Manchester, U.K; 3) Los Angeles, U.S.A; 4) Department of Medical Genetics; 5 Department of Statistics.

Hethcote and Knudson (Proc Natl Acad Sci 1978;75:2453-7) developed a "two-hit" model to describe the incidence of tumours in hereditary and sporadic retinoblastoma. Subsequent molecular genetic analysis has established the validity of this model in retinoblastoma and other inherited forms of cancer. Molecular evidence suggests that a two-hit model is also appropriate for the development of vestibular schwannomas (VS) in patients with neurofibromatosis 2 (NF2). We fit a model analogous to Hethcote and Knudson's to incidence data for sporadic and inherited VS, the latter in NF2 patients, to examine the correlation of epidemiological and molecular evidence in this condition. The data included 72 NF2 patients, all non-probands with bilateral VS, and 50 published sporadic cases of unilateral VS (Clin. Otolaryngol 1999;24:13-18). The age at onset of VS in sporadic cases is later than that in patients with NF2 (mean/median age of onset in years, 52.1/56.5 for sporadic cases, 30.1/26.0 for NF2 cases). The predicted incidence curves for the age at onset of VS from the two-hit model fit the empirical incidence curves very closely. (chi-square(8 df) = 4.59 for goodness of fit, p = 0.80)(See http://mendel.medgen.ubc.ca/friedmanlab/2hitplot.html for the plot). We are extending this model to include provision for the allele-phenotype correlation that has been described in NF2 (e.g., J Med Genet 1998;35:450-455) and to analyze the occurrence of other tumours in this disease. The authors gratefully acknowledge support from the Acoustic Neuroma Association of Canada, the BC Medical Services Foundation, and NSERC.

1861

Risk of breast cancer from benign breast disease: Incidence Rates for breast cancer and intra observer reliability in classifying benign breast disease lesions. *M.J. Worsham[1], C.C. Johnson[2], U. Raju[1], J. Abrams[2], A. Blount[2], S.R. Wolman[3].* 1) Cancer Genetics Research, Dept Pathology, Henry Ford Hosp, Detroit, MI; 2) Josephine Ford Cancer Center, enry Ford Hosp, Detroit, MI; 3) Uniformed Services University of the Health Sciences, Bethesda, MD 20814-4799.

Women with benign breast lesions, particularly those classified as proliferative, are at increased risk for subsequent development of breast cancer. We have identified a cohort of women with benign breast disease (BBD) diagnosed by breast biopsy during the years 1981-1994. Classification was based on risk categories for developing invasive carcinoma defined by Page and Dupont. At the current time, 2263 members of the cohort have been followed for occurrence of breast cancer through 1997. One hundred thirty one cases were identified over 21,317 person-years of follow-up. The average incidence rate per year was 615 per 100,000 (95%) confidence interval of 518-729). The incidence of breast cancer in this BBD cohort appears to be higher than the SEER rate of 350.2 per 100,000 for women 50 years from 1990-1994 in the same metropolitan areas. To evaluate intra observer reliability, a 10% random sample of slides, N=74, from years 1981 through 1983 were independently reviewed a second time by the same pathologist who was blinded at both readings to the identity of the patient. Concordance ranged from 85% for simple apocrine metaplasia to 99% for squamous metaplasia. Average agreement was 91%. Kappa statistics indicated significantly greater than chance agreement ($p<.001$) for all lesions but fibrosis. Concordance ranged from 93% for simple adenoid and hyperplasia to 99%for apocrine hyperplasia with a mean of 96%. All kappa statistics indicated significantly more than chance agreement, $p<.001$. Lesions with moderately increased risk are atypical ductal hyperplasia (ADH) and atypical lobular hyperplasia (ALH). One case of ADH and no cases of ALH were found and the pathologist agreed at both readings. No high-risk lesions i.e. ductal or lobular carcinoma in situ were found. In summary, a trained breast pathologist can reliably classify lesions of different risk categories.

1862

HER2/neu and PS6K (17q23) amplification in breast lesions from women with and without a family history of breast cancer. *G. Wu, K. Anderl, C.A. Soderberg, L.C. Hartmann, R.B. Jenkins, F.J. Couch.* Mayo Clinic, Rochester, MN.

Germline mutations in BRCA1, BRCA2, and other susceptibility loci are involved in the initiation of hereditary breast cancer. However, the somatic events that lead to progression of hereditary cancers are not known. In addition, it is not known whether somatic progression pathways differ in hereditary versus sporadic disease. To address this question we have evaluated the frequency of amplification of HER2/neu and a region of chromosome 17q23 containing the PS6K (p70 S6 kinase) gene in a series of 22 cases of breast cancer from families with strong histories of breast and/or ovarian cancer and 29 matched sporadic cases. Paraffin blocks for 46 in situ carcinomas and 51 invasive carcinomas were identified for these cases, along with 32 regions of apparently benign epithelium (for control purposes). These blocks were subjected to fluorescent in situ hybridization (FISH) analysis using HER2/neu/CEN17 and PS6K/CEN17 dual-BAC probe mixtures.

The incidences of gene amplification in hereditary and sporadic cases, respectively, were 28% (6 of 21) and 0% (0 of 13) for HER2/neu, and 44% (7 of 16) and 25% (3 of 12) for PS6K. The incidences of chromosomal gain in hereditary and sporadic cases, respectively, were 65% (13 of 20) and 38% (5 of 13) for +CEN17. In hereditary cancers 1 of 16 had co-amplification of HER2 and PS6K, 3 of 16 had amplification of HER2 only, and 6 of 16 had amplification of PS6K only. In sporadic cancers, 0 of 12 showed co-amplification, 0 of 12 had amplification of HER2 only, and 3 of 12 had amplification of PS6K only. Our data show that chromosomal alterations, as measured by CEN17 gain and HER2/neu and PS6K gene amplification, are more frequent within breast cancers of women with a strong family history of cancer, consistent with an increased underlying chromosomal instability. Further studies will determine if separate pathways of carcinogenesis exist for hereditary and sporadic breast cancer.

1863

Localization of Transfected B7-1 (CD80) DNA on Human Melanoma Cells after Particle Mediated Gene Transfer. *S. Wu[1], D.O. McCarthy[2], N.J. Glowacki[2], C.A. Emler[3], X. Chen[1], M.R. Albertini[2].* 1) Pediatrics, Children's Hospital, Los Angeles, School of Medicine, University of Southern California, Los Angeles, CA; 2) University of Wisconsin Comprehensive Cancer Center, Madison, WI; 3) Agracetus, Inc., Middleton, WI.

Particle mediated gene transfer (PMGT) is an efficient means to directly deliver transgenes into human melanoma cells for transient or stable gene expression. The aim of this study was to determine the localization of transfected B7-1 cDNA in M-21 melanoma cells following PMGT. Microscopic gold particles coated with a plasmid vector containing B7-1 cDNA and delivered by PMGT were detected in the cytoplasm and nucleus of recipient M-21 cells. Using fluorescence in situ hybridization (FISH), biotin labeled B7-1 DNA was clearly detected in most melanoma cells 24 hours following PMGT. The B7-1 transgene particles were randomly distributed within melanoma cells, and transfected melanoma cells contained between 1 and 14 biotin labeled particles. Stable B7-1 transfectants (M-21-B7) were obtained following PMGT with a plasmid vector containing cDNA for both B7-1 and neomycin phosphotransferase and subsequent selection in media containing G418. While 50-60% of M-21-B7 evaluated by flow cytometry had surface expression of B7-1, analysis by FISH did not detect the B7-1 transgene in these cells. The M-21-B7 were then sorted on the FACStar Plus by brightness of B7 expression to obtain M-21-B7 (bright) cells with 85-90%of cells with B7-1 expression. Analysis by FISH and subsequent chromosome G-banding analysis demonstrated 70% of M-21-B7 (bright) to have two predominant integration sites with extensive amplification of the B7-1 transgene. These integration sites were located on chromosome 15 and 17. These findings demonstrate that B7-1 cDNA can integrate into the chromosomes of recipient M-21 cells following PMGT, and this integration can occur in preferential sites in some cells. The relationship between transgene integration site and expression of the transgene, or other cellular genes, requires further investigation.

1864

Genomic organization and mutation analysis of Mortalin, a candidate for the chromosome 5q31 tumor suppressor gene in AML/MDS. *H. Xie[1], S.K. Horrigan[2], B. Chyna[1], Z.B. Hu[1], C.A. Westbrook[1].* 1) Section of Hematology/Oncology, Univ. of Illinois at Chicago, Chicago, IL; 2) Department of Pediatrics, Lombardi Cancer center, Georgetown University Medical Center, Washington,DC.

In malignant myeloid disorders, including myelodysplasia (MDS) and acute myeloid leukemia (AML), interstitial deletion or loss of chromosome 5 frequently occurs, suggesting the presence of a tumor suppressor gene. By heterozygosity analysis of a small deletion, we have defined a minimal localization for this gene to a 700 kb interval on 5q31, to which we have mapped several candidate genes. Among these candidates, mortalin, HSPA9,is a plausible tumor suppressor. Mortalin is a member of the hsp70 family. The protein exhibits differential cellular localization in mortal and immortal cells of human and mouse by virtue of its cytosolic and perinuclear distribution, respectively. The murine cytosolic form (mot-1) induces senescence in NIH3T3 cells whereas the perinuclear form (mot-2) does not. It has been postulated that loss of cytosolic mortalin may lead to cell immortalization and tumorigenesis. As first step in mutation analysis of mortalin in clinical AML and MDS, we determined the genomic structure and intron-exon boundaries of human mortalin by direct sequencing of BAC DNA. We show that the gene spans 19.5 kb. It contains 17 exons and 16 introns, with similar boundaries to its murine counterpart, and all boundary sequences contained consensus GT/AG sequences at the donor and acceptor site of RNA splicing. Mutation analysis of AML was begun by sequencing DNA from three AML cell lines, including 2 with chromosome 5 loss (KG-1 and HL-60) and one without (AML-193). Using intron-based primers, genomic sequence was completed for all 17 exons, and compared to normal (BAC) DNA. No mutation was detected in any of the cell lines, although two conservative nucleotide sequence variants were identified in exon 16. We have shown by RT-PCR that mortalin is expressed in these AML cell lines and normal CD34+ bone marrow precursor. Mutation and expression analysis of clinical MDS and AML samples is ongoing.

DEPARTMENT OF THE ARMY
US ARMY MEDICAL RESEARCH AND MATERIEL COMMAND
504 SCOTT STREET
FORT DETRICK, MARYLAND 21702-5012

REPLY TO
ATTENTION OF:

MCMR-RMI-S (70-1y) 8 Jan 2003

MEMORANDUM FOR Administrator, Defense Technical Information Center (DTIC-OCA), 8725 John J. Kingman Road, Fort Belvoir, VA 22060-6218

SUBJECT: Request Change in Distribution Statement

1. The U.S. Army Medical Research and Materiel Command has reexamined the need for the limitation assigned to the enclosed. Request the limited distribution statement for the enclosed be changed to "Approved for public release; distribution unlimited." These reports should be released to the National Technical Information Service.

2. Point of contact for this request is Ms. Judy Pawlus at DSN 343-7322 or by e-mail at judy.pawlus@det.amedd.army.mil.

FOR THE COMMANDER:

Encl

PHYLLIS M. RINEHART
Deputy Chief of Staff for
Information Management

ADB265840

ADB266633

ADB282069

ADB279138	ADB251763	ADB265386
ADB264578	ADB281601	ADB282057
ADB281679	ADB258874	ADB258251
ADB281645	ADB281773	ADB264541
ADB261128	ADB281660	ADB241630
ADB261339	ADB259064	ADB281924
ADB273096	ADB266141	ADB281663
ADB281681	ADB281664	ADB281659
ADB259637	ADB258830	
ADB256645	ADB266029	
ADB262441	ADB281668	
ADB281674	ADB259834	
ADB281771	ADB266075	
ADB281612	ADB281661	